The Mu and Delta Opioid Receptors: Mixed Efficacy Ligands and Receptor Trafficking

by

Jessica P. Anand

A dissertation submitted in partial fulfillment
of the requirements for the degree of
Doctor of Philosophy
(Medicinal Chemistry)
in the University of Michigan
2013

Doctoral Committee:

Professor Henry I. Mosberg, Co-chair
Professor John R. Traynor, Co-chair
Associate Professor Roger K. Sunahara
Professor Ronald W. Woodard
Professor James H. Woods

ACKNOWLEDGEMENTS

First and foremost, I would like to thank my mentor, Dr. Henry Mosberg, for his guidance, patience, and support throughout this project. He was always available to help me troubleshoot a problem and gave me a surprising amount of freedom in choosing the direction I wanted to take my research, for which I am very grateful. I would like to Dr. Kate Sobczyk-Kojiro for the innumerable times she has answered my questions and been a sounding board for ideas. Drs. John Traynor, Mary Divin, Adam Kuszak, and Lauren Purington are deserving of thanks for all the training, assistance, and advice they have given me with regards to the pharmacological aspects of my thesis. I also want to thank all the members of the Mosberg and Traynor labs, past and present, for listening to my problems and returning to me advice and sympathy and the students of the Medicinal Chemistry department with whom I have commiserated and exulted, depending on the state of our research.

I would also like to thank the members of my committee, Drs. John Traynor, Roger Sunahara, Ronald Woodard, Oleg Tsodikov, and James Woods. They have helped shape this project and given advice that has been exceedingly valuable. I also want to thank my funding sources, the Pharmacological Sciences Training Program, the Neuroscience Training Grant, and the Fred Lyons Fellowship, for financial support during my graduate school career, without which the research would not have been possible.

Closer to home, I would like to thank my friends and family, both biological and found, my strong, beautiful, Barnard women, and the Michiganders who have welcomed us here in Ann Arbor. Without them, my life would be so much harder. And, last but definitely not least, I want to thank my spouse, Gabe Carlson, who has made my life so much better.

TABLE OF CONTENTS

LIST OF TABLES

LIST OF FIGURES

LIST OF APPENDICES

LIST OF ABBREVIATIONS

[^{35}S]GTPγS [^{35}S] guanosine 5'-O-[gamma-thio]triphosphate

1Nal 1-naphthylalanine

2Nal 2-naphthylalanine

AF488 Alexafluor 488

AF555 Alexafluor 555

AF647 Alexafluor 647

Aib 2-Aminoisobutyric acid

Aic 2-aminoindane-2-carboxylic acid

Ala Alanine

Arg Arginine

Asn Asparagine

Asp Aspartate

Boc Tert-butoxycarbonyl

BOD647 Bodipy dye 647

BODTMRX Bodipy dye TMR-X

C6 C6 rat gliomal cells

CDOR Cyan fluorescent protein labeled delta opioid receptor

CFP Cyan fluorescent protein

Cha Cyclohexylalanine

CHO Chinese hamster ovary cells

Cy3 Cyanine fluorescent dye 3

Cy5 Cyananine fluorescent dye 5

Cys Cysteine

DAMGO [DAla^{2}, N-MePhe^{4}, Gly-ol]-enkephalin

Dhp 3-(2,6-dimethyl-4-hydroxyphenyl)propanoic acid

DIEA *N*,*N*-diisopropylethylamine

DMF Dimethylformamide

Dmt 2,6 dimethyl tyrosine

dns does not stimulate

DOR Delta opioid receptor

DPDPE DPen^{2,5}- enkephalin

DPN Diprenorphine

ESI-MS Electrospray ionization mass spectrometry

Et ethyl

Fmoc 9-fluorenylmethyloxycarbonyl

FRET Förster resonance energy transfer

GAP GTPase activating proteins

GDP guanosine diphosphate

Gln Glutamine

Glu Glutamate

Gly Glycine

GPCR G protein coupled receptor

G Protein Guanine nucleotide binding protein

GTP Guanosine triphosphate

HATU 2-(7-aza-1H-benzotriazole-1-yl)-1,1,3,3-tetramethyluronium hexafluorophosphate

HBTU *O*-benzotriazole-*N*,*N*,*N*',*N*'-tetramethyl-uronium-hexafluorophosphate

Hcp 4'[N-(hexyl)carboxamido]phenylaline]

HDL High density lipoprotein

HEK Human embryonic kidney cells

His Histidine

HOAt 1-hydroxy-7-azabenzotriazole

HOBt *N*-hydroxybenzotriazole

HPLC High performance liquid chromatography

Idg indanylglycine

Ile Isoleucine

KOR Kappa opioid receptor

LC/MS Liquid chromatography/mass spectrometry

Leu Leucine

Lys Lysine

Me Methyl

Met Methionine

MOR Mu opioid receptor

Ncp 4’-[N-(2-napthalen-2-yl)ethyl)carboxamido] phenylalanine

nd not determined

Nle Norleucine

NLX Naloxone

NMP *N*-methylpyrrolidinone

NMR Nuclear magnetic resonance spectroscopy

nt not tested

PDB Protein data bank

Pen penicillamine

Phe Phenylalanine

POPC 1-palmitoyl-2-oleoyl-sn-glycero-3-phosphocholine

POPG 1-palmitoyl-2-oleoyl-sn-glycero-3-phospho-rac-(1-glycerol)

Pro Proline

Sar Sarcosine

SAR Structure-activity relationship

Ser Serine

SEtS Ethylene dithioether

SH SY5Y Human neuroblastomal cell line

SMeS Methylene dithioether

SM-TIRF-M Single molecule total internal reflection fluorescence microscopy

SPPS Solid phase peptide synthesis

TFA Trifluoroacetic acid

THF Tetrahydrofuran

Thr Threonine

Tic Tetrahydro-isoquinoline-3-carboxylic Acid

TIS triisopropylsilane

Trp Tryptophan

Tyr Tyrosine

Val Valine

wt Wild type

YFP Yellow fluorescent protein

YMOR Yellow fluorescent protein labeled mu opioid receptor

ABSTRACT

Opioids are widely used in the treatment of pain; however, the development of tolerance and dependence limit clinical use. The co-administration of a μ opioid receptor (MOR) agonist with a δ opioid receptor (DOR) agonist or antagonist produces analgesia with reduced tolerance and dependence. Elucidating how MOR and DOR interact has the potential to change opioid analgesic treatment.

This work has two branches: firstly, cyclic MOR agonist/DOR antagonist peptides were synthesized. Models of MOR and DOR indicate that the active state conformation of both receptors is narrower than the inactive conformations. DOR has bulkier residues occluding its binding pocket; the active and inactive state conformations of DOR are narrower than their MOR counterparts. Increased steric bulk prevents binding to the active state conformation of DOR and is tolerated in the more open MOR active and DOR inactive conformations, producing MOR agonist/DOR antagonist ligands. Analogues were synthesized with bulkier residues and both the size and stereochemistry of the cycle were varied to explore the active and inactive state MOR and DOR conformations. The structure activity relationships found in the cyclic ligands were then translated to linear peptides, as they are easier to synthesize and have higher yields. However, the flexibility of the linear peptides allowed for more compact binding poses, resulting in MOR/DOR agonist ligands. Promising ligands from both series were glycosylated for improved bioavailability. Secondly, selective fluorescent MOR agonist and DOR antagonist ligands were synthesized and used as probes to explore MOR trafficking in response to DOR and DOR antagonists. The presence of both receptors in the same cell did not alter the trafficking of agonist-bound MOR or antagonist-bound DOR when only one ligand was present. The presence of both ligands in cells that expressed both receptors increased the internalization of agonist-bound MOR, without changing the trafficking of antagonist-bound DOR. Internalization of MOR is involved in receptor recycling and can lead to an increase in surface expressed receptor. By increasing surface expression of MOR, antagonist-bound DOR may reduce the development of tolerance to MOR agonists.

CHAPTER 1
Introduction

1.1 Opioids and the Opioid Receptors

Opioid analgesics, such as opium and morphine, are among the world's oldest known drugs for the treatment of acute and chronic pain and morphine and other opioid compounds are still widely used in the clinic today. Opioids are also prescribed as cough suppressants and antidiarrheals, in spite of the fact that many opioids are known to show euphorigenic and rewarding properties. Opioid compounds fall into two main structural categories: small molecule alkaloids, such as morphine and oxycodone, and opioid peptides, such as the enkephalins, endorphins, and dynorphins, all of which interact with the same binding site deep within the transmembrane helix bundle of the opioid receptors. Although successful use of opioids in pain management is common, there are several side effects, such as constipation and respiratory depression, which can severely limit their clinical utility. To make matters more difficult, both acute and chronic use of opioids can result in neurochemical adaptations which alter the subject's homeostasis; two noteworthy adaptations caused by opioid use are tolerance, which can occur with both acute and chronic use, and dependence, which, in a clinical setting, is primarily seen in long term pain management. Tolerance is an adaptation that results in the clinical efficacy of a given dose decreasing over time or, in other words, needing an escalating dose to achieve the same effect. Dependence is characterized by an alteration of homeostasis, whereby subjects require the presence of drug to maintain a "normal" state and the removal of drug results in a series of negative symptoms known as withdrawal. These adaptations not only complicate dosing regimens for patients and limit the clinical use of opioids, but have been linked to increased addiction liability and may contribute to the prevalence of opioid abuse [1-3].

Opioid compounds exert their analgesic and rewarding properties through interaction with the opioid receptors found in the brain and spinal cord [4]. Opioid receptors belong to the Class A family of G protein-coupled receptors (GPCRs); GPCRs are membrane bound proteins containing seven transmembrane helices, with the N-terminus in the extracellular space and the

C-terminus in the intracellular space. All GPCRs couple with heterotrimeric guanine nucleotide binding proteins (G proteins) which are composed of an α subunit and a β and γ subunit that form an obligate dimer. Upon ligand binding to a GPCR, specific conformations of the receptor are stabilized, a signal is transmitted from the extracellular space to the intracellular space and second messengers are activated to initiate downstream signaling. In the case of agonist binding, the "active" conformation(s) of the transmembrane domains of the GPCR are stabilized; the "active" state(s) of the GPCR promotes a change in conformation of the nucleotide binding site of the associated α subunit of the G protein which favors the exchange of guanosine diphosphate (GDP) for guanosine triphosphate (GTP). Upon GTP binding, the "active" form of the α subunit is stabilized; this allows for dissociation of the G protein from the receptor as well as the dissociation of the α subunit from the βγ subunit. These subunits go on to affect downstream signaling partners and alter cell signaling. Eventually the signal is terminated by hydrolysis of GTP to GDP, either through the intrinsic GTPase activity of the α subunit or through the enzymatic activity of cellular GTPase activating proteins (GAPs). This allows for the re-association of the α and βγ subunits with each other and the receptor, resetting the system for further signaling (**Figure 1.1**). The signal can be terminated either by the removal of the ligand from the extracellular space or by the inactivation of the receptor through phosphorylation, desensitization, and internalization.

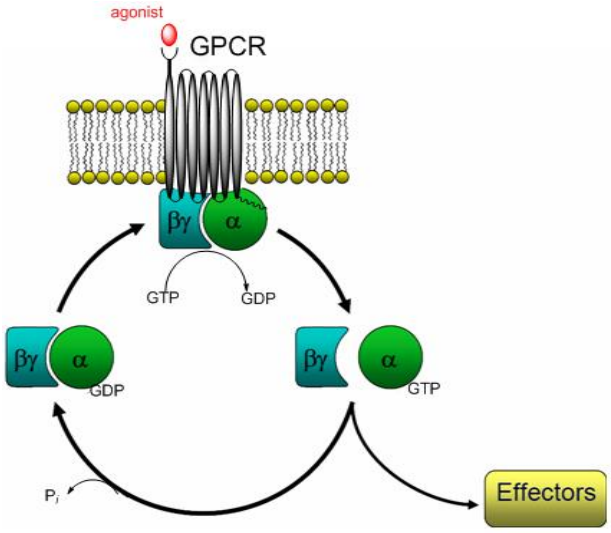

Figure 1.1: GPRC Cycle – Upon agonist binding the "active" form of a GPCR is stabilized. This stabilizes the "active" state of the associated G protein. The "active" G protein conformation favors the exchange of GDP for GTP. This allows for the dissociation of the G protein subunits from each other and the receptor to interact with downstream effectors. The signal is terminated by the hydrolysis of GTP to GDP which allows for the re-association of the G protein subunits with each other and the receptor, resetting the system for further signaling.

There are three classical types of opioid receptor – μ, δ, and κ (MOR, DOR, and KOR respectively) – that couple mainly to the adenylyl cyclase inhibitory $G\alpha_{i/o}$ subfamily of G proteins that stimulate inwardly rectifying K^+ and reduce the opening of voltage gated Ca^+

channels, dampening the firing of neurons; the Gβγ subunits associated with the opioid receptors signal to downstream effectors and alter the signaling of many pathways, including the MAPK pathways [5-9]. All three opioid receptors are distributed widely throughout the body; however the analgesic and rewarding properties of opioids are primarily centrally mediated. MOR is found mainly in the cortex, striatum, thalamus, and locus coeroleus, DOR is found in the striatum and cortex, and KOR is found in the limbic regions of the brain and spinal cord [4, 10]. As will be discussed more in section 1.3, it is worth noting that MOR and DOR occupy similar regions of the brain, especially regions associated with pain signaling, reward, and addiction [11].

Table 1.1: *In vitro* Pharmacology of Opioid Receptors – A summary of the actions of agonists at the three classical opioid receptors. (Levitt unpublished.)

	Opioid Receptor		
in vitro Pharmacology	μ	δ	κ
Antinociception	+	+/-	+/-
Respiratory Depression	+	-	-
Rewarding Effects	+	-	-
Dependence	+	-	+/-
Tolerance	+	+	+

Agonists for MOR, DOR, and KOR each display distinct pharmacological profiles (**Table 1.1**); clinically used opioids are MOR agonists. MOR agonists uniformly display analgesic properties and produce unwanted side effects such as respiratory depression and constipation, though these attributes are sometimes utilized in the form of cough suppressants or antidiarrheals; many MOR agonists are also euphorogenic. Tolerance develops for all of these properties, though at differing rates; normally tolerance develops first to the analgesic and euphoric properties of opioids, while tolerance to constipation or respiratory depression is slower to emerge [12]. This poses a major problem for chronic use of opioids as a given dose will become less effective in pain management, or, in the case of opioid abuse, less effective in providing a high, but remain potent in its ability to repress respiration and gastric transit. In contrast, DOR agonists are not used clinically, nor are they abused. While DOR agonists are capable of producing mild analgesia, DOR agonists also produce seizures [13]. KOR agonists are also somewhat analgesic, but, unfortunately, are also dysphoric, sedating, and may produce psychomimetic effects, and therefore they are not used clinically in pain management [14].

As described above and shown in **Table 1.1,** opioid receptors display a wide range of pharmacological responses which often vary depending on the conditions under which the

receptors are tested. In fact, pharmacological testing predicts a greater number of opioid receptor subtypes (δ^1, δ^2, etc) than gene cloning would suggest. It has been proposed that this increased number of apparent opioid receptor subtypes – as defined by altered ligand binding, efficacy, trafficking, etc – can be explained by opioid receptor/receptor interactions either with other opioid receptors or with other non-opioid GPCRs [15]. It has been suggested that homo- and hetero-oligomers regulate GPCR ligand binding and pharmacology, the association of downstream signaling partners, amplification of signal, and even trafficking and expression of receptors [16-24]. Some groups even feel that oligomerization, usually dimerization, is necessary for normal opioid function and that opioid dimers are the native receptor state, as opposed to the classical view of a GPCR monomer coupling to single G protein to transmit a signal (Figure 1.1) [15, 25-30]. The idea of requisite Class A GPCR oligomerization is highly controversial,[1] especially as it relates to *in vivo* function. While there exists a plethora of indirect evidence suggesting that dimers or higher order oligomers do occur [24] there are also reports of functional monomeric GPCRs [31-33].

1.2 Theories of Tolerance

The development of tolerance with chronic use of opioid analgesics is a major problem facing clinical use. This is particularly problematic as patients often develop tolerance to the analgesic properties of opioids long before they develop tolerance to unwanted side effects, such that in order to achieve the desired analgesic effect one risks major complications, as described in section *1.1*. The cellular mechanism(s) for the development of analgesic tolerance are unclear; however there are several hypotheses to explain this phenomenon.

Opioid receptors, like all GPCRs, are expressed on the plasma membrane of cells such that their binding sites are accessible to the extracellular matrix; many opioid ligands, such as endogenous opioid peptides, are unable to cross the plasma membrane and so the ligand binding site must be surface accessible in order for opioid receptors to be activated. After agonist binding and initiation of downstream signaling, opioid receptors are phosphorylated at serine or threonine residues on the intracellular C-terminal tail by various kinases. This prevents G proteins from accessing the receptor, thus preventing further signal transduction; receptors in this

[1] Oligomerization of other classes of GPCRs, such as Class C receptors, is well established.

state are said to be desensitized, as they can bind ligand, but this does not produce a transduction of signal. This phosphorylation also marks the receptors for recognition by β arrestins which induce internalization of the receptor via clatherin coated pits, sequestering them in vesicles inside the cell [34-37]. One theory addressing the development of tolerance suggests internalization of the targeted receptor produces tolerance by removing receptors from the cell surface rendering the receptor unable to bind extracellular ligand and initiate downstream signaling [2]. Internalization depletes the cell's receptor reserve (number of receptors expressed on the surface but not actively used in signaling at any given time) and so a given amount of drug will stimulate fewer receptors and produce less of an effect than it did prior to receptor internalization, in other words, producing tolerance. Receptor binding studies have shown that MOR surface expression decreases after chronic treatment with MOR agonists and that there is a corresponding loss of opioid mediated signal [38-40].

The degree of receptor reserve for a given ligand may be important in the development of tolerance. Ligands with high intrinsic efficacy will have a large receptor reserve as a single binding event may be able to trigger many second messenger signaling events. This means that fewer receptors need to be occupied to produce a given level of response; so a smaller percentage of the total receptor population will be lost when agonist bound receptors are desensitized or internalized. As a result, there will be a larger store of unoccupied receptors to take the place of the desensitized or internalized receptors – a receptor reserve – and so tolerance will be slower to develop. Ligands with lower intrinsic efficacy will have a smaller receptor reserve as more receptors will need to be occupied to produce a given response, so when the agonist occupied receptors are desensitized or internalized a smaller percentage of the total receptor population will remain active, and tolerance will develop more quickly. This theory is supported in the case of MOR agonists. High efficacy MOR agonists such as [D-Ala^2, N-Me-Phe^4, Gly-ol]-enkephalin (DAMGO) and fentanyl are slow to develop analgesic tolerance [40, 41], whereas lower efficacy agonists, such as morphine, rapidly develop tolerance [42, 43].

Another theory suggests that receptor endocytosis is the first step in resensitization of the receptor and that tolerance emerges from desensitization via phosphorylation while receptor is still on the cell surface. Here, after agonist binding and phosphorylation, the receptors are internalized, re-sensitized through dephosphorylation and recycled to the surface in a functional

state [36, 40, 44]. This idea is supported by the fact that some MOR agonists, such as DAMGO and fentanyl, undergo robust internalization, but are slow to develop analgesic tolerance [40, 41], whereas morphine, in many systems, does not undergo internalization, but rapidly develops tolerance [42, 43]. This would suggest that morphine binds ligand and the receptor is phosphorylated and desensitized, but the receptor conformation that is stabilized by morphine does not undergo internalization. This would leave non-functional receptor on the plasma membrane and reduce the overall number of functional receptors on the cell surface, leading to tolerance as described above. In the case of DAMGO or fentanyl, the receptor conformation that is stabilized is capable of undergoing internalization and can therefore be dephosphorylated and returned to the surface in a functional state, maintaining surface expression of functional receptors.

Whether internalization causes or helps prevent the development of tolerance, the trafficking of MOR to and from the plasma membrane seems to play a key role. Exploring the relationship between altered opioid trafficking and the development of tolerance will lay the groundwork for a better understanding of opioid signaling and the development of better opioid analgesics with extended clinical use. In this work I will develop mixed efficacy ligands and explore how various ligand combinations alter the trafficking of MOR and DOR in live cell systems, monitored with fluorescently tagged ligands and receptors.

1.3 DOR Modulation of MOR Tolerance

1.3.1 DOR Antagonists

It is well established that the analgesic effects of opioids and the tolerance to opioid analgesia are both mediated through MOR. However, it has been shown that MOR does not act in isolation *in vivo* or *in vitro*; of particular note are the ways in which MOR and DOR have been shown to interact [45]. It has been demonstrated that the co-administration of a MOR agonist and a DOR antagonist mitigates the development of tolerance and dependence, while preserving the desired analgesia [46-49]. The role of DOR blockade in the development of MOR tolerance and dependence is of significant clinical importance, as it could potentially extend the use and reduce the abuse of opioid drugs. The role of DOR itself, as opposed to DOR ligands, in the development of MOR tolerance has also been explored; it has been shown that the knock-down

or knock-out of DOR in mice slows the development of tolerance to a MOR agonist [50, 51]. Taken together, these data strongly suggest that there is a clinically significant interaction between the two receptors, MOR and DOR, which modulates the development of tolerance to and dependence on MOR agonists. Several theories have been proposed to explain how a DOR antagonist can decrease the development of tolerance to MOR agonists, two of which involve MOR/DOR heterodimers (**Figure 1.2**). One theory proposes that upon DOR antagonist treatment DOR surface expression is increased, either through blockade of basal DOR signaling such that

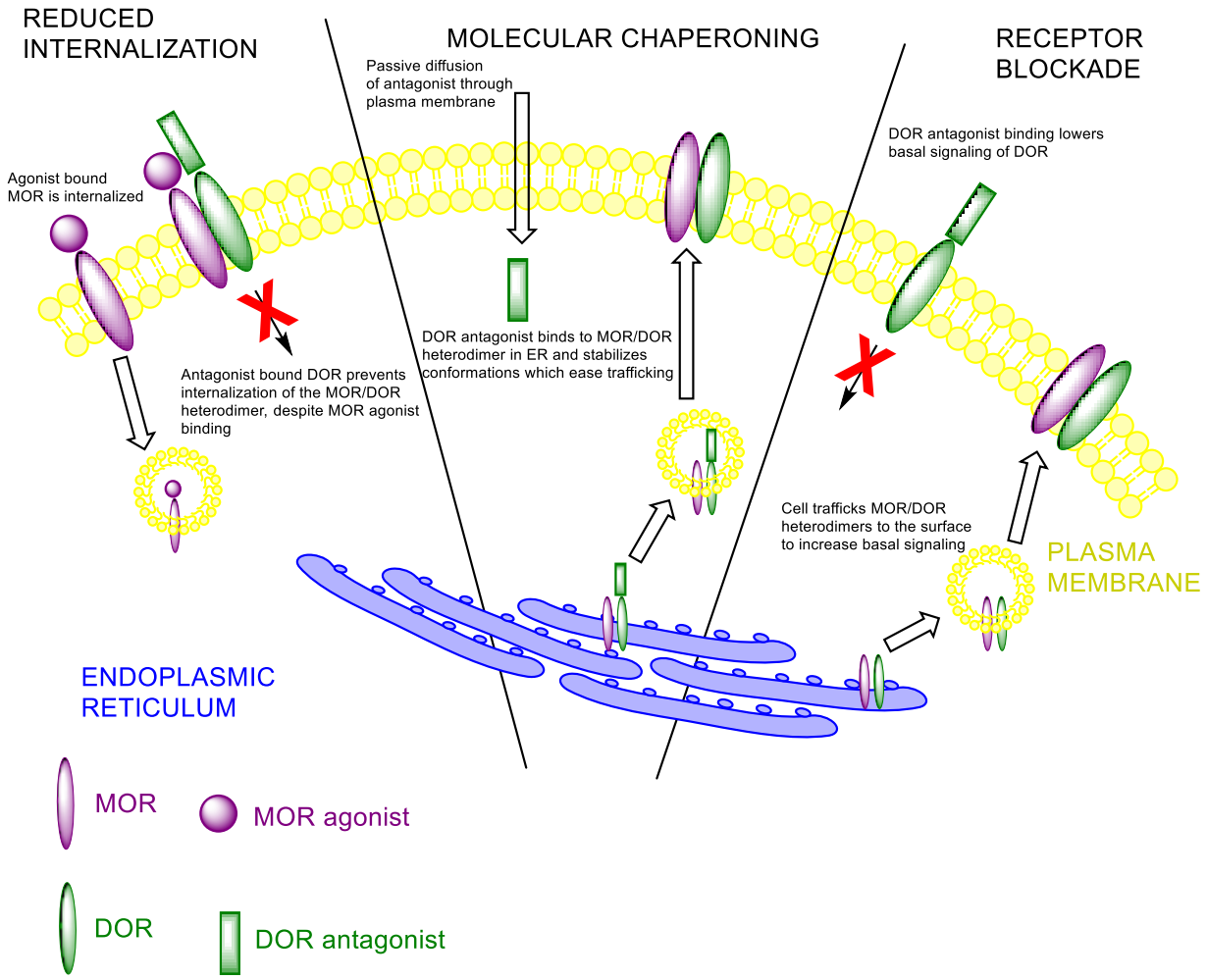

Figure 1.2: Mechanisms by which Opioid MOR/DOR Heterodimers may Effect Receptor Trafficking – Mechanisms by which DOR receptor blockade may regulate the surface expression of MOR via MOR/DOR heterodimers. (**A**) MOR/DOR heterodimers expressed on the cell surface are not internalized with DOR antagonist is bound. (**B**) DOR antagonists act as molecular chaperones which facilitate trafficking of MOR/DOR heterodimer to the cell surface from the endoplasmic reticulum. (**C**) DOR antagonists block basal DOR signaling on the cell surface. The cell increases trafficking of MOR/DOR heterodimers to the cell surface from the endoplasmic reticulum to maintain enkephalinergic tone.

the cell traffics more DOR to the surface from intracellular stores to maintain enkephalinergic tone or through molecular chaperoning which stabilizes the receptor and enhances trafficking to the surface of the cell from the endoplasmic reticulum [52, 53]. MOR is then co-trafficked to the plasma membrane in the form of a MOR/DOR heterodimer from the endoplasmic reticulum or vesicular stores, thereby making more MOR binding sites available on the plasma membrane and preventing the development of tolerance through loss of cell surface binding [15, 54]. Another hypothesis proposes that if MOR/DOR heterodimers occur on the plasma membrane, antagonist bound DOR will prevent the internalization of agonist bound MOR through their receptor/receptor dimerization, thereby maintaining surface expression of MOR [28]. These theories are supported by the fact that MOR and DOR have been shown to co-localize in the same cell in the dorsal root ganglion [55-57], a region associated with pain signaling. There also exists a third set of possibilities which do not involve the dimerization of MOR and DOR: it is possible that MOR and DOR signal to a central location, either inter- or intracellularly, and the confluence of these signals attenuates the development of tolerance and dependence. It is likely that these signals would alter the trafficking pattern of the receptors, but do not necessarily do so through a direct physical interaction between MOR and DOR. Regardless of the mechanism, it is clear that DOR antagonists have the ability to modulate the activity and function of MOR ligands as well as the ligand-receptor interactions and trafficking patterns of MOR.

1.3.2 DOR Agonists

Endorphins and enkephalins are the body's endogenous MOR and DOR agonist peptides; though endorphins and enkephalins are referred to as MOR and DOR ligands respectively, they are somewhat promiscuous and both groups of peptides are capable of stimulating both MOR and DOR. This may have clinical significance, as it has been shown that the co-administration of DOR agonist with a MOR agonist lessens the development of tolerance to and dependence on MOR agonists, as well as reducing the incidence of other unwanted side effects [58-60] without affecting MOR mediated analgesia. It has also been demonstrated that sub-analgesic doses of DOR agonists potentiate the affinity and antinociceptive potency of MOR agonists in a dose dependent manner [59, 61-63]. While these are intriguing observations, they have been pursued less vigorously than MOR agonist/DOR antagonist interactions, perhaps because of the severe unwanted effects which can result from stimulation of DOR by some non-endogenous ligands,

such as mood alteration, convulsions, and seizures [13], all significant drawbacks for any chronic therapeutic.

1.4 Multifunctional Ligands as Tools to Explore MOR/DOR Interactions

It has been recognized that the simultaneous modulation of multiple targets often generates a more desirable drug profile, in some cases even reducing the development of negative side effects [64-68]. Given the data presented above in section 1.3.1, the idea of mixed efficacy ligands displaying MOR agonism/DOR antagonism has been the object of much investigation, both as leads for new analgesics and as tools to illuminate the mechanism(s) by which DOR influences the development of MOR tolerance. It is possible that these novel ligands might not only affect neurochemical adaptations involving analgesic tolerance and dependence, but also the emergence of negative side effects such as constipation and respiratory depression or tolerance to these effects [14, 66]. This has generated a whole new field of research directed toward developing novel mixed opioid efficacy ligands, as opposed to new formulations of multiple pre-existing drugs. Such a multifunctional ligand would possess considerable advantages over the traditional approach of using a combination of selective opioid drugs; combination therapies often contain active ingredients with differing pharmacokinetic properties which complicate dosing regimens and reduce patient compliance. Complicated drug cocktails also increase the risk of patient to patient variation in efficacy and adverse drug reactions. As a result, many groups have investigated the development of mixed efficacy ligands, both peptidic and non-peptidic, displaying varying degrees of MOR and DOR agonism or antagonism [69-75]. These compounds fall into two main categories: bivalent ligands, in which two separate pharmacophores, in this case a MOR agonist pharmacophore and a DOR antagonist pharmacophore, are linked by a flexible spacer [75-77], and bifunctional ligands, which contain a single set of binding elements which can interact with both targets, in this case the MOR agonist binding site and the DOR antagonist binding site [72, 73] (**Figure 1.3**).

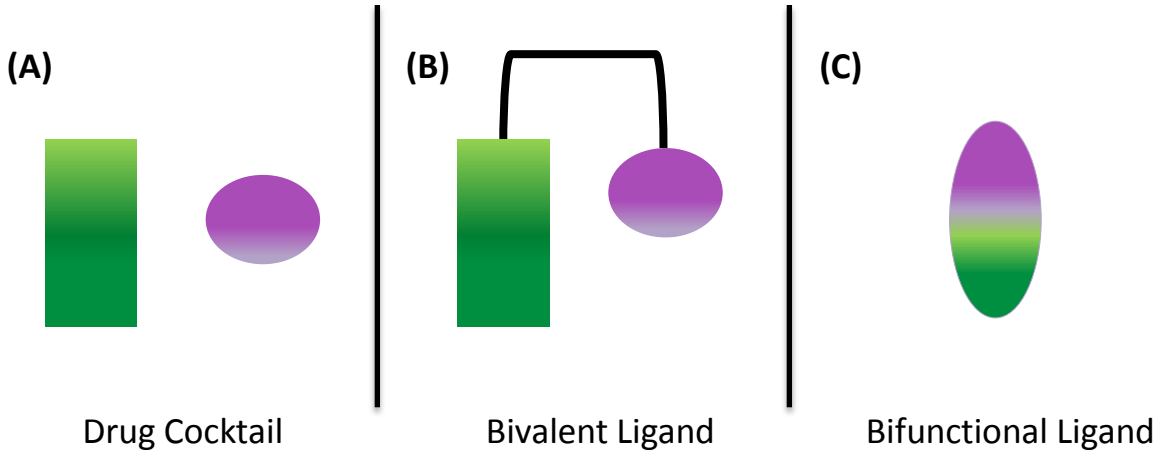

Figure 1.3: Drug Cocktail vs. Bivalent Ligands vs. Bifunctional Ligands – (**A**) A drug cocktail containing two selective drugs with distinct pharmacophores (**B**) A bivalent ligand in which two separate pharmacophores are connected by a flexible linker to form a single molecule (**C**) A bifunctional drug in which two separate pharmacophores are merged into a single ligand which displays properties of both pharmacophores.

Peptides provide a convenient starting point for the development of multifunctional opioid ligands to study the interactions between MOR and DOR. Many endogenous and synthetic opioid peptides have been studied and their structure-activity relationships (SAR) have been well characterized, providing the foundation for applying rational design to existing ligands to explore the MOR and DOR active (agonist) and inactive (antagonist) binding pockets. Peptides also possess the distinct advantage of making multiple contacts within the receptor binding site which can be easily modified by making minor alterations to the constituent residues; this allows for the fine tuning of binding and efficacy profiles and greater flexibility in ligand generation. Additionally, most peptides are unable to cross the plasma membrane; as we are interested in the trafficking of MOR and DOR to and from the cell surface knowing that the ligand-receptor interaction occurs at the plasma membrane will help to elucidate at what point in the receptor trafficking cycle a ligand produces its effect.

1.5 Objectives

The development of tolerance to the analgesic properties of opioids is a major problem facing the clinical use of opioids and may contribute to the development of physical dependence on opioids, a risk factor for abuse and addiction [1-3]. Although the mechanism(s) by which altered opioid trafficking are linked to the development of tolerance are unclear, it is well

established that both acute and chronic tolerance to opioid agonists is concomitant with altered opioid receptor trafficking [38-40].

My thesis project takes two different approaches to explore the development of tolerance to and dependence on opioid analgesics. The first branch aims to develop mixed efficacy MOR/DOR ligands that display reduced development of tolerance and dependence. In Chapter 2, I will explore the development of cyclic mixed efficacy ligands displaying MOR agonism and DOR antagonism with similar affinity for both MOR and DOR, with selectivity relative to KOR. In Chapter 3 I will translate these ligands to linear scaffolds to simplify the structures in an effort to increase yields and ease purification. The second branch explores how various ligand treatments alter the trafficking patterns of MOR and DOR in live cell systems to determine if ligand profiles which slow the development of tolerance and dependence display distinctive receptor trafficking. I will attempt to relate patterns of receptor co-trafficking to the development of tolerance and dependence. In Chapter 4, I will use fluorescent ligands and fluorescently tagged receptors to explore how different drug cocktails alter the trafficking pattern of receptors in live cell systems which express both MOR and DOR. In Appendix B, I will utilize the fluorescent ligands developed in Chapter 4 to explore the necessity of receptor dimerization for basic opioid function using receptors isolated in high density lipoprotein (HDL) discs and design selective fluorescent ligands for use with total internal reflection fluorescence microscopy (TIRF-M).

1.6 References

1. Ross, S. and E. Peselow, *The Neurobiology of Addicitive Disorders.* Clinical Neuropharmacology, 2009. **32**(5): p. 269-276.
2. Bailey, C.P. and M. Connor, *Opioids: Cellular Mechanisms of Tolerance and Physical Dependence.* Current Opinion in Pharmacology, 2005. **5**(1): p. 60-8.
3. Johnston, L.D., et al., *Monitoring the Future: National Survey Results on Drug Use.* National Institute on Drug Abuse, 2009. **1**: p. 1-721.
4. Mansour, A., et al., *Opioid-receptor mRNA Expression in the Rat CNS: Anatomical and Functional Implications.* Trends in Neuroscience, 1995. **18**(1): p. 22-29.
5. Burt, A.R., et al., *Agonist Activation of the p42 and p44 Mitogen-activated Protein Kinases Following Expression of the Mouse Delta Opioid Receptor in Rat-1 Fibroblasts: Effects of Receptor Expression Levels and Comparisons with G Protein Activation.* Biochemistry, 1996. **320**: p. 227-235.
6. Henry, D.J., et al., *Kappa Opioid Receptors Couple to Inwardly Rectifying Potassium Channels When Coexpressed by Xenopus Oocytes.* Molecular Pharmacology, 1995. **47**: p. 551-557.
7. Hescheler, J., et al., *The GTP-binding protein, Go, Regulated Neuronal Calcium Channels.* Nature, 1987. **325**: p. 445-447.
8. Jin, W., et al., *Dual Excitator and Inhibitory Effects of Opioids on Intracellular Clacium in Neuroblastom X Glioma Hybrid NG-108-15 Cells.* Molecular Pharmacology, 1992. **42**: p. 1083-1089.
9. Surprenant, A., et al., *Inhibition of Calcium Currents by Noradrenaline, Somatostatin, and Opioids in Guinea-pig Submuscosal Neurons.* Journal of Physiology, 1990. **431**: p. 585-608.
10. Trescot, A.M., et al., *Opioid Pharmacology.* Pain Physician, 2008. **11**(Second Supplememt): p. S133-S153.
11. Gray, A.C., I.M. Coupar, and P.J. White, *Comparison of opioid receptor distributions in the rat central nervous system.* Life Sciences, 2006. **79**: p. 674-685.
12. Ling, G.S.F., et al., *Differential Development of Acute Tolerane to Analgesia, Respiratory Depression, Gastrointestinal Transit and Hormone Release in a Morphin Infusion Model.* Life Sciences, 1989. **45**: p. 1627-1636.
13. Jutkiewicz, E.M., *The Antidepressant-like Effects of Delta-Opioid Receptor Agonists.* Molecular Interventions, 2006. **6**(3): p. 162-169.
14. Schiller, P.W., *Bi- or Multifunctional Opioid Peptide Drugs.* Life Sciences, 2010. **86**(15-16): p. 598-603.
15. George, S.R., et al., *Oligomerization of mu and delta Opioid Receptors: Generation of Novel Functional Properties.* Journal of Biological Chemistry, 2000. **275**(34): p. 26128-26135.
16. Breitwieser, G.E., *G Protein coupled Receptor Oligomerization: Implications for G Protein Activation and Cell Signaling.* Circulation Research, 2004. **94**: p. 17-27.
17. Fotiadis, D., et al., *Rhodopsin dimers in native disc membranes.* Nature, 2003. **421**: p. 127-8.
18. Gether, U. and B.K. Kobilka, *G Protein-coupled Receptors.* Journal of Biological Chemistry, 1998. **273**(29): p. 17979-17982.

19. Lee, C., et al., *Two Defective Heterozygous Lutenizing Hormone Receptors can Rescue Hormone Action.* Journal of Biological Chemistry, 2002. **277**: p. 15795-15800.
20. Maggio, R., Z. Vogel, and J. Wess, *Co-expression studies with mutant muscarinic/adrenergic receptors provide evidence for intermolecular ''cross-talk'' between G-protein linked receptors.* Proc Natl Acad Sci USA, 1993. **90**: p. 3103–3107.
21. McVey, M., et al., *Monitoring Receptor Oligomerization Using Time-resolved Fluorescence Resonance Energy Transfer and Bioluminescence Resonance Enerty Transfer.* Journal of Biological Chemistry, 2001. **276**(17): p. 14092-14099.
22. Milligan, G., *G Protein Coupled Receptor Dimerization: Function and Ligand Pharmacology.* Molecular Pharmacology, 2004. **66**: p. 1-7.
23. Ramsay, D., et al., *Homo- and Heterooligomeric Interactions Between G Protein-Coupled Receptors in Living Cells Monitored by Two Variants of Bioluminesence Resonance Energy Transfer. Heterooligomers Between Receptor Subtypes form More Effiency than between less Closely Related Sequences.* Biochemistry, 2002. **365**: p. 429-440.
24. Rios, C.D., et al., *G-protein-coupled Receptor Dimerization: Modulation of Receptor Function.* Pharmacology and Therapeutics, 2001. **92**: p. 71-87.
25. Gomes, I., et al., *Heterodimerization of mu and delta Opioid Receptors: A Role in Opiate Synergy.* Journal of Neuroscience, 2000. **20**: p. 1-5.
26. Hazum, E., K.-J. Chang, and P. Cuatrecasas, *Opiate (Enkaphalin) Receptors of Neuroblastoma Cells: Occurrene in Clusters on the Cell Surface.* Science, 1979. **206**(4422): p. 1077-1079.
27. Hazum, E., K.-J. Chang, and P. Cuatrecasas, *Cluster Formation of Opiate (enkaphalin) Receptors in Neuroblastoma Cells: Differences between Agonists and Antagonists and Possible Relationships to Biological Functions.* Proceedings of the National Academy of Science USA, 1980. **77**(5): p. 3038-3041.
28. Law, P.-Y., et al., *Heterodimerization of mu - and delta-Opioid Receptors Occurs at the Cell Surface Only and Requires Receptor-G Protein Interactions.* Journal of Biological Chemistry, 2005. **280**(12): p. 11152-62.
29. Li-Wei, C., et al., *Homodimerization of the Human Mu-Opioid Receptor Overexpressed in Sf9 Insect Cells.* Protein and Peptide Letters, 2002. **9**: p. 145-152.
30. Pascal, G. and G. Millligan, *Functional Complementation and the Ananlysis of Opioid Receptor Homodimerization.* Molecular Pharmacology, 2005. **68**: p. 905-915.
31. Whorton, M.R., et al., *A Monomeric G Protein-coupled Receptor Isolated in a High-density Lipoprotein Particle Efficiently Activates its G Protein.* Proc Natl Acad Sci USA, 2007. **104**(18): p. 7682-7687.
32. Whorton, M.R., et al., *Efficient coupling of transducin to monomeric rhodopsin in a phospholipid bilayer.* J Biol Chem, 2008. **283**(7): p. 4387-94.
33. Kuszak, A.J., et al., *Purification and reconstitution of a mu-opioid receptor monomer: functional G protein activation and allosteric regulation.* Journal of Biological Chemistry, 2009. **284**(39): p. 26732-41.
34. Vives, E. and B. Lebleu, *One-pot Labeling and purification of peptides and proteins with fluorescein maleimide.* Tetrahedron Letters, 2003. **44**: p. 5389-5391.
35. Bailey, C.P., et al., *How Important is Protein Kinase C in Mu Opioid Receptor Desensitization and Morphine Tolerance?* Trends in Pharmacological Sciences, 2006. **27**: p. 558-565.

36. Martini, L. and J.L. Whistler, *The Role of Mu Opioid Receptor Desensitization and Endocytosis in Morphine Tolerance and Dependence.* Current Opinion in Neurobiology, 2007. **17**(5): p. 556-564.
37. von Zastrow, M., *Regulation of Opioid Receptors by Endocytic Membrane Traffics: Mechanisms and Translational Implications.* Drug and Alcohol Dependence, 2010. **108**(3): p. 166-171.
38. Elliot, J., L. Guo, and J.R. Traynor, *Tolerance to Mu-opioid Agonists in Human Neuroblastoma SH-SY5Y Cells as Determined by Changes in Guanosine-5'-O-(3-[35S]-thio)triphosphate Binding.* British Journal of Pharmacology, 1997. **121**(7): p. 1422-1428.
39. Alt, A., et al., *Mu and Delta Opioid Receptors Activate the Same G Proteins in Human Neuroblastoma SH-SY5Y Cells.* British Journal of Pharmacology, 2002. **135**(1): p. 217-225.
40. Alvarez, V.A., et al., *Mu Opioid Receptors: Ligand Dependent Activation of Potassium Conductance, Desensitization, and Internalization.* Journal of Neuroscience, 2002. **22**: p. 5769-5776.
41. Von Zastrow, M., D.E. Keith, and C.J. Evans, *Agonist-induced State of the Delta Opioid Receptor that Discriminates Between Opioid Peptides and Opiate Alkaloids.* Molecular Pharmacology, 1993. **44**(1): p. 166-172.
42. Keith, D.E., et al., *Morphine Activates Opioid Receptors without Causing their Rapid Internalization.* Journal of Biological Chemistry, 1996. **271**(32): p. 19021-19024.
43. Sternini, C., et al., *Agonist Selective Endocytosis of the Mu Opioid Receptor by Neurons in vivo.* Proc Natl Acad Sci USA, 1996. **93**(17): p. 9241-9246.
44. Koch, T., et al., *C-terminal Splice Variants of the Mouse Mu Opioid Receptor Differ in Morphin-induced Internalization and Receptor Desensitization.* Journal of Biological Chemistry, 2001. **276**(3): p. 31408-31412.
45. Traynor, J.R. and J. Elliot, *Delta Opioid Receptor Subtypes and Cross-talk with Mu Receptors.* Trends in Pharmacological Sciences, 1993. **14**(3): p. 84-86.
46. Abdelhamid, E.E., et al., *Selective Blockage of the Delta Opioid Receptors Prevents the Development of Morphine Tolerance and Dependence in Mice.* The Journal of Pharmacology and Experimental Therapeutics, 1991. **258**(1): p. 299-301.
47. Fundytus, M.E., et al., *Attenuation of Morphine Tolerance and Dependence with the Highly Selective d-Opioid Receptor antagonist TIPP (psi).* European Journal of Pharmacology, 1995. **286**(1): p. 105-8.
48. Hepburn, M.J., et al., *Differential Effects of Naltrindole on Morphine-Induced Tolerance and Physical Dependence in Rats.* Journal of Pharmacology and Experimental Therapeutics, 1997. **281**(3): p. 1350-6.
49. Miyamoto, Y., P.S. Portoghese, and A.E. Takemori, *Involvement of the Delta 2 Opioid Receptors in Acute Dependence on Morphin in Mice.* Journal of Pharmacology and Experimental Therapeutics, 1993. **265**(3): p. 1325-1327.
50. Kest, B., et al., *An Antisense Oligodeoxynucleotide to the Delta Opioid Receptor (DOR-1) Inhibits Morphine Tolerance and Acute Dependence in Mice.* Brain Research Bulletin, 1996. **39**(3): p. 185-8.
51. Zhu, Y., et al., *Retention of Supraspinal Delta-like Analgesia and Loss of Morphine Tolerance in d Opioid Receptor Knockout Mice.* Neuron, 1999. **24**: p. 243-52.

52. Cahill, C.M., S.V. Holdridge, and A. Morinville, *Trafficking of the Delta Opioid Receptors and other G Protein-Coupled Receptors: Implications for Pain and Analgesia.* Trends in Pharmacological Sciences, 2007. **28**(1): p. 23-31.
53. Dunham, J.H., Hall, R. A., *Enhancement of the surface expression of G protein-coupled receptors.* Trends in Biotechnology, 2009. **27**(9): p. 541-545.
54. Cvejic, S. and L.A. Devi, *Dimerizatoin of the delta-Opioid Receptor: Implication for a Role in Receptor Internalization.* Journal of Biological Chemistry, 1997. **272**: p. 26959-26964.
55. Wang, H.-B., et al., *Co-expression of the Delta and My Opioid Receptors in Nociceptive Sensory Neurons.* Proceedings of the National Academy of Science, 2010. **107**(29): p. 13117-13122.
56. Peng, J., S. Sarkar, and S.L. Chang, *Opioid Receptor Expression in Human Brain and Peripheral Tissues using Absolute Quantitative Real-Time RT-PCR.* Drug and Alcohol Dependence, 2012. **124**: p. 223-228.
57. Liu, N.-J., et al., *Cholecystokinin Octapeptide Reverses Mu-Opioid-Receptor Mediated Inhibition of Calcium Current in Rat Dorsal Root Ganglion Neurons.* The Joural of Pharmacology and Experimental Therapeutics, 1995. **275**(3): p. 1293-1299.
58. Li, Y., et al., *Opioid Glycopeptide Analgesics Derived from Endogenous Enkephalins and Endorohins.* Future Medicinal Chemistry, 2012. **4**(2): p. 205-226.
59. Lowery, J.J., et al., *In Vivo Characherization of MMP-2200, a Mixed Mu/Delta Opioid Agonist, in Mice.* The Journal of Pharmacology and Experimental Therapeutics, 2011. **336**: p. 767-778.
60. Rozenfeld, R., et al., *An Emerging Role for the Delta Opioid Receptor in the Regulation of Mu Opioid Receptor Function.* Science World Journal, 2007. **7**: p. 4-73.
61. Heyman, J.S., et al., *Modulation of Mu Mediated Antinociception by Delta Agonists in the Mouse: Selective Potentiation of Morphine and Normorphine by [DPen2,DPen5]enkephalin.* European Journal of Pharmacology, 1989. **165**: p. 1-10.
62. Heyman, J.S., et al., *Modulation of Mu-Mediated Antinociception by Delta Agonists: Characterization with Antagonists.* European Journal of Pharmacology, 1989. **169**: p. 43-52.
63. Horan, P., et al., *Antinociceptive Interactions of Opioid Delta Receptor Agonists with Morphine in Mics: Supra- and Sub-Additivity.* Life Sciences, 1992. **50**: p. 1535-1541.
64. Morphy, R., C. Kay, and Z. Rankovic, *From Magic Bullets to Designed Multiple Ligands.* Research Focus Reviews, 2004. **9**(15): p. 641-652.
65. Morphy, R. and Z. Rankovic, *Designing Multiple Ligands - Medicinal Chemistry Strategies and Challenges.* Current Pharmaceutical Design, 2009. **15**(6): p. 587-600.
66. Dietis, N., et al., *Simultaneous Targeting of Multiple Opioid Receptors: A Strategy to Improve Side-effect Profile.* British Journal of Anaesthesia, 2009. **103**(1): p. 38-49.
67. Balboni, G., et al., *Evaluation of the Dmt-Tic Pharmacophore: Conversion of a Potent Delta-opioid Receptor Antagonist into a Potent Delta Agonist and Ligands with Mixed Properties.* Journal of Medicinal Chemistry, 2002. **45**: p. 713-720.
68. Balboni, G., et al., *Further Studies on the Effect of Lysine at the C-terminus of the Dmt-Tic Opioid Pharmacophore.* Bioorganic and Medicinal Chemistry 2007. **15**: p. 3143-3152.

69. Ananthan, S., *Opioid Ligands with Mixed u/d Opioid Receptor Interactions: An Emerging Approach to Novel Analgesics.* The American Association of Pharmaceuctical Sciences Journal, 2006. **8**(1): p. 118-125.
70. Anathan, S., et al., *Synthesis, Opioid Receptor Binding, and Biological Activities of Naltrexone-derived Pyrido- and Pyrimidomorphans.* Journal of Medicinal Chemistry, 1999. **42**: p. 3527-3538.
71. Anathan, S., et al., *Identification of Opioid Ligands Possessing Mixed Mu Agonist/Delta Antagonist Activity Among Pyridomorphans Derived from Naloxone, Oxymorphone, and Hydromorphone.* Journal of Medicinal Chemistry, 2004. **47**: p. 1400-1412.
72. Purington, L.C., et al., *Pentapeptides Displaying Mu Opioid Receptor Agonist and Delta Opioid Receptor Partial Agonist/Antagonist Properties.* Journal of Medicinal Chemistry, 2009. **52**: p. 7724-7731.
73. Purington, L.C., et al., *Development and in Vitro Characterization of a Novel Bifunctional Mu-Agonist/Delta-Antagonist Opioid Tetrapeptide.* Journal of Chemical Biology, 2011. **6**: p. 1375-1381.
74. Schiller, P.W., et al., *The TIPP Opioid Peptide Family: Development of detla Antagonists, delta Agonists, and Mixed mu Agonist/ delta Antagonists.* Biopolymers (Peptide Synthesis), 1999. **51**: p. 411-425.
75. Yamamoto, T., et al., *A Structure-Activity Relationship Study and Combinatorial Synthetic Approach to C-Terminal Modified Bifunctional Peptides that are Delta/Mu Opioid Receptor Agonists and Neurokinin 1 Receptor Antagonists.* Journal of Medicinal Chemistry, 2008. **51**: p. 1369-1376.
76. Daniels, D.J., et al., *Opioid Induced Tolerance and Dependence in Mice is Modulated by the Distance Between Pharmacophores in a Bivalent Ligand Series.* Proc Natl Acad Sci USA, 2005. **102**(52): p. 19208-19213.
77. Portoghese, P.S., *Bivalent Ligands and the Message-Address Concept in the Design of Selective Opioid Receptor Antagonists.* Trends in Pharmacological Sciences, 1989. **10**(6): p. 230-235.

CHAPTER 2

Cyclic Mixed Efficacy Ligands

2.1 Introduction

The recognition that a specific receptor often plays a pivotal role in a disease state shifted the drug discovery paradigm toward a "one disease, one target" approach. The driving force behind this shift was the idea that the more specific a drug, the fewer negative side effects it will elicit. However, it has since been recognized that the simultaneous modulation of multiple targets often generates a more desirable drug profile, in some cases even reducing the development of negative side effects [1-3]. As described in Chapter 1.3, this concept is illustrated in the field of opioid analgesics, where the co-administration of a mu opioid receptor (MOR) agonist with a delta opioid receptor (DOR) antagonist provides all the expected analgesia of a MOR agonist, but with reduced negative side effects, especially reduced tolerance and dependence liabilities [4-8], features that limit the clinical use of opioid analgesics [10]. As a result, the idea of bifunctional mixed efficacy ligands displaying MOR agonism/DOR antagonism has been the source of much investigation, both as leads for new analgesics and as tools to illuminate the mechanism(s) by which DOR ligands influence the development of MOR tolerance.

Our lab and others [7, 8, 10-18] have explored the development of bifunctional mixed efficacy ligands where MOR agonist activity is combined with DOR antagonism in the same molecule using a "merged" pharmacophore [2]. Such a multifunctional ligand would possess considerable advantages over the traditional approach of using a combination of selective opioid drugs with possibly differing pharmacokinetic or pharmacodynamic properties, as described in Chapter 1.4. Peptides provide a convenient starting point for the development of multifunctional opioid ligands. The synthetic ease with which peptide sequences may be altered and the wealth

of knowledge about opioid peptide structure-activity relationships provide the foundation for applying structure based design to existing compounds directed toward exploring the MOR and DOR binding pockets. In addition, peptides are generally larger molecules and make many contacts within the binding pocket; this allows for multiple sites of alteration to fine tune the binding and efficacy profiles of the resultant ligands to achieve balanced binding to both receptors and full MOR efficacy and functional DOR antagonism. Previous work in our lab resulted in a lead peptide **MP-143** (MP compounds were synthesized by Maggie Przydzial) with a linear sequence of Tyr-DCys-Phe-Phe-Cys-NH_2, cyclized through a disulfide bridge between the D-Cys in position 2 and the L-Cys in position 5, hereafter denoted with c(S-S) with the cyclized residues in square brackets (e.g. Tyr-c(SS)[DCys-Phe-Phe-Cys]NH_2) [20]. Peptide **MP-143** displays full agonism[2] at MOR and slightly reduced efficacy at DOR as well as high affinity for both receptors (**Table 2.1**). Since **MP-143** has appreciable DOR efficacy, we then focused our efforts on designing ligands that retain MOR agonist activity, but with reduced stimulation of DOR [7]. Using our receptor models for both active, or agonist binding, and inactive, or antagonist binding, states of MOR and DOR [7, 10, 21-25] we predicted that adding bulky aromatic substituents in the third or fourth position of peptide **MP-143** would produce a steric clash in the DOR active state binding site which would not be seen in the DOR inactive site, thus favoring binding to the DOR inactive state and consequently resulting in lower DOR efficacy [7]. Docking to corresponding active and inactive state MOR models revealed no analogous receptor state-specific adverse interactions; we therefore predicted that increasing steric bulk at position 3 or 4 would provide the desired MOR agonist/DOR antagonist profile. It is important to note that these models of the active and inactive conformations of the opioid receptors are based on crystal structures of antagonist bound receptors; there are no crystal structures for the active conformations of the opioid receptors. More detail can be found in *Section 2.5.8*.

Incorporation of 1-Nal (1-naphthylalanine) or 2-Nal (2-naphthylalanine) into position 3 or 4 of **MP-143** did indeed yield analogs with high MOR/ low DOR efficacy, but all analogs also retained high kappa opioid receptor (KOR) affinity [7]. Such KOR activity is less than desirable; while KOR agonists are known to be effective against mild pain, they are also known to cause dysphoria and other psychomimetic effects, which severely limits their usefulness [26]. The

[2] N.B. In this work "agonism" and "efficacy" refer to the ability of compounds to stimulate G protein turnover in the GTPγS assay. Details can be found in *Section 2.5.7*.

compounds discussed in this chapter make further use of our receptor-ligand models to design analogues that maintain high affinity for both MOR and DOR, but not KOR, and display full MOR agonism and DOR antagonism.

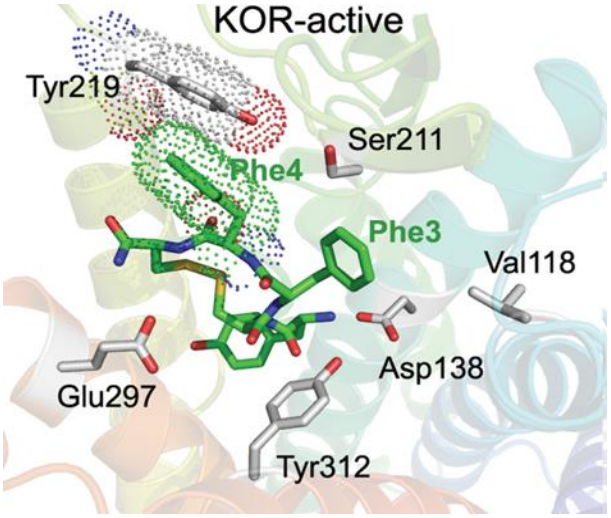

Figure 2.1: Modeling of peptide MP143 in the KOR Active Site – MP143 (Tyr-c(S-S)[DCys-Phe-Phe-Cys]NH_2) docked in the KOR active state model. Highlighted is the π-π interaction between Phe^4 of **MP143** with Tyr^{219} of KOR (shown by dots). This favorable interaction appears to contribute to the high affinity of **MP143** for KOR as well as its agonist character.

2.2 Development Cyclic Pentapeptide MOR Agonist/DOR Antagonist Ligands

To understand the basis for the relatively high KOR binding affinity of **MP-143** and related compounds in the series [20] we docked **MP-143** to our previously developed active state model of KOR [25, 27]. The docking suggested an important role for Phe^4 of **MP-143** in interacting with KOR. An improved active state model generated from the recently released crystal structure of KOR [28] demonstrates that Phe^4 of **MP-143** indeed can form π-π stacking interactions in the KOR active site with Tyr^{219} from extracellular loop 2 located at the beginning of helix 5 (**Figure 2.1**). These interactions likely contribute to the binding and agonist character

Table 2.1: Non-Aromatic Phe^4 Replacements in Cyclic Mixed Efficacy Pentapeptides

Sequence		Binding (nM)			Efficacy					
					MOR		DOR		KOR	
		MOR	DOR	KOR	%	EC50 (nM)	%	EC50 (nM)	%	EC50 (nM)
MP143	Tyr(SS)[DCys-Phe-Phe-Cys]NH2	0.3± 0.2	0.8± 0.3	8.6±0.5	77±9	1.4 ± 0.8	69± 1.6	45 ± 9	80± 4	74 ±17
LP-26	Tyr(SS)[DCys-Phe-Leu-Cys]NH2	1.3±0.7	2.0±0.8	>1000	100± 0.5	9.6 ± 4.2	74±13	6.4±3.8	dns	nd
LP-29	Tyr(SS)[DCys-Phe-Ile-Cys]NH2	1.5±0.7	0.3± 0.2	>1000	93±4	3.0±0.6	86±7	2.6±0.1	dns	nd
LP-09	Tyr(SS)[DCys-Phe-Nle-Cys]NH2	1.6±0.1	1.7± 0.3	>1000	100±10	nd	103±1.5	nd	nd	nd
LP-08	Tyr(SS)[DCys-Phe-Nle-DCys]NH2	0.6±0.1	1.3±0.4	>1000	64±6	nd	47±9	nd	nd	nd

Binding affinities (K_i) were obtained by competitive displacement of radiolabeled [^{3}H] diprenorphine. Efficacy data were obtained using [^{35}S] GTPγS binding assay. Efficacy is represented as percent maximal stimulation relative to standard agonists DAMGO (MOR), DPDPE (DOR) or U69,593 (KOR) at 10μM concentrations. All values are expressed as mean ± SEM of three separate assays performed in duplicate. Cyclization abbreviated as SS for disulfide linkage, nd = not determined, dns = does not stimulate.

of peptide **MP-143**. DOR and MOR lack a corresponding aromatic residue in the binding site – DOR has a Ser^{206} and MOR has a Thr^{225} in the analogous position. We hypothesized that changing the Phe^4 of peptide **MP-143** to a non-aromatic hydrophobic residue would eliminate this favorable aromatic interaction with Tyr^{219} and thus decrease affinity to KOR. As shown in **Table 2.1**, replacing Phe^4 of peptide **MP-143** with the aliphatic residues Leu, Ile, or Nle resulted in the predicted decreased binding to KOR (**Table 2.1**).

As all three analogues with an aliphatic residue in position 4 displayed similar opioid profiles, high affinity and efficacy for MOR and DOR with low KOR activity, we chose, for convenience, to carry forward analogs containing the Nle^4 substitution. Since cyclic opioid pentapeptides with either D- or L-stereochemistry in residue 5 displayed similar MOR and DOR affinities in the initial examples of this series [20], we also examined the opioid profile of **LP-08**, the $D\text{-}Cys^5$ diastereomer of **LP-09** (LP compounds were synthesized by Lauren Purington). This analog displayed a similar binding profile as **LP-09**, but with somewhat reduced efficacy at both MOR and DOR (**Table 2.1**). Thus, we chose both **LP-09** and **LP-08** as starting points for modifications to reduce DOR efficacy.

To achieve this, we again relied on our previously described receptor models [7, 10, 21-25] that suggested that bulkier aromatic side chains replacing Phe^3 or Phe^4 of the ligands would better fit the large and more open antagonist binding pocket of the receptors in the inactive state, while having steric clashes in the more narrow agonist binding pocket of

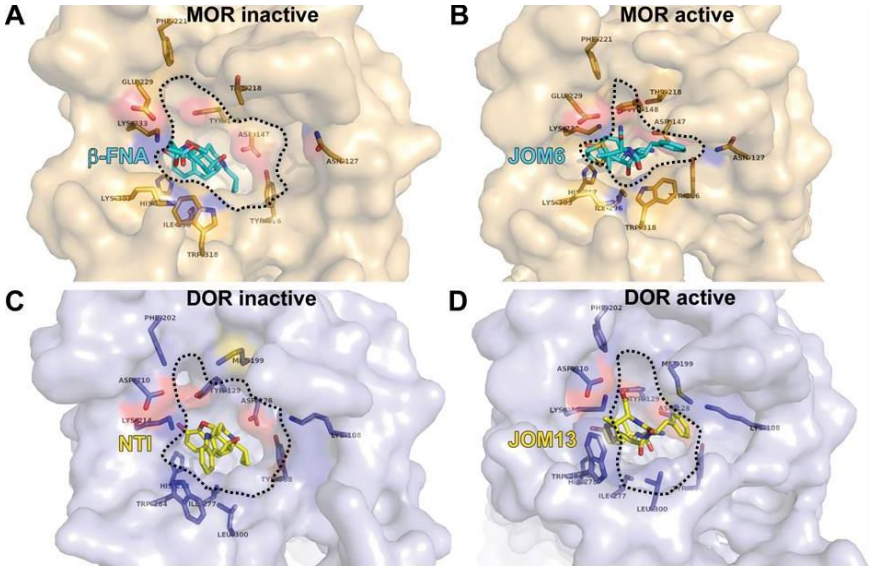

Figure 2.2: Modeling of the Inactive and Active Conformations of MOR and DOR – (A) the inactive conformation of MOR bound to the MOR antagonist β-Funaltrexamine, **(B)** the active conformation of MOR bound to the MOR agonist JOM6 [9], **(C)** the inactive conformation of DOR bound to the DOR antagonist naltrindole, **(D)** the active conformation of DOR bound to the DOR agonist JOM13 [19]. The edges of the binding pockets are shown with dashed lines. For both MOR and DOR the active conformation of the receptor is narrower than the inactive conformation.

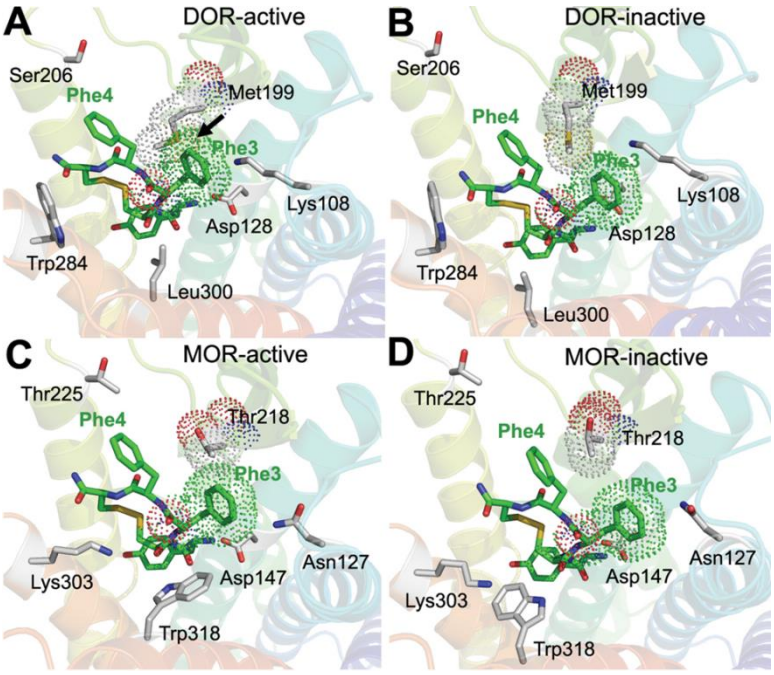

Figure 2.3: Modeling of MP143 in the MOR and DOR Active and Inactive Binding Pockets – MP143 (Tyr-c(S-S)[DCys-Phe-Phe-Cys]NH_2) docked in the active and inactive state models of DOR (**A** and **B**) and MOR (**C** and **D**). Docking of **MP143** to the active state of DOR shows a steric clash between Phe^3 of **MP143** and Met^{199} of DOR, highlighted by an arrow in **2A**; this steric clash is not seen when **MP-143** is docked in the DOR inactive state binding site or the MOR active or inactive state binding sites.

the active receptor conformation (**Figure 2.2**). A greater effect was expected for DOR which has more bulky residues – Lys^{108}, Met^{199}, and Trp^{284} – occluding the ligand binding pocket than MOR – Asn^{127}, Thr^{218} and Lys^{303} – at the corresponding positions. Examination of our current, refined models of DOR and MOR in complex with **MP-143** supported our previous suggestions (**Figure 2.3**). Of particular importance here is the observation that Phe^3 of peptide **MP-143** is in close proximity to Met^{199} in the DOR agonist binding pocket. (**Figure 2.2A**) However, in the DOR antagonist binding conformation (**Figure 2.2B**), Met^{199} is angled away from the ligand, enlarging the binding pocket. Replacing the Phe^3 of peptide **MP-143** with a larger residue would be expected to increase the steric clash between the ligand and the active conformation of DOR, disfavoring the binding of the ligand to the active conformation and thus reducing its agonist character, as we have observed before [10]. However, due to the presence of the smaller side chain of Thr^{218} in the MOR binding pocket (**Figure 2.2C**) instead of Met^{199} in the DOR binding pocket, adding steric bulk in the 3 position of peptide **MP-143** should have less of an effect on MOR efficacy. Consequently, we prepared and pharmacologically assessed a series of pentapeptides based on **LP-09** and **LP-08**, in which the Phe^3 residue was replaced by 1-Nal or 2-Nal, increasing steric bulk at the third position (**Table 2.2**).

The 1-Nal^3 and 2-Nal^3 analogs of **LP-08** and **LP-09** were synthesized and are shown in **Table 2.2**; replacing the Phe^3 of **LP-08** or **LP-09** with 2-Nal (analogues **LP-17** and **LP-21**) greatly reduces efficacy at both MOR and DOR, consistent with our earlier observations [7],

Table 2.2: Bulky Aromatic Phe[3] Replacements in Cyclic Pentapeptides

	Sequence	Binding (nM)			Efficacy					
					MOR		DOR		KOR	
		MOR	DOR	KOR	%	EC50 (nM)	%	EC50 (nM)	%	EC50 (nM)
LP-21	Tyr(SS)[DCys-2Nal-Nle-Cys]NH2	2.4±1.3	240±70	>1000	25±1	nd	32±11	nd	dns	nd
LP-19	Tys(SS)[DCys-2Nal-Nle-DCys-]NH2	2.1±0.9	>1000	>1000	9.3±0.9	nd	dns	nd	dns	nd
JPAM3 (SS)	Tyr(SS)[DCys-1Nal-Nle-Cys]NH2	0.7±0.3	12±2.7	730±330	100±2	5.1±1.4	22±0.9	160± 70	<10	nd
JPAM2 (SS)	Tyr(SS)[DCys-1Nal-Nle-DCys]NH2	1.4±0.3	56±2.5	>1000	43.0±2.7	17.5±5.0	dns	nd	<10	nd
JPAM3 (SEtS)	Tyr(SEtS)[DCys-1Nal-Nle-Cys]NH2	1.3±0.1	37.0±1.5	180±90	51±6	8.3±1.3	24±1	440±110	<10	nd
JPAM2 (SEtS)	Tyr(SEtS)[DCys-1Nal-Nle-DCys]NH2	1.4±0.4	23± 2.9	770±140	30.5±1.2	34±13	dns	nd	<10	nd
LP-32	Tyr(SS)[DCys-1Nal-Nle-Cys]OH	4±2	11±3	>5000	94±1	3.4± 0.8	17±2	nd	30±8	nd
JPAM1 (SS)	Tyr(SS)[DCys-1Nal-Nle-DCys]OH	2.7±0.3	4.0±0.5	>5000	dns	nd	dns	nd	dns	nd
JPAM4 (SEtS)	Tyr(SEtS)[DCys-1Nal-Nle-Cys]OH	8.6±1.4	58±8	>1000	47±4	36±5	11±8	300 ±100	nd	nd
JPAM1 (SEtS)	Tyr(SEtS)[DCys-1Nal-Nle-DCys]OH	3.1± 0.04	29±4	>1000	38.6 ± 3.4	25±13	7.3±1.4	64±8	nd	nd

Binding affinities (K_i) were obtained by competitive displacement of radiolabeled [^{3}H] diprenorphine. Efficacy data were obtained using [^{35}S] GTPγS binding assay. Efficacy is represented as percent maximal stimulation relative to standard agonists DAMGO (MOR), DPDPE (DOR) or U69,593 (KOR) at 10μM concentrations. All values are expressed as mean ± SEM of three separate assays performed in duplicate. Cyclization abbreviated as SS for disulfide linkage and SEtS for an ethylene dithioether linkage, nd = not determined, dns = does not stimulate.

while also greatly reducing affinity at DOR. By contrast, the 1-Nal[3] analogues **JPAM3 (SS)** and **JPAM2 (SS)** display a more promising profile in which DOR efficacy is more selectively affected and DOR affinity is less drastically reduced. In these analogues the DCys[5] diastereomer exhibits a greater ability to reduce efficacy than the corresponding LCys[5], but this effect is equally expressed at MOR and DOR.

In compounds **JPAM3 (SEtS)** and **JPAM2 (SEtS)** we examined the effect of increasing the ring size of the 14-membered disulfide scaffold of **JPAM3 (SS)** and **JPAM2 (SS)** to a 16-membered ethylene dithioether-containing cycle, an approach we have often used to modulate opioid activity [7, 20, 27]. In the present case increasing the cycle size had little effect on binding affinity or efficacy, with the exception of a rather large reduction in maximal stimulation at MOR (51% vs. 100% stimulation relative to the standard, DAMGO) and a slight increase in KOR affinity displayed by **JPAM3 (SEtS)** compared to **JPAM3 (SS)**.

Of these analogues, the most promising is **JPAM3 (SS)** which possesses high MOR affinity, full agonist behavior at MOR in this assay and greatly reduced DOR efficacy (22% of DOR standard DPDPE). Furthermore, **JPAM3 (SS)** lacks the undesired KOR activity, which makes it a promising ligand for the exploration of functional MOR/DOR interactions. However **JPAM3 (SS)** displays ~18 fold lower affinity at DOR compared to MOR. The C-terminal carboxylic acid analogues of the carboxamide terminal peptides described above were designed to restore a balance in MOR and DOR affinity, as negatively charged C-terminal groups often interfere with MOR binding [29]. As seen in **Table 2.2**, the carboxy-terminal analogs displayed the expected decrease in MOR affinity, decreased KOR affinity, but little significant effect on DOR binding. Peptide **JPAM1 (SS)** was an exception, in that DOR affinity improved approximately 14-fold compared with **JPAM2 (SS)** (K_i = 4 nM vs. 56 nM). Both disulfide-containing, C-terminal carboxylic acids, **LP-32** and **JPAM1 (SS)**, display the desired binding profile: high affinity for MOR and DOR, low affinity for KOR. The dithioether-containing analogs, **JPAM4 (SEtS)** and **JPAM1 (SEtS)** have less desirable binding profiles displaying somewhat lower and/or less balanced MOR and DOR affinity and reduced MOR efficacy.

Examination of the efficacy profiles of **LP-32** and **JPAM1 (SS)** reveals an interesting observation. While **LP-32**, like its carboxamide terminal counterpart **JPAM3 (SS)**, is a full agonist at MOR, with low partial DOR agonism (~20% maximal stimulation vs. DPDPE), peptide **JPAM1 (SS)**, which differs from **LP-32** only in the stereochemistry of the C-terminal Cys, acts as an antagonist at both MOR and DOR. Reduced efficacy of $DCys^5$ vs $LCys^5$-containing analogs is a consistent feature among the compounds shown in **Table 2.2**; however the complete elimination of MOR efficacy for **JPAM1**

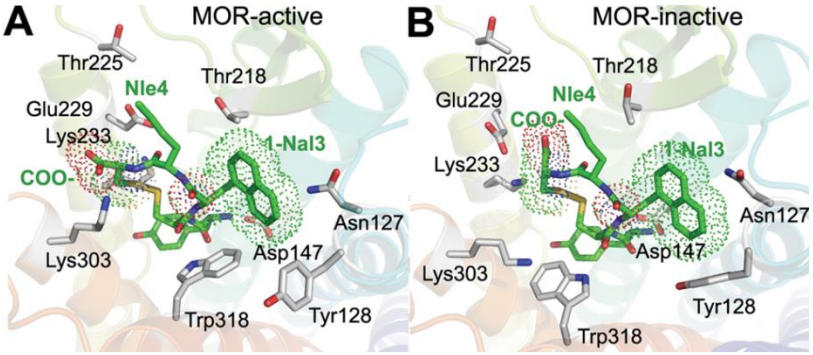

Figure 2.4: Comparison of LP-32 and JPAM1 (SS) in the MOR Active and Inactive Binding Sites – (**A**) **LP32** (Tyr-c(SS)[DCys-1-Nal-Nle-Cys]OH) docked in the active state model of MOR and (**B**) **JPAM1 (SS)** (Tyr-c(SS)[DCys-1-Nal-Nle-DCys]OH) docked in the inactive state model of MOR. The C-terminal COO- of **LP-32** forms a favorable ionic interaction with Lys^{303}. However, when **JPAM1 (SS)** is docked in the active site the C-terminal COO- is angled toward Glu^{229}, resulting in an unfavorable repulsion (not shown); in the inactive state, rotation of Glu^{229} and Lys^{233} relieves this repulsion and allows a favorable interaction with Lys^{233}.

(SS) was unexpected. An explanation for this behavior can be deduced from examination of **LP-32** and **JPAM1 (SS)** docked to the active and inactive states of MOR. **Figure 2.4A** depicts **LP-32** bound to our model of the MOR active receptor. In this model, the C-terminal COO^- of **LP-32**, while being close to Glu^{229} from transmembrane helix 5, may also form an ionic bridge with the positively charged side chain of Lys^{303} from helix 6. This ionic bridge can be formed only in MOR and only in the active conformation, but not in DOR or KOR which have Trp^{284} (DOR) or Glu^{297} (KOR) in the corresponding position in helix 6. The favorable ionic interactions of **LP-32** in the agonist binding pocket of MOR may explain its behavior as an efficacious MOR agonist. The unfavorable ionic interaction between the C-terminal carboxylate of **LP-32** and Glu^{229} from helix 5 in MOR or Glu^{297} from helix 6 in KOR is consistent with the 6- and 7-fold decreased affinity of **LP-32** to MOR and KOR, respectively, as compared to **JPAM2 (SS)** with a C-terminal amide. For **JPAM1 (SS)**, the change in stereochemistry of residue 5 orients the terminal COO^- away from Lys^{303} and toward Glu^{229}, resulting in an unfavorable ionic repulsion. However, in the inactive conformation of MOR (**Figure 2.4B**) rotation of Glu^{229} and Lys^{233} relieve this repulsion. In the DOR models the C-terminus of **JPAM1 (SS)** is close to the Asp^{210}-Lys^{214} pair from helix 5 and can form favorable ionic interactions with Lys^{214} in the inactive receptor conformation. These ligand-receptor interactions help explain the antagonist activity of **JPAM1 (SS)** in MOR and its improved binding and antagonist activity at DOR.

Two of the ligands described in this series, **JPAM3 (SS)** and **LP-32**, displayed nanomolar binding to both MOR and DOR with selectivity relative to KOR. These ligands displayed high efficacy at MOR with reduced DOR efficacy, making progress towards achieving our goal of developing a potent mixed efficacy MOR agonist/DOR antagonist ligand. Both ligands, however, display appreciable DOR agonist character and a slight preference for binding to MOR over DOR. We next sought to further reduce this DOR agonist activity and to balance the binding between MOR and DOR by exploring a new tetrapeptide scaffold.

2.3 Development Cyclic Tetrapeptide MOR Agonist/DOR Antagonist Ligands

Previous work in our lab generated a series of cyclic tetrapeptide ligands which display MOR agonist and DOR antagonist character, with low nanomolar affinities for both receptors. This series is similar to the pentapeptide series described above in that it is composed of cyclic ligands with hydrophobic residues between the bridging thiol containing amino acids. However,

Table 2.3: Development of Bioactive Cyclic MOR Agonist/DOR Antagonist Ligands

Sequence		Binding (nM)			Efficacy					
					MOR		DOR		KOR	
		MOR	DOR	KOR	%	EC50 (nM)	%	EC50 (nM)	%	EC50 (nM)
KSK102	Dmt(SEtS)[DCys-Aci-DPen]NH2	0.6±0.1	0.9±0.2	10±4	58±8	0.4±0.02	37±4	1.4±0.4	dns	nd
JPAM22 (SMeS)	Dmt(SMeS)[DCys-Aci-DPen]NH2	1.33±0.06	12±1	332±28	21.5± 0.4	41±6	dns	nd	dns	nd
VRP26	Dmt(SEtS)[DCys-Aci-DPen]Ser(Glc)-NH2	4.7 ± 0.3	4.7 ± 0.1	810 ± 160	55 ± 7	15 ± 5	2.6±1.4	56±37	nd	nd

Binding affinities (K_i) were obtained by competitive displacement of radiolabeled [^{3}H] diprenorphine. Efficacy data were obtained using [^{35}S] GTPγS binding assay. Efficacy is represented as percent maximal stimulation relative to standard agonists DAMGO (MOR), DPDPE (DOR) or U69,593 (KOR) at 10μM concentrations. All values are expressed as mean ± SEM of three separate assays performed in duplicate. Cyclization abbreviated as SMeS for methylene dithioether linkage and SEtS for an ethylene dithioether linkage, nd = not determined, dns = does not stimulate.

in place of DCys^5 in the pentapeptide series described above, ligands in this series contain a D-penicillamine (DPen) and one less residue within the cycle (**Table 2.3**). One of the ligands in this series, **KSK-102**, displayed well balanced MOR and DOR binding, with moderate efficacy at MOR and slightly reduced efficacy at DOR. Because of its promising profile, **KSK-102** has been modified with a C-terminal β-glucoserine, in which the side chain hydroxyl of Ser is covalently O-linked to a β-glucose, hereafter referred to as "glucoserine" (**VRP-26**). This modification was made to improve stability and bioavailability after peripheral administration [30-32]. (KSK compounds were synthesized by Katarzyna Sobczyk-Kojiro and VRP compounds were synthesized by Vanessa Porter-Barrus) While the addition of a glucoserine reduced MOR and DOR affinity somewhat, it also improved the overall *in vitro* drug profile in two key ways: it drastically improved selectivity relative to KOR and significantly reduced DOR efficacy, rendering the ligand a DOR antagonist. We have tested **VRP-26** in the warm water tail withdrawal assay in mice (data not shown); **VRP-26** produced dose-dependent antinociception after peripheral administration, demonstrating that it is able to cross membranes to reach its site of action in the CNS.

VRP-26 provides proof of concept that our potent mixed efficacy opioid ligands are effective at producing antinociception after peripheral administration. These ligands address the problems of residual DOR efficacy and unbalanced MOR/DOR binding found in the pentapeptide series described above. There is, however, room for improvement in the ability of these ligands to stimulate MOR; **VRP-26** only displays partial agonist behavior at MOR, a more

efficacious agonist with similar potency would likely require smaller doses to achieve the same analgesic effect, further limiting the development of tolerance and dependence, as these negative adaptations occur in a dose dependent manner. I therefore designed and synthesized a series of analogues containing various aromatic residues in the third position cyclized through either a methylene or ethylene dithioether bridge (**Table 2.3**).

As described above in Chapter 2.2, we have utilized our homology models to approximate how a representative cyclic ligand, **MP-143**, fits in the active and inactive sites of MOR and DOR. We found that the active sites of both MOR and DOR are narrower than their inactive counterparts, and that increased steric bulk reduces efficacy, with a greater effect seen at DOR than MOR. We hypothesized that the hydrophobic bulk and conformational restriction of Aci in **KSK-102** and **VRP-26** played a role in the decreased efficacy at MOR; the conformational restriction of Aci kinks the peptide backbone of **KSK-102** somewhat and likely

Table 2.4: Flexible Hydrophobic Aci[3] Replacements in Cyclic Tetrapeptides

Sequence		Binding (nM)			Efficacy					
					MOR		DOR		KOR	
		MOR	DOR	KOR	%	EC50 (nM)	%	EC50 (nM)	%	EC50 (nM)
JPAM10 (SEtS)	Dmt(SEtS)[DCys-1Nal-DPen]NH2	0.22±0.06	0.4±0.2	1.5±0.2	68± 6	0.14 ±0.03	73±1	1.0±0.3	dns	nd
JPAM11 (SEtS)	Dmt(SEtS)[DCys-2Nal-DPen]NH2	0.29±0.03	0.4±0.1	7.4±0.6	32±2	1.1±0.6	dns	nd	<10	nd
JH6	Tyr(SEtS)[DCys-Hfe-DPen]NH2	0.67±0.02	2.77±0.09	>1000	95 ± 4	4.7±0.9	22± 3	nd	nd	nd
JPAM13 (SEtS)	Dmt(SEtS)[DCys-Hfe-DPen]NH2	0.22±0.02	0.73±.0.04	7±1.8	21±2	27±2	18±3	9±7	<10	nd
JPAM13 (SMeS)	Dmt(SMeS)[DCys-Hfe-DPen]NH2	0.49±0.09	1.9±0.3	33±14	87±4	1.0±0.05	dns	nd	<10	nd
JPAM14 (SEtS)	Dmt(SEtS)[DCys-Idg-DPen]NH2	0.39±0.03	1.0±0.3	5.3±1.2	73±5	0.73±0.03	50±8	28±18	<10	nd
JPAM14 (SMeS)	Dmt(SMeS)[DCys-Idg-DPen]NH2	0.48±0.08	1.0±0.1	9.2±2	60±3	0.3±0.1	13±8	nd	dns	nd
JPAM18 (SEtS)	Tyr(SEtS)[DCys-Hfe-DPen]Ser(Glc)-NH2	4.7±1.3	4.2±0.3	>5000	86±5	440±70	25±3	200±95	dns	nd
JPAM19 (SMeS)	Dmt(SMeS)[DCys-Hfe-DPen]Ser(Glc)-NH2	1.8±0.1	2.38±0.05	79±6	30±2	30±7	32±2	34±10	15±3	nd

Binding affinities (K_i) were obtained by competitive displacement of radiolabeled [^{3}H] diprenorphine. Efficacy data were obtained using [^{35}S] GTPγS binding assay. Efficacy is represented as percent maximal stimulation relative to standard agonists DAMGO (MOR), DPDPE (DOR) or U69,593 (KOR) at 10μM concentrations. All values are expressed as mean ± SEM of three separate assays performed in duplicate. Cyclization abbreviated as SMeS for methylene dithioether linkage and SEtS for an ethylene dithioether linkage, nd = not determined, dns = does not stimulate.

makes it more difficult for it to fit into the narrower active conformation of MOR. I therefore replaced the Aci[3] of **KSK-102** with various bulky but flexible aromatic residues and then cyclized these linear sequences with either a methylene or ethylene dithioether bridge between the DCys[2] and DPen[5] side chains. By making both the methyl and ethyl bridged compounds we were able to further explore how the angle of the side chain in the third position and of the ligand as a whole in the active site affected binding and efficacy to MOR and DOR. The binding affinities and efficacies for this series are listed below in **Table 2.4**.

It is interesting to note that while the Tyr[1], Hfe[3], ethyl bridged analogue (**JH6**) displayed the desired profile, of the two Dmt[1], Hfe[3], analogues (**JPAM13**) it was the methyl bridged compound that displayed the desired profile (JH compounds were synthesized by Jeff Ho). To explain the large difference in MOR efficacies that relatively small changes in cycle size and steric bulk in the first position make, we again turned to our homology models. We found that the cycle size (methyl vs. ethyl bridged) greatly affects the angle of the side chain in the first position and that the added bulk of the two methyl groups in Dmt can produce a steric clash in the active site of MOR, reducing efficacy. When comparing **JH6**, **JPAM13 SMeS,** and **JPAM SEtS** we found that the first residue (Tyr[1] or Dmt[1]) is located between Tyr[148] and Ile[296] in MOR and that the distance between these residues is larger in the inactive conformation than in the active conformation of the receptor (**Figure 2.5**). In order to accommodate the extra bulk of the two methyl groups of Dmt[1] the ligand as a whole must tilt to fit into the narrower active site; as these ligands are conformationally restricted, the tilt of the Dmt[1] is determined by the cyclization. In **JPAM13 SMeS** and **JPAM13 SEtS**, tilt of Dmt[1] is different due to its interaction with

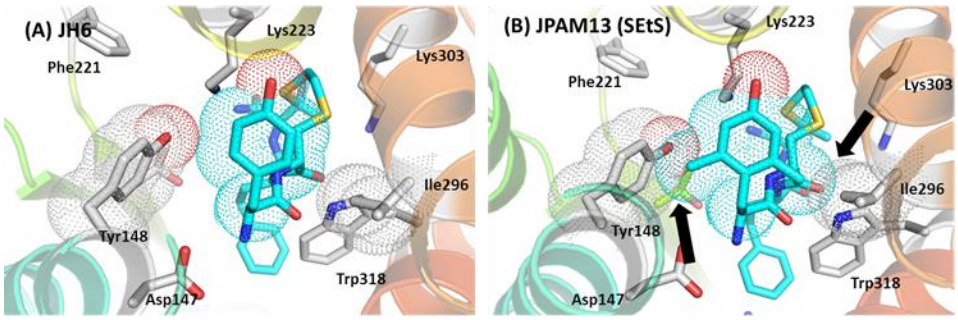

Figure 2.5: Comparison of JH6 and JPAM13 (SEtS) in the MOR Active Site – (**A**) **JH6** (Tyr-c(SEtS)[DCys-Hfe-DPen]NH_2) and (**B**) **JPAM(SEtS)** (Dmt-c(SEtS)[DCys-Hfe-DPen]NH_2) in th e active state model of MOR. The 2,6 methyl groups of Dmt[1] in **JPAM13 (SEtS)** clash with Tyr[148] and Ile[296] of MOR in the active conformation (highlighted with arrows). The steric clash reduces the affinity of **JPAM13 (SEtS)** for the active conformation of MOR, reducing its ability to stimulate the receptor.

SMeS or SEtS groups, respectively. The larger cycle size produces a steric clash in the active site of MOR between Dmt^1 of the ligand and Tyr^{148} of the receptor, reducing MOR efficacy, while the smaller cycle size allows the Dmt^1 to tilt such that it can fit in the MOR active site, granting higher efficacy. However, **JH6**, which contains a Tyr^1, has reduced steric bulk as compared to **JPAM13 SEtS**, and so there is less of a steric clash in the active conformation of the receptor, allowing for full MOR agonist behavior (**Figure 2.5**).

The most promising ligands, **JH6** and **JPAM13 (SMeS)** both contained a homo-phenylalanine (Hfe) residue as the aromatic amino acid in the third position. This fits with our hypothesis that a flexible but bulky side chain within the cyclized portion of the molecule would balance high MOR efficacy with low DOR efficacy, while preserving binding affinity at both receptors. As these ligands possess the desired binding and efficacy profiles, they present an opportunity to generate a bioavailable mixed efficacy peptide. I therefore modified both of these sequences with a C-terminal glucoserine to yield compounds **JPAM18 (SEtS)** and **JPAM19 (SMeS)**. Both of these glycosylated ligands displayed promising binding profiles, however, their efficacy profiles were less than ideal. **JPAM 19 (SMeS)** displayed partial agonism at both MOR and DOR and was discarded as a viable *in vivo* ligand. **JPAM18 (SEtS)** displayed full MOR agonism, but, unfortunately, also displayed partial DOR agonism and low potency at both receptors, unlike its unglycolsylated counterpart **JH6**. To more fully explore Hfe^3 analogues **JPAM18 (SMeS)** was also synthesized, but could not be tested due to solubility issues.

2.4 Conclusions

The studies discussed in this chapter were aimed toward developing opioid ligands that display high affinity and efficacy for MOR, high affinity and low efficacy for DOR and low affinity for KOR as tools for exploring MOR/DOR interactions and the development of tolerance to and dependence on opioid analgesics. Using our validated receptor models of the active and inactive states of all three receptors for structure-based design, we were able to achieve this goal by selectively modulating the affinity and efficacy of our lead peptide **MP-143**. First, examination of docking of the lead peptide, **MP-143**, to active state KOR suggested the participation of the ligand's Phe^4 residue in an aromatic $\pi-\pi$ interaction unavailable in MOR or DOR. Replacement of this Phe^4 with an aliphatic residue achieved the desired result of greatly reducing KOR affinity and efficacy. Next, predicted differences in ligand docking to the DOR

active and inactive conformations were exploited by incorporating bulkier residues in the third position of peptide **MP-143** to favor binding to the DOR inactive conformation. As predicted, the use of bulky aromatic groups within the cyclized portion of the peptide greatly reduced DOR efficacy. Of our pentapeptide analogs, **JPAM3 (SS)** and **LP-32** in particular, with 1-Nal[3], exhibited the desired profile of high MOR/ low DOR efficacy; among the tetrapeptide analogues those with a flexible Hfe residues in the third position, **JH6** and **JPAM13 (SMeS)**, displayed the desired binding and efficacy profiles *in vitro*. Unfortunately, the addition of a C-terminal glucoserine significantly altered the binding, efficacy, and potency of the resulting compounds, **JPAM18 (SEtS)** and **JPAM19 (SMeS)**. These ligands are being set aside for now, though future directions may include the exploration of other glycosylation alternatives which move the sugar away from the opioid pharmacophore, with the goal of maintaining the desired pharmacological profile. Such glycosylation alternatives may include using a lactose instead of a glucose, conjugation through a Thr as opposed to Ser, or extension of the sugar away from the main peptide either through a homo-serine or by incorporating Gly before the C-terminal glycosylated amino acid. Arginine and homo-arginine analogues of promising sequences will also be synthesized as a means of improving bioavailability, as Arg rich peptides also show improved membrane penetration [33]. Future work may also include Tyr[1] replacements to explore how the removal of the 2, 6 dimethyl groups of Dmt effect the efficacy of ligands in this series.

The wide range of affinity and efficacy shown by the closely related analogs in **Table 2.2** and **Table 2.3** reflects both the structural sensitivity of the ligand-receptor interaction and the utility of peptides, whose structures can be easily and subtly manipulated for probing the details of the ligand-receptor interaction. Of particular note is the profound functional difference observed for **LP-32** and **JPAM1 (SS)**, which differ only in stereochemistry of the C-terminal residue and which possess similar affinity, but quite different efficacy profiles. Similar effects can be seen the tetrapeptide series, as with **JPAM10 (SEtS)** and **JPAM11 (SEtS)** which differ only in the connectivity of the napthyl ring in the third position. This ligand pair also display similar binding profiles, but have profoundly different MOR and DOR stimulation.

The results reported here further validate our receptor models and our approach of using these models for rational design to exploit differences in the opioid receptors highly homologous binding pockets. We have demonstrated that we can successfully generate MOR agonist/DOR

antagonist ligands using information from our models and that we can fine tune our binding and efficacy profiles in predictable ways. While we have not generated a glycosylated ligand with which to explore *in vivo* activity in this series, we have designed several mixed efficacy tools which can be used to probe the *in vitro* pharmacology of tolerance.

The most promising ligands from this series will then be carried forward into *in vivo* studies. Literature precedent states that the co-administration of a MOR agonist with a DOR antagonist limits the development of tolerance, dependence, and self-administration, features that limit the clinical use of opioid analgesics [4-8], but we have not yet confirmed if our mixed efficacy ligands also display these desirable properties. We will, therefore, test the ability of our most promising mixed efficacy ligands to produce both acute and chronic tolerance, physical dependence, and conditioned place preference.

2.5 Methods and Materials

2.5.1 Materials

All reagents and solvents were purchased from commercial sources and used without further purification. All chemicals and biochemicals were purchased from Sigma Aldrich (St. Louis, MO, USA) or Fisher Scientific (Hudson, NH, USA), unless otherwise noted. All tissue culture reagents were purchased from Gibco Life Sciences (Grand Island, NY, USA). Radioactive compounds were purchased from Perkin-Elmer (Waltham, MA, USA). Peptide synthesis reagents, amino acids, and Rink resin were purchased from Advanced Chem Tech (Louisville, KY, USA). Wang resins were purchased from Nova Biochem, EMD (Gibbstown, NJ, USA). Fmoc-Ser (b-GlcAc4)-OH (the glycosylated serine building block) was synthesized by Larisa Yeomans accordingly to previously published protocols [34].

2.5.2 Solid-Phase Peptide Synthesis

Peptides were synthesized using standard solid phase Fmoc (fluorenylmethyloxycarbonyl) chemistry on a CS Bio CS336X Peptide Synthesizer (CS Bio Company, Menlo Park, CA, USA), using previously described protocols. [35] C-terminal amide peptides were synthesized using Rink resin, C-terminal acid peptides were synthesized using

Fmoc-Wang resin preloaded with the C-terminal amino acid. A 20% solution of piperidine in N-methyl-2-pyrrolidone (NMP) was used to remove the first Fmoc protecting group before synthesis and again to remove the Fmoc-protecting group after each coupling cycle. Coupling was performed using a four-fold excess of amino acid and a solution of 0.4 M hydroxybenzotriazole (HOBt) and O-benzotriazole-N,N,N',N'-tetramethyl-uroniumhexafluoro-phosphate (HBTU) in dimethylformamide (DMF), in the presence of diisopropylethylamine (DIEA). After the synthesis was complete, the resin was washed with NMP, then with dichloromethane, and dried under vacuum. The peptides were cleaved from the resin and side-chain-protecting groups removed by treatment at room temperature for 2 h with a cleavage cocktail consisting of 9.5 mL trifluoroacetic (TFA) acid, 0.25 mL triisopropylsilane (TIS) and 0.25 mL H_2O. The solution was concentrated *in vacuo*, and peptides were precipitated using cold, fresh diethylether. The filtered crude material was then purified using a Waters semipreparative HPLC (Waters Corporation, Milford, MA, USA) with a Vydac Protein and Peptide C18 column, using a linear gradient 10% Solvent B (0.1% TFA acid in acetonitrile) in Solvent A (0.1% TFA acid in water) to 60% Solvent B in Solvent A, at a rate of 1% per minute. The identity all peptides were determined ESI-MS performed on an Agilent Technologies LC/MS system using a 1200 Series LC and 6130 Quadrupole LC/MS (Agilent Technologies, Santa Clara, CA, USA) in positive mode with 50–100 µL injection volume and a linear gradient of 0% Solvent D (0.02% TFA and 0.1% acetic acid (AcOH) in acetonitrile) in Solvent C (0.02% TFA and 0.1% AcOH in water) to 60% Solvent D in Solvent C in 15 min. The purity of all peptides was determined using a Waters Alliance 2690 Analytical HPLC (Waters Corporation, Milford, MA, USA) and Vydac Protein and Peptide C18 reverse phase column, using a linear gradient of 0–70% Solvent B in Solvent A at a rate of 1% per minute. Linear peptides were purified to ≥ 95% purity by UV absorbance at 230 nm.

2.5.3 Disulfide Cyclization of Linear Peptides

Pure linear disulfhydryl-containing peptide was dissolved at 1mg/mL in argon saturated solution of 1% (v/v) AcOH in H_2O at 4C. The pH of the peptide solution was raised to 8.5 using NH_4OH, followed by the addition of 4 molar equivalents of $K_3Fe(CN)_6$. The reaction mixture was stirred on ice, under argon for two minutes and quenched by addition of glacial acetic acid to pH 3.5. The reaction mixture was incubated with 100-200 mesh anion exchange resin AG-3-X4

(Biorad, Hercules, CA, USA) and swirled occasionally at room temperature until the solution was colorless. The crude mixture was then filtered, concentrated *in vacuo*, and purified to ≥98% purity as determined by UV absorbance at 230 nm as described above to yield the disulfide linked cyclized peptides. The identity of cyclic peptides was determined by ESI-MS as described above.

2.5.4 Dithioether Cyclization of Linear Peptides

A DMF solution of the linear peptide (15 mg/40 mL) containing 5 molar equiv of 1,2-dibromoethane was added dropwise to a round-bottom flask containing 10 molar equiv of potassium tert-butoxide in 100 mL of anhydrous DMF saturated with argon, on ice. The reaction was stirred for 2 h under argon, on ice, and then quenched with to pH 3.5 with glacial acetic acid. Solvents were removed *in vacuo*, and the residue was purified to ≥ 98% purity as determined by UV absorbance at 230 nm as described above to afford the alkyl dithioether cyclized peptide. The identity of cyclic peptides was determined by ESI-MS as described above.

2.5.5 Cell Lines and Membrane Preparations

C6-rat glioma cells stably transfected with a rat μ (C6-MOR) or rat δ (C6-DOR) opioid receptor [36] and Chinese hamster ovary (CHO) cells stably expressing a human κ (CHO-KOR) opioid receptor [37] were used for all in vitro assays. Cells were grown to confluence at 37ºC in 5% CO_2 in Dulbecco's Modified Eagle's Medium containing 10% fetal bovine serum and 5% penicillin/streptomycin. Membranes were prepared by washing confluent cells three times with ice cold phosphate-buffered saline (0.9% NaCl, 0.61 mM Na_2HPO_4, 0.38 mM KH_2PO_4, pH 7.4). Cells were detached from the plates by incubation in warm harvesting buffer (20 mM HEPES, 150 mM NaCl, 0.68 mM EDTA, pH 7.4) and pelleted by centrifugation at 200xg for 3 min. The cell pellet was suspended in ice-cold 50 mM Tris-HCl buffer, pH 7.4 and homogenized with a Tissue Tearor (Biospec Products, Inc, Bartlesville, OK, USA) for 20 s at setting 4. The homogenate was centrifuged at 20,000xg for 20 min at 4 C, and the pellet was rehomogenized in 50 mM Tris-HCl with a Tissue Tearor for 10 s at setting 2, followed by recentrifugation. The final pellet was resuspended in 50mM Tris-HCl and frozen in aliquots at -80ºC. Protein concentration was determined via Bradford assay using bovine serum albumin as the standard.

2.5.6 Radioligand Binding Assays

Opioid ligand-binding assays were performed using competitive displacement of 0.2 nM [^{3}H]diprenorphine (250 μCi, 1.85TBq/mmol) by the test compound from membrane preparations containing opioid receptors. The assay mixture, containing membrane suspension (20 μg protein/tube) in 50 mM Tris-HCl buffer (pH 7.4), [^{3}H]diprenorphine, and various concentrations of test peptide, was incubated at room temperature for 1 h to allow binding to reach equilibrium. The samples were rapidly filtered through Whatman GF/C filters using a Brandel harvester (Brandel, Gaithersburg, MD, USA) and washed three times with 50 mM Tris-HCl buffer. The radioactivity retained on dried filters was determined by liquid scintillation counting after saturation with EcoLume liquid scintillation cocktail in a Wallac 1450 MicroBeta (Perkin-Elmer, Waltham MA, USA). Nonspecific binding was determined using 10 μM naloxone. K_i values were calculated using nonlinear regression analysis to fit a logistic equation to the competition data using GraphPad Prism version 5.01 for Windows. The results presented are the mean ± standard error from at least three separate assays performed in duplicate.

2.5.7 Stimulation of [^{35}S]GTPγS Binding

Agonist stimulation of [^{35}S] guanosine 5'-O-[gamma-thio]triphosphate ([^{35}S]GTPγS, 1250 Ci, 46.2TBq/mmol) binding was measured as described previously [38]. Briefly, membranes (10-20 μg of protein/tube) were incubated 1 h at room temperature in GTPγS buffer (50 mM Tris-HCl, 100 mM NaCl, 5 mM $MgCl_2$, pH 7.4) containing 0.1 nM [^{35}S]GTPγS, 30 μM guanosine diphosphate **(**GDP), and varying concentrations of test peptides. Peptide stimulation of [^{35}S]GTPγS was compared with 10 μM standard compounds [D-Ala^2, N-MePhe^4, Gly-ol]-enkephalin (DAMGO) at MOR, D-Pen^{2,5}- enkephalin (DPDPE) at DOR, or U69,593 at KOR. The reaction was terminated by rapidly filtering through GF/C filters and washing ten times with GTPγS buffer, and retained radioactivity was measured as described above. The results presented are the mean ± standard error from at least three separate assays performed in duplicate; maximal stimulation was determined using nonlinear regression analysis with GraphPad Prism.

2.5.8 Opioid Receptor Modeling

The homology modeling of opioid receptors in complexes with peptide ligands was performed as previously described [7, 10, 39]. The procedure included the following steps: 1) residue substitution in corresponding structural template(s); 2) rigid body helix movement to reproduce structural rearrangement during receptor activation observed in crystal structures of rhodopsin and adrenergic receptor; [40] 3) peptide ligand docking in accordance with mutagenesis-derived constraints; and 4) refinement of receptor-ligand complex using distance geometry and energy minimization with CHARMm. The validity of this modeling procedure has been assessed in blind prediction experiments of structural modeling of MOR, [7, 10] A_{2a}-adenosine receptor, [41] CXCR4, and D3 dopamine receptor [39] performed before the release of the corresponding crystal structures. The following comparison with experimental structures showed relatively high accuracy of our homology models: rmsd were between 1.5 and 2.5 Å for seven transmembrane helices [39, 41]. A comparison of our previously developed opioid receptor models [7, 10, 25, 27] and recently released crystal structures of the mouse MOR [42] and the human KOR [28] demonstrated the high reliability in prediction of ligand-receptor interactions in the more conserved "message" region located deeply in the ligand binding pocket, and less precise modeling in the "address" region of flexible extracellular loops which are responsible for ligand selectivity. Despite some inaccuracies, the previous models suggested the important role of interactions between Met^{199} and Trp^{284} of DOR and pentapeptide Phe^3 and Phe^4 side chains, respectively, and aromatic interactions between pentapeptide Phe^4 side chain and residues from the extracellular loop 2. [7, 8, 25, 27] Here we used X-ray structures of MOR (PDB ID: 4dkl) and KOR (PDB ID: 4djh) to refine the models of MOR and KOR complexes with antagonists, especially in the variable loop regions, and to develop the homology model of antagonist-bound conformation of the human DOR (UniProt ID: P41143, residues 46-333). Further, we used the crystal structure of the human KOR (PDB ID: 4djh) together with our previous models of active conformations of opioid receptors [7, 10] for modeling of the active conformations of MOR, DOR, and KOR, which are appropriate for agonist docking. Low-energy conformations of cyclic pentapeptides were generated using previously developed pharmacophore models of tetrapeptides [43] with additional conformational search in the region of the fifth residue and disulfide bridge. Coordinates of MOR (active and inactive states), DOR

(inactive state), and KOR (active state) with peptide **1** can be downloaded from our web site (http://mosberglab.phar.umich.edu/resources/).

2.6 References

1. Morphy, R., C. Kay, and Z. Rankovic, *From Magic Bullets to Designed Multiple Ligands.* Research Focus Reviews, 2004. **9**(15): p. 641-652.
2. Morphy, R. and Z. Rankovic, *Designing Multiple Ligands - Medicinal Chemistry Strategies and Challenges.* Current Pharmaceutical Design, 2009. **15**(6): p. 587-600.
3. Dietis, N., et al., *Simultaneous Targeting of Multiple Opioid Receptors: A Strategy to Improve Side-effect Profile.* British Journal of Anaesthesia, 2009. **103**(1): p. 38-49.
4. Abdelhamid, E.E., et al., *Selective Blockage of the Delta Opioid Receptors Prevents the Development of Morphine Tolerance and Dependence in Mice.* The Journal of Pharmacology and Experimental Therapeutics, 1991. **258**(1): p. 299-303.
5. Fundytus, M.E., et al., *Attenuation of Morphine Tolerance and Dependence with the Highly Selective Delta Opioid Receptor Antagonist TIPP(psi).* European Journal of Pharmacology, 1995. **286**: p. 105-108.
6. Hepburn, M.J., et al., *Differential Effects of Naltrindole on Morphine-Induced Tolerance and Physical Dependence in Rate.* The Journal of Pharmacology and Experimental Therapeutics, 1997. **281**(3): p. 1350-1356.
7. Purington, L.C., et al., *Pentapeptides Displaying Mu Opioid Receptor Agonist and Delta Opioid Receptor Partial Agonist/Antagonist Properties.* Journal of Medicinal Chemistry, 2009. **52**: p. 7724-7731.
8. Schiller, P.W., *Bi- or Multifunctional Opioid Peptide Drugs.* Life Sciences, 2009. **86**: p. 598-603.
9. McFayden, I.J., et al., *Tetrapeptide Derivatives of [DPen2, DPen5]-Enkephalin (DPDPE) Lacking an N-Terminal Tyrosine Residue are Agonists at the Mu Opioid Receptor.* Journal of Phamacology and Experimental Therapeutics, 2000. **295**(3): p. 960-966.
10. Purington, L.C., et al., *Development and in Vitro Characterization of a Novel Bifunctional Mu-Agonist/Delta-Antagonist Opioid Tetrapeptide.* ACS Chemical Biology, 2011. **6**: p. 1375-1381.
11. Anathan, S., et al., *Synthesis, Opioid Receptor Binding, and Biological Activities of Naltrexone-derived Pyrido- and Pyrimidomorphans.* Journal of Medicinal Chemistry, 1999. **42**: p. 3527-3538.
12. Anathan, S., et al., *Identification of Opioid Ligands Possessing Mixed Mu Agonist/Delta Antagonist Activity Among Pyridomorphans Derived from Naloxone, Oxymorphone, and Hydromorphone.* Journal of Medicinal Chemistry, 2004. **47**: p. 1400-1412.
13. Balboni, G., et al., *Evaluation of the Dmt-Tic Pharmacophore: Conversion of a Potent Delta-opioid Receptor Antagonist into a Potent Delta Agonist and Ligands with Mixed Properties.* Journal of Medicinal Chemistry, 2002. **45**: p. 713-720.
14. Balboni, G., et al., *Potent Delta-opioid Receptor Agonists Containing the Dmt-Tic Pharmacophore.* Journal of Medicinal Chemistry, 2002. **45**: p. 5556-5563.
15. Cheng, K., et al., *Opioid Ligands with Mixed Properties from Substituted Enatiomeric N-phenethyl-5-phenylmorphans: Synthesis of Mu-Agonist Delta-Antagonist and Delta-Inverse Agonists.* Organic and Biomolecular Chemistry, 2007. **5**: p. 1177-1190.
16. Heibel, A.C., et al., *Synthesis and Structure-Activity Relationships of a Potent Mu-Agonist Delta-Antagonist and an Exceedingly Potent Antinociceptive in the Enantiomeric*

C9-substituted 5-(3-hydroxyphenyl)-N-phenylethylmorphan Series. Journal of Medicinal Chemistry, 2005. **50**: p. 3765-3776.
17. Salvadori, S., et al., *Further Studies on the Dmt-Tic Pharmacophore: Hydrophobic Substituents at the C-terminus Endow Delta Antagonists to Manifest Mu Agonism or Mu Antagonism.* Journal of Medicinal Chemistry, 1999. **42**: p. 5010-5019.
18. Yamamoto, T., et al., *A Structure-Activity Relationship Study and Combinatorial Synthetic Approach to C-Terminal Modified Bifunctional Peptides that are Delta/Mu Opioid Receptor Agonists and Neurokinin 1 Receptor Antagonists.* Journal of Medicinal Chemistry, 2008. **51**: p. 1369-1376.
19. Mosberg, H.I., et al., *Development of a Model for the Delta Opioid Receptor Pharmacophore: Conformationally Restricted Phe3 Replacements in the Cycylic Delta Opioid Receptor Selective Tetrapeptide Tyr-c[DCys-Phe-DPen]OH (JOM-13).* Journal of Medicinal Chemistry, 1994. **37**: p. 4384-4391.
20. Przydzial, M.J., et al., *Design of High Affinity Cyclic Pentapeptide Ligands for the Kappa Opioid Receptors.* Journal of Peptide Research, 2005. **66**: p. 255-262.
21. Fowler, C.B., et al., *Refinement of a Homology Model of the Mu-opioid Receptor Using Distance Constraints from Intrinsic and Engineered Zinc-binding Sites.* Biochemistry, 2004. **43**: p. 8700-8710.
22. Fowler, C.B., et al., *Complex of an Active Mu-opioid Receptor with a Cyclic Peptide Agonist Modeled from Experimental Constraints.* Biochemistry, 2004. **43**: p. 15796-15810.
23. Pogozheva, I.D., A.L. Lomize, and H.I. Mosberg, *The Transmembrane 7-alpha-bundle of Rhodopsin: Distance Geometry Calculations with Hydrogen Bonding Constraints.* Biophysics, 1997. **72**: p. 1963-1985.
24. Pogozheva, I.D., A.L. Lomize, and H.I. Mosberg, *Opioid Receptor Three-Dimensional Structures from Distance Geometry Calculations with Hydrogen Bonding Constraints.* Biophysics, 1998. **75**: p. 612-634.
25. Pogozheva, I.D., M.J. Przydzial, and H.I. Mosberg, *Homology Modeling of Opioid Receptor-Ligand Complexes Using Experimental Constraints.* AAPS Journal, 2005. **7**: p. 43-57.
26. Pfeiffer, A., et al., *Psychotomimesis Mediated by Kappa Opioid Receptors.* Science, 1986. **233**: p. 774-776.
27. Mosberg, H.I., et al., *Cyclic Disulfide and Dithioether-Containing Opioid Tetrapeptides: Development of a Ligand with Enhanced Delta Opioid Receptor Selectivity and Potency.* Life Sciences, 1988. **43**: p. 1013-1020.
28. Wu, H., et al., *Structure of the Human Kappa Opioid Receptor in Complex with JDTic.* Nature, 2012: p. doi:10.1038/nature10939.
29. Mosberg, H.I. and C.B. Fowler, *Development and Validation of Opioid Ligand-Receptor Interaction Models: The Structural Basis of Mu vs. Delta Selectivity.* Journal of Peptide Research, 2002. **60**(6): p. 329-335.
30. Li, Y., et al., *Opioid Glycopeptide Analgesics Derived from Endogenous Enkephalins and Endorohins.* Future Medicinal Chemistry, 2012. **4**(2): p. 205-226.
31. Lowery, J.J., et al., *In Vivo Characherization of MMP-2200, a Mixed Mu/Delta Opioid Agonist, in Mice.* The Journal of Pharmacology and Experimental Therapeutics, 2011. **336**: p. 767-778.

32. Polt, R., M. Dhanasekaran, and C.M. Keyari, *Glycosylated Neuropeptides: A New Vista for Neuropsychopharmacology?* Medicinal Research Reviews, 2005. **25**(5): p. 557-585.
33. Schmidt, N., et al., *Arginine-rich Cell-Penetrating Peptides.* FEBS Letters, 2012. **584**(9): p. 1806-13.
34. Lefever, M.R., et al., *Glyscoslation of a-Amino Acids by Sugar Acetate Donors with InBR3 Minimally Competent Lewis Acids.* Carbohydrate Research, 2012. **351**: p. 121-125.
35. Przydzial, M.J., et al., *Roles of Residues 3 and 4 in Cyclic Tetrapeptide Ligand Recognition by the Kappa Opioid Receptor.* Journal of Peptide Research, 2005. **26**: p. 333-342.
36. Lee, K.O., et al., *Differential Binding Properties of Oripavines at Cloned Mu- and Delta-Opioid Receptors.* European Journal of Pharmacology, 1999(378): p. 323-330.
37. Husbands, S.M., et al., *BU74, A Complex Oripavine Derivative with Potent Kappa Opioid Receptor Agonism and Delayed Opioid Antagonism.* European Journal of Pharmacology, 2005(509): p. 117-135.
38. Traynor, J.R. and S.R. Nahorski, *Modulation by Mu-Opioid Agonists of Guanosine-5'-O(3-[35S]thio)triphosphate Binding to Membranes from Human Neuroblastoma SHY5Y Cells.* Molecular Pharmacology, 1995(47): p. 848-854.
39. Kufareva, I., et al., *Status of GPCR Modeling and Docking as Reflected by Community-wide GPCR Dock 2010 Assesment.* Structure, 2011. **19**: p. 1108-1126.
40. Congreve, M., et al., *Progress in Structure Based Drug Design for G Protein-Coupled Receptors.* Journal of Medicinal Chemistry, 2011. **54**: p. 4283-4311.
41. Michino, M., et al., *Community-wide Assesment of GPCR Structure Modeling and Ligand Docking.* Nature Reviews Drug Discovery, 2008. **8**: p. 455-463.
42. Manglik, A., et al., *Crystal Structure of the Mu Opioid Receptor Bound to a Morphinan Antagonist.* Nature, 2012. **doi: 10.1038/nature10954**.
43. Lomize, A.L., et al., *Conformational Analysis of the Delta Receptor Selective Cyclic Opioid Peptide Tyr-c[DCys-Phe-DPen]OH (JOM13). Comparison of X-ray Cystallographic Structures, Molecular Mechanics Simulations, and 1H NMR Data.* Journal of the American Chemical Society, 1994. **116**: p. 429-436.

CHAPTER 3

Linear Mixed Efficacy Ligands

3.1 Introduction

Many of the negative side effects associated with opioid analgesic use, such as tolerance to and dependence on opioid compounds, are closely tied to their mechanism of action; in fact, as discussed in Chapters 1.1 and 1.2, both the analgesia associated with opioids and the development of tolerance and dependence are primarily modulated through the mu opioid receptor (MOR). In Chapters 1.3, 1.4, and 2, we examined how mixed efficacy opioid ligands with MOR agonism and delta opioid receptor (DOR) agonism [1-4] or antagonism [5-9] display reduced tolerance and dependence liabilities as compared to conventional opioid analgesics, while maintaining the analgesia expected of MOR agonists. As discussed in Chapter 2.3, our lab has had success in developing cyclic mixed efficacy MOR/DOR tetrapeptides [8, 10, 11]. The best compounds from that series**,** **KSK-102**, **JH6**, and **JPAM13 (SMeS)**, displayed low nanomolar affinity for MOR and DOR, with selectivity relative to the kappa opioid receptor (KOR), and moderate to high efficacy at MOR and little to no stimulation of DOR (**Table 2.3**) (KSK and JH compounds synthesized by Katarzyna Sobczyk-Kojiro and Jeff Ho respectively).

While these peptides display our desired binding and efficacy[3] profiles, we anticipated that they would make poor drug candidates not only because their synthesis is low yielding, but also because they are peptides. Peptides are particularly susceptible to enzymatic degradation and often have low membrane permeability and therefore low bioavailability [12-14]. This is particularly problematic for opioid peptides as they must cross membranes in the digestive tract and the blood brain barrier (BBB) to be orally active in the central nervous system (CNS), where opioids exert their analgesic properties [15-17]; in fact BBB penetration is considered one of the biggest hurdles that needs to be overcome to have viable peptide therapeutics [18, 19]. While this

[3] N.B. In this work "agonism" and "efficacy" refer to the ability of compounds to stimulate G protein turnover in the GTPγS assay. Details can be found in *Section 3.5.6.*

may seem to argue against using peptides as the basis for effective pain treatment, peptides do offer an array of unique opportunities. Peptides have a high density of chemical information, making many ligand-receptor contact points, allowing for the fine tuning of binding and efficacy profiles for multiple targets, a key advantage in mixed efficacy ligands. Additionally, peptides are broken down into smaller peptide fragments and amino acids after metabolism and degradation; this means that the incidence of negative off target effects due to active metabolites is lessened for peptide therapeutics relative to their small molecule counterparts. It is also worth noting that in the case of opioid peptides we already have well characterized structure-activity relationships (SAR) and good lead compounds for drug development, especially for mixed efficacy MOR/DOR ligands.

In an effort to make out peptide ligands more "druggable" we planned to use the peptide ligands developed in this chapter as the basis for blood brain barrier (BBB) penetrating glycosylated peptides, an approach which has been convincingly demonstrated by Polt and coworkers in the field of mixed efficacy opioid ligands [4, 14, 20, 21] and which we have ourselves tested in the cyclic tetrapeptide series described in Chapter 2.3. Literature precedent and our own initial attempts at glycosylated peptides (see **KSK-102** and **VRP-26** in Chapter 2.3, VRP compounds synthesized by Vanessa Porter-Barrus) predict that these glycopeptides will have increased membrane permeability and CNS activity relative to their parent compounds, without greatly altering the binding or efficacy profiles of the resultant ligands. We are therefore incorporating a C-terminal serine residue as a site for sugar modifications and plan on testing the glucoserine analogues, where the Ser is covalently O-linked to a β-glucose, of the most promising peptides described below for *in vivo* activity in the future.

As described in Chapter 2, we have had success in developing potent mixed efficacy opioid ligands [8, 10, 11]. However, to date all of these ligands have been cyclic in nature. A long-time focus in our lab has been on cyclic peptides as a means to improve receptor selectivity by "freezing out" unwanted conformations; for mixed efficacy ligands conformational restriction may not be advantageous. Furthermore, the synthesis of linear peptides involves fewer chemical modifications and purifications while also providing higher yields than cyclic ligands. Consequently, we shifted our focus to examine linearized versions of previously described MOR agonist/DOR antagonist cyclic peptides [22] and explored the effect of phenylalanine

replacements on agonist activity to determine if the SAR found in cyclic peptides [8, 11] is mirrored in linear analogues. In parallel, we also used the known linear opioid agonist peptides developed by Roques, Tyr-DThr-Gly-Phe-Leu-X-NH_2, where X = DSer (**DTLES**) or X = DThr (**DTLET**) [23], as templates for installing the Phe replacements to modulate efficacy in a manner similar to that found in our cyclic analogues. Although initially reported as DOR selective, **DTLES** and **DTLET** actually bind to both MOR and DOR with similar affinity and display some selectivity relative to KOR [14]. In this chapter we will make a two series of analogues based on our previously described cyclic series and the Roques compounds in an effort to make linear mixed efficacy MOR agonist/DOR antagonist ligands.

3.2 Direct Translation of Cyclic Mixed Efficacy Tetrapeptides to Linear Ligands

In our first series we sought to directly translate our successful cyclic tetrapeptide, **KSK-102** (Chapter 2.3), into a linear ligand, substituting the $DCys^2$ with either a D-Serine (DSer) or D-Threonine (DThr) and the $DPen^5$ with a D-Leucine (DLeu), thereby removing reactive thiol groups, while maintaining similar shape and bulk in the second and fifth positions. For the initial sequences in this series we used a Tyr^1 in place of Dmt^1 for cost concerns. We hypothesized that we would find a ligand which bound tightly to MOR and DOR and stimulated MOR, but not DOR, yielding a mixed efficacy MOR agonist/DOR antagonist (**Table 3.1**). Unfortunately, the initial direct translations of **KSK-102** (**VRP-29** and **VRP-31**) did not bind to either MOR or DOR and were abandoned. However, our models[4] [8, 22, 24-28] suggested that an L- (as opposed to D-) Leu in the fifth position would significantly improve binding. We therefore made the $DThr^2$, Leu^5 analogue (**VRP-35**), which did, in fact, display mid-range nanomolar binding to MOR and DOR with moderate stimulation of MOR and very low efficacy at DOR (**Table 3.1**). Like its cyclic counterpart, **VRP-35** displayed selectivity relative to KOR and no measurable KOR agonist activity. There was, however, room for significant improvement in increasing the affinity of these ligands for MOR and DOR and, in the case of **VRP-35**, increasing its ability to stimulate MOR. I therefore synthesized a series of ligands with various aromatic and aliphatic residues in the third position in hopes of finding a ligand which would make appropriate hydrophobic contacts with MOR and DOR, improving binding to both receptors, while

[4] N.B. Models of the opioid receptors are based on X-ray crystal structures of antagonist bound receptor. No crystal structures exist for the active conformation of the receptors. For more details see *Section 3.5.7.*

preserving or improving the efficacy profile found in **VRP-35**; these ligands are listed in **Table 3.1** (HVW compounds synthesized by Helen V. Waldschmidt.)

While we made several hydrophobic substitutions in the third position, no one compound exactly meets our desired profile of nanomolar binding to MOR and DOR while displaying agonism only at MOR. In fact, many of the compounds in the series displayed low MOR stimulation and poor binding to DOR and/or MOR. However, two compounds stand out as different from the rest of the analogues in this series. **JPAM7** is unique among the Tyr^1 pentapeptide analogues in that it displays nanomolar binding to MOR and DOR, with selectivity relative to KOR; this is the only Tyr^1 compound in the series with single digit nanomolar binding

Table 3.1: Direct Linear Translations of Cyclic Tetrapeptides

	Sequence	Binding (nM)			Efficacy					
					MOR		DOR		KOR	
		MOR	DOR	KOR	%	EC50 (nM)	%	EC50 (nM)	%	EC50 (nM)
VRP-29	Tyr-DSer-Aci-DLeu-Ser-NH2	>1000	>1000	nd	nd	nd	nd	nd	nd	nd
VRP-31	Tyr-DThr-Aci-DLeu-Ser-NH2	>1000	>1000	nd	nd	nd	nd	nd	nd	nd
VRP-35	Tyr-DThr-Aci- Leu-Ser-NH2	21 ± 4	160± 26	>10000	68 ±10	264 ±9	12 ±4	nd	nd	nd
HVW-4	Tyr-DThr-Idg-Leu-Ser-NH2	64±3	58±16	>10000	dns	nd	dns	nd	nd	nd
JPAM20	Tyr-DThr-Phe-Leu-Ser-NH2	272±13	105±14	>10000	10.8 ±0.4	nd	dns	nd	dns	nd
JPAM21	Tyr-DThr-Cha-Leu-Ser-NH2	11±2	78±3	>10000	dns	nd	dns	nd	dns	nd
JPAM7	Tyr-DThr-Hfe-Leu-Ser-NH2	3.6 ± 0.5	1.4 ±0.1	>10000	22 ±9	275 ±36	122 ±5	520 ±60	dns	nd
HVW-3	Tyr-DThr-Nle-Leu-Ser-NH2	68±20	145±6	>10000	dns	nd	dns	nd	nd	nd
JPAM6	Tyr-DThr-1Nal-Leu-Ser-NH2	24 ±3	>1000	900 ±280	dns	nd	dns	nd	dns	nd
JPAM5	Tyr-DThr-2Nal-Leu-Ser-NH2	90 ±30	660 ±220	>1000	dns	nd	dns	nd	dns	nd
HVW-1	Dmt-DThr-Aci- Leu-Ser-NH2	1.57±0.08	7±0.5	>10000	dns	nd	dns	nd	nd	nd
JPAM12	Dmt-DThr-Idg-Leu-Ser-NH2	0.6±0.2	1.6±0.1	390±90	dns	nd	dns	nd	dns	nd
HVW-5	Dmt-DSer-Idg-Leu-Ser-NH2	0.53±0.06	1.2±0.3	93±2	68±7	14±2	75±2	49±4	dns	nd

Binding affinities (K_i) were obtained by competitive displacement of radiolabeled [^{3}H] diprenorphine. Efficacy data were obtained using [^{35}S] GTPγS binding assay. Efficacy is represented as percent maximal stimulation relative to standard agonists DAMGO (MOR), DPDPE (DOR) or U69,593 (KOR) at 10μM concentrations. All values are expressed as mean ± SEM of three separate assays performed in duplicate. nd = not determined, dns = does not stimulate.

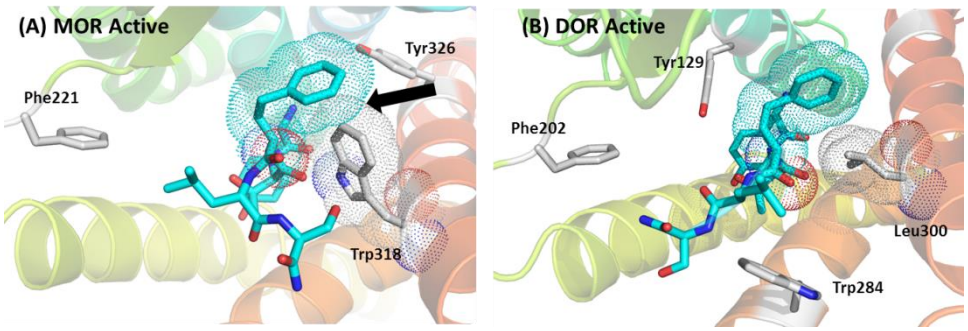

Figure 3.1: Modeling of peptide JPAM7 in the MOR and DOR Active Sites – JPAM7 (Tyr-DThr-Hfe-Leu-Ser-NH_2) docked in the active state model of MOR (**A**) and the active state model of DOR (**B**). The Hfe^3 of **JPAM7** forms a steric clash in the MOR active site with Trp^{318} (highlighted by an arrow). This clash is relieved in the DOR active site as it has a less bulky Leu in the corresponding position.

to MOR and DOR. It is also unusual in that it also displays full DOR agonist character; all the other compounds in this series are DOR antagonists or weak partial agonists. Docking studies of **JPAM7** in the DOR active site show that the added flexibility of the Hfe^3 contributes greatly to its agonist character and nanomolar binding. All of the other analogues in this series have either bulky groups, such as 1- or 2Nal, or inflexible residues like Aci or Idg in the third position; these groups produce a steric clash in the DOR active site, reducing efficacy as intended. However the side chain of Hfe is flexible enough to assume a conformation which relieves this steric clash, allowing the ligand to assume a more compact binding pose to fit into the narrower DOR active site. Furthermore, because of this somewhat unique binding position, the Leu^4 of **JPAM7** may be able to make some favorable hydrophobic interactions with Trp^{284} in the DOR active site which are not seen in the other ligands in this series. The side chain flexibility of Hfe^3 and the narrow binding pose that it produces allows **JPAM7** to assume a conformation which fits into the binding site of MOR and DOR better than the bulky and inflexible analogues in this series, contributing to the tight binding of **JPAM7** (**Table 3.1; Figure 3.1**).

While **JPAM7** is able to assume a more compact conformation than many of the other ligands in this series it does not fit well in the MOR active site. Modeling studies show that in order for **JPAM7** to sit far enough down in the binding pocket of MOR to stimulate receptor turnover the Hfe^3 of **JPAM7** forms a steric clash with Trp^{308} in the receptor; DOR has Leu^{300} in the corresponding positions which are less bulky and do not produce a steric clash in the DOR active site (**Figure 3.1**). To relieve this clash, the ligand must sit higher in the active site, reducing its ability to stimulate MOR. This may explain why **JPAM7** displays only partial agonism at MOR.

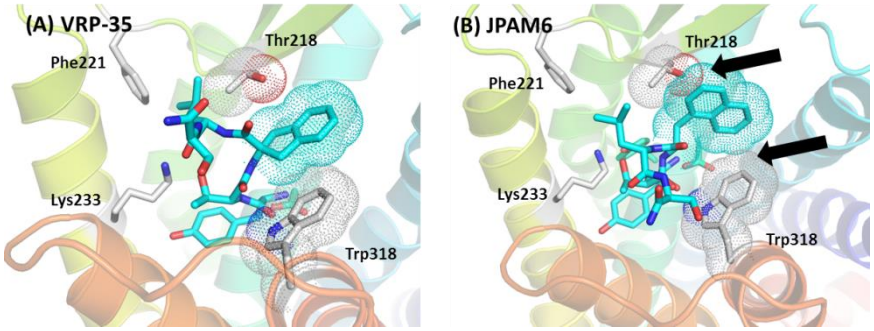

Figure 3.2: Comparison of VRP-35 and JPAM6 in the MOR Active Site – VRP-35 (Tyr-DThr-Aci-Leu-Ser-NH_2) (**A**) and **JPAM6** (Tyr-DThr-1Nal-Leu-Ser-NH_2) (**B**) docked in the active state model of MOR. The Aci^3 of **VRP-35** sits close to the peptide backbone, whereas the $1Nal^3$ of **JPAM6** assumes a more extended pose away from the peptide backbone and forms a steric clash in the MOR active site with Trp^{318} and Thr^{218} (highlighted by arrows). This clash prevents **JPAM6** (and similarly extended analogues) from binding to the MOR active site reducing MOR efficacy.

VRP-35 (**Table 3.1**) also stands out in this series, as it actually displays the desired efficacy profile of MOR efficacy coupled with relatively low DOR efficacy. Modeling studies comparing **VRP-35** and **JPAM6** (**Figure 3.2**), show that the two ligands assume a similar shape in the MOR active site, but that the $1Nal^3$ in **JPAM6** forces the ligand into more extended shape than **VRP-35**, which has an Aci in the third position. Because the $1Nal^3$ extends out from the backbone of **JPAM6**, it forms a steric clash with Thr^{218} and Asp^{216} of extracellular loop 2 in the MOR active site. Our modeling shows that in an effort to relieve this steric clash the ligand as a whole shifts toward helix 5 of the MOR active site (relative to the position of **VRP-35** in the MOR active site), but that this then produces a steric clash between a $DThr^2$ and Lys^{233}. In other words, because Aci^3 is close to the backbone of **VRP-35** the ligand assumes a more compact shape than other ligands in this series, allowing it to fit more comfortably into the narrow MOR active site, contributing to its agonist character. We therefore generated a new analogue, **HVW-1**, in which Tyr^1 of **VRP-35** is substituted with a Dmt^1 in hopes of improving binding without drastically effecting the efficacy profile. **HVW-1** displays a much improved binding profile as compared to **VRP-35**, however **HVW-1** is an

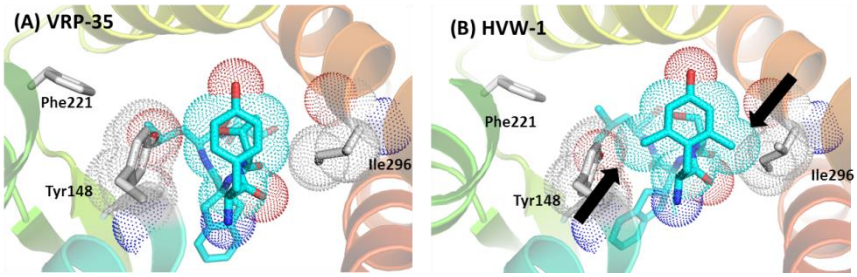

Figure 3.3: Comparison of VRP-35 and HVW-1 in the MOR Active Site – VRP-35 (Tyr-DThr-Aci-Leu-Ser-NH_2) (**A**) and **HVW-1** (Dmt-DThr-Aci-Leu-Ser-NH_2) (**B**) docked in the active state model of MOR. The 2,6 methyl groups of Dmt^1 in **HVW-1** from a steric clash in the MOR active site with Tyr^{148} and Ile^{196} (highlighted by arrows). This clash prevents **HVW-1** from binding to the MOR active site reducing MOR efficacy.

antagonist at both MOR and DOR. Information from molecular modeling studies suggests that the added bulk of the 2, 6 methyl groups on Dmt[1] form a steric clash with Tyr[148] and Ile[296] in the active site of MOR, making **HVW-1** a MOR antagonist. As **VRP-35** has a Tyr[1], it fits easily into the narrow active site of MOR and displays MOR agonism. (**Figure 3.3**)

These same modeling studies suggest that a smaller DSer[2] may relieve some of this steric hindrance and rescue MOR agonist activity. We therefore synthesized a pair of ligands with a Dmt[1] which differ only in the residue in the second position (**Table 3.1; Figure 3.4**), **JPAM12**, which contains DThr[2], and **HVW-5**, which contains a DSer[2]. Both of these ligands display nanomolar binding to both MOR and DOR, with some selectivity relative to KOR. **JPAM12** is an antagonist at both MOR and DOR. The substitution of a DSer[2] for a DThr[2] (**HVW-5**) does, as predicted, rescue MOR agonist activity. However, this substitution also confers DOR agonist character, resulting in a MOR agonist/DOR agonist compound. While unexpected, this profile is still desirable, as is discussed in the next section.

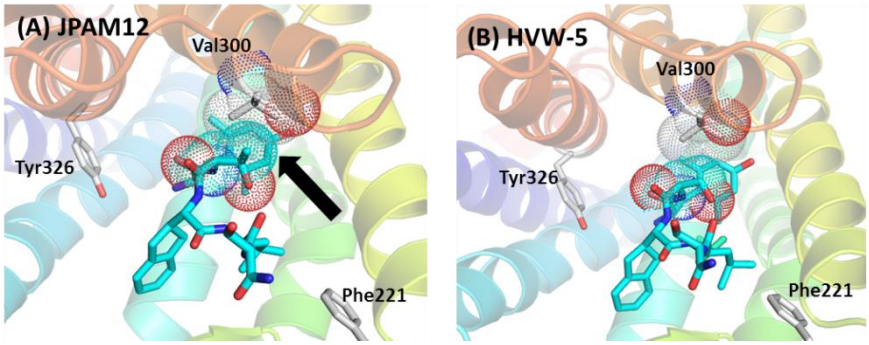

Figure 3.4: Comparison of JPAM12 and HVW-5 in the MOR Active Site – JPAM12 (Tyr-DThr-Idg-Leu-Ser-NH_2) (**A**) and **HVW-5** (Tyr-DSer-Idg-Leu-Ser-NH_2) (**B**) docked in the active state model of MOR. The DThr[2] of **JPAM12** forms a steric clash in the MOR active site with Val[300] (highlighted by an arrow). This clash is relieved in **HVW-5** which has a less bulky DSer[2].

3.3 Modifications to Roques Scaffolds to Produce Mixed Efficacy MOR/DOR Ligands

For our parallel series of linear peptides based on the Roques compounds **DTLES** and **DTLET** we installed various bulky hydrophobic Phe[4] replacements with the thought that this substitution might selectively confer DOR antagonism as it did in our cyclic ligands described in Chapter 2. We initially installed an Aci[4] in place of Phe[4] in hopes of mimicking the *in vitro* binding and efficacy profile of **KSK-102**, unfortunately, this compound, **VRP-33**, displayed micromolar binding to all three opioid receptors. We also made analogues with less constrained, bulky hydrophobic residues in the fourth position as we did in the linear series described above; their binding and efficacy profiles are listed in **Table 3.2**. Most of the ligands in this series

Table 3.2: Modification of Roques Linear Hexapeptides

	Sequence	Binding (nM)			Efficacy					
					MOR		DOR		KOR	
		MOR	DOR	KOR	%	EC50 (nM)	%	EC50 (nM)	%	EC50 (nM)
VRP-33	Tyr-DThr-Gly-Aci-Leu-Ser-NH2	>1000	>5000	>10000	nd	nd	nd	nd	nd	nd
JPAM16	Tyr-DThr-Gly-Idg-Leu-Ser-NH2	200±20	300±55	>10000	709±9	>2000	dns	nd	nd	nd
JPAM8	Tyr-DThr-Gly-1Nal-Leu-SerNH2	0.8±0.2	0.9 ±0.1	25±3	93.0±0.6	31±7	144±7	35±6	75±2	>1000
VRP-39	Tyr-DThr-Gly-2Nal-Leu-Ser-NH2	2.7 ± 0.08	0.47 ± 0.07	125 ±22	101±3	13±2	196±2	11.3±0.8	25±4	>1000
JPAM9	Tyr-DThr-Gly-Hfe-Leu-SerNH2	52±7	3.4±0.9	>1000	56±2	>1000	105±3	>1000	nd	nd
JPAM15	Dmt-DThr-Gly-2Nal-Leu-Ser-NH2	0.5±0.1	0.7±0.1	2.3±0.5	81±5	1.5±0.6	164±7	0.3±0.05	dns	nd
JPAM17	Dmt-DThr-Gly-Idg-Leu-Ser-NH2	3.4±0.7	2.1±0.3	270±120	dns	nd	dns	nd	nd	nd
HVW-2	Tyr-DThr-Gly-2Nal-Leu-Ser(Glc)-NH2	4.9±0.3	0.87±0.03	130±10	73±4	400±140	144±15	26±11	<10	nd

Binding affinities (K_i) were obtained by competitive displacement of radiolabeled [^{3}H] diprenorphine. Efficacy data were obtained using [^{35}S] GTPγS binding assay. Efficacy is represented as percent maximal stimulation relative to standard agonists DAMGO (MOR), DPDPE (DOR) or U69,593 (KOR) at 10μM concentrations. All values are expressed as mean ± SEM of three separate assays performed in duplicate. nd = not determined, dns = does not stimulate.

display nanomolar binding to both MOR and DOR, with some selectivity relative to KOR, and both MOR and DOR agonist activity. It is interesting to note that the ligands with the more constrained residues in the fourth position (**VRP-33** with and Tyr^1, Aci^4 and **JPAM16** with Tyr^1, Idg^4) displayed significantly lower affinity for MOR and DOR than the other compounds in this series, which contained more flexible residues in the fourth position. Despite its relatively poor binding, we were able to obtain efficacy data for **JPAM16**. Perhaps unsurprisingly, **JPAM16** is the only ligand in this series which displays a MOR agonist/DOR antagonist profile. This is likely due to the fact that some conformational restriction is necessary to selectively produce a steric clash in the DOR active site to reduce DOR efficacy, without effecting MOR efficacy; more flexible residues will be able to assume conformations which can be accommodated in the narrower DOR active site and will display DOR agonism. We next attempted to improve the binding of **JPAM16** by replacing the Tyr^1 with a Dmt^1 (**JPAM17**). While this slight modification did produce the expected increase in affinity, yielding a better binding profile, the substitution of a Dmt^1 for a Tyr^1 also completely abolished MOR efficacy. We saw a similar

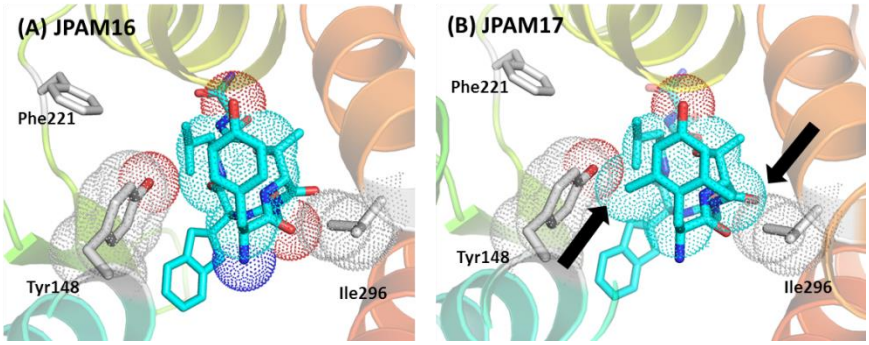

Figure 3.5: Comparison of JPAM16 and JPAM17 in the MOR Active Site – JPAM16 (Tyr-DThr-Idg-Leu-Ser-NH_2) (**A**) and **JPAM17** (Dmt-DThr-Idg-Leu-Ser-NH_2) (**B**) docked in the active state model of MOR. The 2, 6 methyl groups of Dmt^1 in **JPAM17** forms a steric clash in the MOR active site with Tyr^{148} and Ile^{296} (highlighted by arrows). This clash prevents **JPAM17** from binding to the MOR active site, causing it to be an antagonist.

effect when we substituted a Dmt^1 for a Tyr^1 in our cyclic series with **JH6** and **JPAM13 (SEtS)** and in the **VRP-35/HVW-1** ligand pair; binding of the Dmt^1 analogue was increased, but MOR efficacy was drastically reduced. In the case of **JH6/JPAM13 (SEtS)** and **VRP-35/HVW-1** we posited that in order for the phenolic hydroxyl of the Dmt to anchor correctly in the MOR binding site the ligand must assume a conformation which causes the 2, 6 methyl groups of the Dmt to form a steric clash in the MOR active site with Tyr^{148} and Ile^{296}. This steric clash is relieved in the more open MOR inactive site, allowing for nanomolar binding, but low efficacy at MOR. We may be seeing a similar effect with our **JPAM16** and **JPAM17** ligand pair, where the added bulk of the two methyl groups in the first position combined with a $DThr^2$ prohibits binding to the MOR active conformation, as seen in the linear pentapeptide series described in the previous section (**Figure 3.5**). Whatever the reason, neither **JPAM16** nor **JPAM17** fit our desired profile of nanomolar binding to MOR and DOR, with MOR agonist and DOR antagonist behavior.

While we were not able to selectively reduce DOR efficacy while retaining nanomolar binding to MOR and DOR, these hexapeptide ligands remain promising as a MOR agonist/DOR agonist profile is also desirable. It has been demonstrated that the co-administration of a MOR agonist with a DOR agonist potentiates the binding and antinociceptive potency of MOR agonists [1-4]. The synergistic effect between MOR and DOR agonists has been shown to lessen the development of tolerance and dependence, as well as other unwanted side effects [4, 14, 29]. The Polt group has already successfully developed mixed efficacy MOR agonist/DOR agonist peptide ligands, which they report as displaying reduced tolerance and dependence liabilities and reduced self-administration [4, 14, 21]. However, when the *in vitro* pharmacology for the lead

Table 3.3: *In vitro* Pharmacological Data for MMP-2200

Sequence		Binding (nM)			Efficacy					
					MOR		DOR		KOR	
		MOR	DOR	KOR	%	EC50 (nM)	%	EC50 (nM)	%	EC50 (nM)
MMP-2200	Tyr-D-Thr-Gly-Phe-Leu-Ser-(Lac)-NH2	5*	2.5*	75*	92±5	120±30	152±16	94±16	82±11	1800±300

Binding affinities (K_i) were obtained by competitive displacement of radiolabeled [^{3}H] diprenorphine. Efficacy data were obtained using [^{35}S] GTPγS binding assay. Efficacy is represented as percent maximal stimulation relative to standard agonists DAMGO (MOR), DPDPE (DOR) or U69,593 (KOR) at 10μM concentrations. All values are expressed as mean ± SEM of three separate assays performed in duplicate, except values denoted with * where n=1. Ser(Lac) is a Ser is covalently O-linked to a β-lactose.

ligand in this series, **MMP-2200**, was first published, no efficacy data at KOR was reported, though the ligand displayed low nanomolar KOR affinity [4]. We therefore tested this compound in our own assays, and found that **MMP-2200** displays full agonist behavior at KOR, albeit with poor potency. The binding for **MMP-2200** at MOR, DOR and KOR was similar to reported values, as was efficacy at MOR and DOR. (**Table 3.3**; **MMP-2200** was a kind gift from Dr. Robin Polt.) KOR agonists have been shown to cause dysphoria [30] and psychomimetic effects [31] and patients describe KOR agonists as unpleasant. For these reasons KOR agonist often display aversive effects [32]. These are undesirable characteristics in a drug designed to treat chronic pain and often lead to decreased patient compliance. The ligands that I have described in this section provide an answer to this problem, in that they not only display a preference for binding to MOR and DOR over KOR, but also, for the most part, act as KOR antagonists. The lack of KOR activity in the ligands developed in this chapter will help to deconvolute the effects that DOR agonists have on MOR agonist behavior and provide a more acceptable drug profile for use in human subjects.

Of the Tyr^1 hexapeptide MOR agonist/DOR agonist ligands **VRP-39** displays the best binding profile, with nanomolar binding to both MOR and DOR and some selectivity relative to KOR. We next decided to modify **VRP-39** with an N-terminal Dmt to balance the MOR and DOR binding (**JPAM15**). While this modification did balance MOR and DOR binding and increase potency at MOR and DOR it also significantly reduced selectivity relative to KOR. However, as **VRP-39** already displays the desired pharmacological profile, we added a C-terminal glucoserine improve its bioavailability. The resulting compound, **HVW-2**, still displays the desired binding and efficacy profile (**Table 3.2**) and will be carried forward into animal studies in future work.

3.4 Conclusions

The studies discussed in this chapter were aimed toward developing linear mixed efficacy opioid ligands displaying MOR agonist and DOR antagonist behavior. Two series of linear ligands were developed: a series of pentapeptides designed as linear translations of the cyclic tetrapeptides described in Chapter 2.3 with a C-terminal Ser as a handle for sugar modification and a series of hexapeptides, also with a C-terminal Ser, based on linear peptides designed by Roques [23] and Polt [4, 14, 20, 21].

Most of the analogues synthesized in the pentapeptide series displayed lower affinity for MOR and DOR and greater selectivity relative to KOR than their cyclic counterparts described in Chapter 2.3. The DThr^{2} analogues in this series also displayed antagonist behavior at both MOR and DOR, with **VRP-35** and **JPAM7** standing out as notable exceptions. Preliminary modeling studies suggest that, for the most part, these linear ligands adopt a less compact binding pose than their cyclic counterparts. This extended conformation prevents these ligands from binding in the narrow active sites of MOR and DOR, likely contributing to their antagonist character. This extended pose also forces the ligands to sit higher in the opioid binding pocket, preventing the Tyr^{1} of the ligand from making favorable electrostatic interactions with the receptor. Most tight binding opioid peptide ligands form a salt bridge between the N-terminus of the peptide and a conserved Asp residue (Asp^{147} in MOR and Asp^{145} in DOR) deep in the opioid binding pocket. This higher binding pose also prevents a water mediated H-bond from forming between the hydroxyl group of Tyr^{1} of the ligand and a conserved His residue (His^{297} in MOR and His^{278} in DOR). This lack of electrostatic interactions likely contributes to the lower affinities for MOR and DOR seen in this series as compared to their cyclic counterparts.

Two compounds stand out in the DThr^{2} linear pentapeptide series: **VRP-35** and **JPAM7**. Both of these compounds display appreciable agonism, **VRP-35** at MOR and **JPAM7** at DOR. Preliminary modeling studies suggest that this is because both of these ligands assume a more compact shape than the other ligands in this series, **VRP-35** because the Aci^{3} kinks the peptide backbone of the ligand and **JPAM7** because the Hfe^{3} is flexible enough to allow the ligand to fold in on itself. As **VRP-35** displays the desired efficacy profile, it was modified with a Dmt^{1} to improve its binding profile. The resulting ligand, **HVW-1**, displays the desired binding profile, but the addition of two methyl group abolished all agonist activity at MOR. This is in line with a

trend observed in the cyclic mixed efficacy ligands where the addition of two methyl groups produces a steric clash in the active site with Tyr^{148} and Ile^{296} in MOR, reducing efficacy. On the surface this observation appears to be at odds with previous reports of additional steric bulk conferring agonist character to **TIPP** analogues [33, 34]. However, the rationale for increased hydrophobic bulk lending agonist character to **TIPP** analogues rests on the idea that increased hydrophobicity in the first position allows the ligand to undergo so-called "hydrophobic collapse," decreasing the overall size of the ligand and allowing it to fit into the narrower active site conformation. In our case, the added bulk in the first position does not significantly decrease the overall size of the molecule; in fact it increases the steric bulk at the N-terminus and consequently does not confer agonist character.

Fortunately, the converse is also true: reducing steric bulk at the N-terminus of the molecule rescues agonist activity. This is illustrated by the ligand pair **JPAM12** and **HVW-5**, where a $DSer^2$ is substituted for a $DThr^2$. **JPAM12** displays nanomolar binding, largely due to the Dmt^1 (compared to **HVW-4**), but does not stimulate MOR, by removing a methyl ($DThr^2$ to $DSer^2$) we are able to rescue MOR efficacy. However, this effect is limited to MOR and **HVW-5** also displays DOR agonism.

While we did not generate a mixed efficacy MOR agonist/DOR antagonist ligand in our linear pentapeptide series, we have made several observations that will help direct future SAR efforts in this series. When comparing this series of ligands to the cyclic tetrapeptides described in Chapter 2.3 it becomes clear that making direct translations from cyclic to linear ligands did not achieve the desired result. By linearizing the peptides we lose the conformational restriction which gives our cyclic ligands their compact shape and allows them to selectively reduce DOR agonism. We are able to mimic this somewhat by introducing conformational restriction, as with **VRP-35**, or extreme flexibility, as with **JPAM7**, into the aromatic residue in the third position and reducing steric bulk in the second position, as with **HVW-5**. The next logical step would be to make a series of analogues which contain $DSer^2$ with some conformational restriction in an attempt to selectively rescue MOR agonist activity.

For the hexapeptide series based on the Roques compounds we sought to add steric bulk in the fourth position to selectively reduce DOR agonism as we saw with the tetra- and pentapeptides described in Chapter 2. The only difference in sequence between this series and

the pentapeptide series described above is a Gly^3 residue. While this may seem small, the added flexibility from a glycine is enough to confer full agonism at both MOR and DOR, where most ligands in the pentapeptide series were MOR and DOR antagonists. Given this extra flexibility it is unsurprising that the extra hydrophobic bulk in the fourth position was unable to reduce DOR efficacy – the ligand is not constrained enough to form a steric clash in the active site. **JPAM16** stands out in this series as it is the only compound to selectively display MOR agonism. Unfortunately, **JPAM16** also displays poor binding to MOR and DOR. The incorporation of a Dmt^1 (**JPAM17**) increased binding at MOR and DOR as expected, but also abolished all agonist activity. Future directions will include the $DSer^2$ analogue of **JPAM17**, to see if the decreased bulk of a DSer, relative to a DThr, will selectively rescue MOR agonist activity, resulting in a potent MOR agonist/DOR antagonist ligand.

While we did not achieve our desired profile of MOR agonist/DOR antagonist, a potent MOR agonist/DOR agonist is also a desirable profile [4, 14, 29]. We have therefore appended a C-terminal glucoserine to our most promising MOR agonist/DOR agonist compound, **VRP-39**. The resulting ligand, **HVW-2**, retains low nanomolar binding to MOR and DOR, with selectivity relative to KOR, and displays MOR and DOR agonism. This ligand will be carried forward into animal studies to compare how a MOR agonist/DOR agonist ligand compares to a MOR agonist/DOR antagonist compound in tolerance, dependence, and self-administration assays.

3.5 Materials and Methods

3.5.1 Materials

All reagents and solvents were purchased from commercial sources and used without further purification. All chemicals and biochemicals were purchased from Sigma Aldrich (St. Louis, MO, USA) or Fisher Scientific (Hudson, NH, USA), unless otherwise noted. All tissue culture reagents were purchased from Gibco Life Sciences (Grand Island, NY, USA). Radioactive compounds were purchased from Perkin-Elmer (Waltham, MA, USA). Peptide synthesis reagents, amino acids, and Rink resin were purchased from Advanced Chem Tech (Louisville, KY, USA). Wang resins were purchased from Nova Biochem, EMD (Gibbstown, NJ, USA). MMP-2200 was a kind gift from Dr. Robin Polt. Fmoc-Ser (b-GlcAc4)-OH (the glycosylated

serine building block) was synthesized by Larisa Yeomans accordingly to previously published protocols [35].

3.5.2 Solid-Phase Peptide Synthesis on CS Bio

Peptides were synthesized using standard solid phase Fmoc (fluorenylmethyloxycarbonyl) chemistry on a CS Bio CS336X Peptide Synthesizer (CS Bio Company, Menlo Park, CA, USA), using previously described protocols. [36] C-terminal amide peptides were synthesized using Rink resin, C-terminal acid peptides were synthesized using Fmoc-Wang resin preloaded with the C-terminal amino acid. A 20% solution of piperidine in N-methyl-2-pyrrolidone (NMP) was used to remove the first Fmoc protecting group before synthesis and again to remove the Fmoc-protecting group after each coupling cycle. Coupling was performed using a four-fold excess of amino acid and a solution of 0.4 M hydroxybenzotriazole (HOBt) and O-benzotriazole-N,N,N',N'-tetramethyl-uroniumhexafluoro-phosphate (HBTU) in dimethylformamide (DMF), in the presence of diisopropylethylamine (DIEA). After the synthesis was complete, the resin was washed with NMP, then with dichloromethane, and dried under vacuum. The peptides were cleaved from the resin and side-chain-protecting groups removed by treatment at room temperature for 2 h with a cleavage cocktail consisting of 9.5 mL trifluoroacetic (TFA) acidand 0.5 mL water. The solution was concentrated *in vacuo*, and peptides were precipitated using cold diethylether. The filtered crude material was then purified using a Waters semipreparative HPLC (Waters Corporation, Milford, MA, USA) with a Vydac Protein and Peptide C18 column, using a linear gradient 10% Solvent B (0.1% TFA acid in acetonitrile) in Solvent A (0.1% TFA acid in water) to 60% Solvent B in Solvent A, at a rate of 1% per minute. The identity all peptides were determined ESI-MS performed on an Agilent Technologies LC/MS system using a 1200 Series LC and 6130 Quadrupole LC/MS (Agilent Technologies, Santa Clara, CA, USA) in positive mode with 50–100 µL injection volume and a linear gradient of 0% Solvent D (0.02% TFA and 0.1% acetic acid (AcOH) in acetonitrile) in Solvent C (0.02% TFA and 0.1% AcOH in water) to 60% Solvent D in Solvent C in 15 min. The purity of all peptides was determined using a Waters Alliance 2690 Analytical HPLC (Waters Corporation, Milford, MA, USA) and Vydac Protein and Peptide C18 reverse phase column, using a linear gradient of 0–70% Solvent B in Solvent A at a rate of 1% per minute. Linear peptides were purified to ≥ 95% purity by UV absorbance at 230 nm.

3.5.3 Solid Phase Peptide Synthesis on Microwave

Peptides were synthesized using solid phase Fmoc (fluorenylmethyloxycarbonyl) chemistry as described above on a Discover S-Class CEM microwave using Synergy software. Deprotection of the first Fmoc protecting group was performed using a 20% solution (*v/v*) of piperidine in *N*-methyl-2-pyrrolidone (NMP) with "Fmoc deprotection" program (power: 20 W, Time: 1:30 min, Temperature: 75˚C, Δ Temperature: 0˚C) on the microwave synthesizer followed by three washes of NMP. Double coupling was then preformed using a 4.0x equivalence of the amino acids, 0.4M *O*-(7-azabenzotriazol-1-yl)-*N*,*N*,*N*′,*N*′-tetramethyluronium hexafluorophosphate (HATU) and 1-hydroxy-7-azabenzotriazole (HOAt) in dimethylformamide (DMF) (2.5mL), 0.125M diisopropylethylamine (DIEA) (1mL), NMP (2.5mL), and the "Coupling" program (power: 20W, Time: 5:00 min, Temperature: 75˚C, Δ Temperature: 5˚C) on the microwave synthesizer. After each double coupling the resin was washed with three times with NMP. After the final "Fmoc deprotection" the resin was washed three times with NMP then three times with methylene chloride (DCM) and dried under vacuum. Cleavage, deprotection, and purification were then performed as described in *Section 3.4.3.*

3.5.4 Cell Lines and Membrane Preparations

C6-rat glioma cells stably transfected with a rat μ (C6-MOR) or rat δ (C6-DOR) opioid receptor [37] and Chinese hamster ovary (CHO) cells stably expressing a human κ (CHO-KOR) opioid receptor [38] were used for all in vitro assays. Cells were grown to confluence at 37ºC in 5% CO_2 in Dulbecco's Modified Eagle's Medium containing 10% fetal bovine serum and 5% penicillin/streptomycin. Membranes were prepared by washing confluent cells three times with ice cold phosphate-buffered saline (0.9% NaCl, 0.61 mM Na_2HPO_4, 0.38 mM KH_2PO_4, pH 7.4). Cells were detached from the plates by incubation in warm harvesting buffer (20 mM HEPES, 150 mM NaCl, 0.68 mM EDTA, pH 7.4) and pelleted by centrifugation at 200xg for 3 min. The cell pellet was suspended in ice-cold 50 mM Tris-HCl buffer, pH 7.4 and homogenized with a Tissue Tearor (Biospec Products, Inc, Bartlesville, OK, USA) for 20 s at setting 4. The homogenate was centrifuged at 20,000xg for 20 min at 4 C, and the pellet was rehomogenized in 50 mM Tris-HCl with a Tissue Tearor for 10 s at setting 2, followed by recentrifugation. The final pellet was resuspended in 50mM Tris-HCl and frozen in aliquots at -80ºC. Protein concentration was determined via Bradford assay using bovine serum albumin as the standard.

3.5.5 Radioligand Binding Assays

Opioid ligand-binding assays were performed using competitive displacement of 0.2 nM [^{3}H]diprenorphine (250 μCi, 1.85TBq/mmol) by the test compound from membrane preparations containing opioid receptors. The assay mixture, containing membrane suspension (20 μg protein/tube) in 50 mM Tris-HCl buffer (pH 7.4), [^{3}H]diprenorphine, and various concentrations of test peptide, was incubated at room temperature for 1 h to allow binding to reach equilibrium. The samples were rapidly filtered through Whatman GF/C filters using a Brandel harvester (Brandel, Gaithersburg, MD, USA) and washed three times with 50 mM Tris-HCl buffer. The radioactivity retained on dried filters was determined by liquid scintillation counting after saturation with EcoLume liquid scintillation cocktail in a Wallac 1450 MicroBeta (Perkin-Elmer, Waltham MA, USA). Nonspecific binding was determined using 10 μM naloxone. K_i values were calculated using nonlinear regression analysis to fit a logistic equation to the competition data using GraphPad Prism version 5.01 for Windows. The results presented are the mean ± standard error from at least three separate assays performed in duplicate.

3.5.6 Stimulation of [^{35}S]GTPγS Binding

Agonist stimulation of [^{35}S] guanosine 5'-O-[gamma-thio]triphosphate ([^{35}S]GTPγS, 1250 Ci, 46.2TBq/mmol) binding was measured as described previously [39]. Briefly, membranes (10-20 μg of protein/tube) were incubated 1 h at room temperature in GTPγS buffer (50 mM Tris-HCl, 100 mM NaCl, 5 mM $MgCl_2$, pH 7.4) containing 0.1 nM [^{35}S]GTPγS, 30 μM guanosine diphosphate **(**GDP), and varying concentrations of test peptides. Peptide stimulation of [^{35}S]GTPγS was compared with 10 μM standard compounds [D-Ala^2, N-MePhe^4, Gly-ol]-enkephalin (DAMGO) at MOR, D-Pen^{2,5}- enkephalin (DPDPE) at DOR, or U69,593 at KOR. The reaction was terminated by rapidly filtering through GF/C filters and washing ten times with GTPγS buffer, and retained radioactivity was measured as described above. The results presented are the mean ± standard error from at least three separate assays performed in duplicate; maximal stimulation was determined using nonlinear regression analysis with GraphPad Prism.

3.5.7 Receptor Modeling

The homology modeling of opioid receptors in complexes with peptide ligands was performed as previously described. [8, 22, 40] The procedure included the following steps: 1) residue substitution in corresponding structural template(s); 2) rigid body helix movement to reproduce structural rearrangement during receptor activation observed in crystal structures of rhodopsin and adrenergic receptor; [41] 3) peptide ligand docking in accordance with mutagenesis-derived constraints; and 4) refinement of receptor-ligand complex using distance geometry and energy minimization with CHARMm. The validity of this modeling procedure has been assessed in blind prediction experiments of structural modeling of MOR, [8, 22] A_{2a}-adenosine receptor, [42] CXCR4, and D3 dopamine receptor [40] performed before the release of the corresponding crystal structures. The following comparison with experimental structures showed relatively high accuracy of our homology models: rmsd were between 1.5 and 2.5 Å for seven transmembrane helices [40, 42]. A comparison of our previously developed opioid receptor models [8, 22, 28, 43] and recently released crystal structures of the mouse MOR [44] and the human KOR [45] demonstrated the high reliability in prediction of ligand-receptor interactions in the more conserved "message" region located deeply in the ligand binding pocket, and less precise modeling in the "address" region of flexible extracellular loops which are responsible for ligand selectivity. Despite some inaccuracies, the previous models suggested the important role of interactions between Met^{199} and Trp^{284} of DOR and pentapeptide Phe^3 and Phe^4 side chains, respectively, and aromatic interactions between pentapeptide Phe^4 side chain and residues from the extracellular loop 2. [8, 9, 28, 43] Here we used X-ray structures of MOR (PDB ID: 4dkl) and KOR (PDB ID: 4djh) to refine the models of MOR and KOR complexes with antagonists, especially in the variable loop regions, and to develop the homology model of antagonist-bound conformation of the human DOR (UniProt ID: P41143, residues 46-333). Further, we used the crystal structure of the human KOR (PDB ID: 4djh) together with our previous models of active conformations of opioid receptors [8, 22] for modeling of the active conformations of MOR, DOR, and KOR, which are appropriate for agonist docking.

3.6 References

1. Heyman, J.S., et al., *Modulation of Mu-Mediated Antinociception by Delta Agonists: Characterization with Antagonists.* European Journal of Pharmacology, 1989. **169**: p. 43-52.
2. Heyman, J.S., et al., *Modulation of Mu Mediated Antinociception by Delta Agonists in the Mouse: Selective Potentiation of Morphine and Normorphine by [DPen2,DPen5]enkephalin.* European Journal of Pharmacology, 1989. **165**: p. 1-10.
3. Horan, P., et al., *Antinociceptive Interactions of Opioid Delta Receptor Agonists with Morphine in Mics: Supra- and Sub-Additivity.* Life Sciences, 1992. **50**: p. 1535-1541.
4. Lowery, J.J., et al., *In Vivo Characherization of MMP-2200, a Mixed Mu/Delta Opioid Agonist, in Mice.* The Journal of Pharmacology and Experimental Therapeutics, 2011. **336**: p. 767-778.
5. Abdelhamid, E.E., et al., *Selective Blockage of the Delta Opioid Receptors Prevents the Development of Morphine Tolerance and Dependence in Mice.* The Journal of Pharmacology and Experimental Therapeutics, 1991. **258**(1): p. 299-303.
6. Fundytus, M.E., et al., *Attenuation of Morphine Tolerance and Dependence with the Highly Selective Delta Opioid Receptor Antagonist TIPP(psi).* European Journal of Pharmacology, 1995. **286**: p. 105-108.
7. Hepburn, M.J., et al., *Differential Effects of Naltrindole on Morphine-Induced Tolerance and Physical Dependence in Rate.* The Journal of Pharmacology and Experimental Therapeutics, 1997. **281**(3): p. 1350-1356.
8. Purington, L.C., et al., *Pentapeptides Displaying Mu Opioid Receptor Agonist and Delta Opioid Receptor Partial Agonist/Antagonist Properties.* Journal of Medicinal Chemistry, 2009. **52**: p. 7724-7731.
9. Schiller, P.W., *Bi- or Multifunctional Opioid Peptide Drugs.* Life Sciences, 2009. **86**: p. 598-603.
10. Purington, L.C., et al., *Development and in Vitro Characterization of a Novel Bifunctional Mu-Agonist/Delta-Antagonist Opioid Tetrapeptide.* Journal of Chemical Biology, 2011. **6**: p. 1375-1381.
11. Anand, J.P., et al., *Modulation of opioid receptor ligand affinity and efficacy using active and inactive state receptor models.* Chemical biology & drug design, 2012. **80**(5): p. 763-70.
12. Egelton, R.D. and T.P. Davis, *Development of Neuropeptide Drugs that Cross the Blood-Brain Barrier.* NeuroRx, 2005: p. 44-53.
13. El-Andaloussi, S., T. Holm, and U. Langel, *Cell Penetrating Peptides: Mechanisms and Applications.* Current Pharmaceutical Design, 2005. **11**: p. 3597-3611.
14. Li, Y., et al., *Opioid Glycopeptide Analgesics Derived from Endogenous Enkephalins and Endorohins.* Future Medicinal Chemistry, 2012. **4**(2): p. 205-226.
15. Gray, A.C., I.M. Coupar, and P.J. White, *Comparison of opioid receptor distributions in the rat central nervous system.* Life Sciences, 2006. **79**: p. 674-685.
16. Mansour, A., et al., *Opioid-receptor mRNA Expression in the Rat CNS: Anatomical and Functional Implications.* Trends in Neuroscience, 1995. **18**(1): p. 22-29.
17. Trescot, A.M., et al., *Opioid Pharmacology.* Pain Physician, 2008. **11**(Second Supplememt): p. S133-S153.

18. Banks, W.A., *Delivery of Peptides to the Brain: Emphasis on Therapeutic Development.* Peptide Science, 2008. **90**(5): p. 589-594.
19. Begley, D.J., *Delivery of Therapeutic Agents to the Central Nervous System: Problems and Possibilities.* Pharmacology and Therapeutics, 2004. **104**: p. 29-45.
20. Keyari, C.M., et al., *Glycosylenkephalins: Synthesis and Binding at the Mu, Delta, and Kappa Opioid Receptors. Antinocicpetion in Mice.* Advances in Experimental Medicine and Biology, 2009. **611**: p. 495-496.
21. Polt, R., M. Dhanasekaran, and C.M. Keyari, *Glycosylated Neuropeptides: A New Vista for Neuropsychopharmacology?* Medicinal Research Reviews, 2005. **25**(5): p. 557-585.
22. Purington, L.C., et al., *Development and in Vitro Characterization of a Novel Bifunctional Mu-Agonist/Delta-Antagonist Opioid Tetrapeptide.* ACS Chemical Biology, 2011. **6**: p. 1375-1381.
23. Zajac, J.M., et al., *Deltakephailn, Tyr-DThr-Gly-Phe-Leu-Thr: A New Highly Potent and Fully Specific Agonist for Opiate Delta Receptors.* Biochemical and Biophysical Research Communications, 1983. **111**(2): p. 390-397.
24. Fowler, C.B., et al., *Refinement of a Homology Model of the Mu-opioid Receptor Using Distance Constraints from Intrinsic and Engineered Zinc-binding Sites.* Biochemistry, 2004. **43**: p. 8700-8710.
25. Fowler, C.B., et al., *Complex of an Active Mu-opioid Receptor with a Cyclic Peptide Agonist Modeled from Experimental Constraints.* Biochemistry, 2004. **43**: p. 15796-15810.
26. Pogozheva, I.D., A.L. Lomize, and H.I. Mosberg, *The Transmembrane 7-alpha-bundle of Rhodopsin: Distance Geometry Calculations with Hydrogen Bonding Constraints.* Biophysics, 1997. **72**: p. 1963-1985.
27. Pogozheva, I.D., A.L. Lomize, and H.I. Mosberg, *Opioid Receptor Three-Dimensional Structures from Distance Geometry Calculations with Hydrogen Bonding Constraints.* Biophysics, 1998. **75**: p. 612-634.
28. Pogozheva, I.D., M.J. Przydzial, and H.I. Mosberg, *Homology Modeling of Opioid Receptor-Ligand Complexes Using Experimental Constraints.* AAPS Journal, 2005. **7**: p. 43-57.
29. Rozenfeld, R., et al., *An Emerging Role for the Delta Opioid Receptor in the Regulation of Mu Opioid Receptor Function.* Science World Journal, 2007. **7**: p. 4-73.
30. Land, B.B., et al., *The Dysphoric Component of Stress is Encoded by Activation of the Dynorphin Kappa-Opioid System.* Journal of Neuroscience, 2008. **28**(2): p. 407-414.
31. Pfeiffer, A., et al., *Psychotomimesis Mediated by Kappa Opioid Receptors.* Science, 1986. **233**: p. 774-776.
32. Xuei, X., et al., *Association of the Kappa-Opioid System with Alcohol Dependence.* Molecular Psychiatry, 2006. **11**(11): p. 1016-1024.
33. Berezowska, I., et al., *Replacement of the Tyr1 Hydroxyl Group of TIPP Peptides with N-(Alkyl)carboxamido Groups Results in Potent and Selective d Opioid Agonists or Antagonists.* Proceedings of the 21st American Peptide Symposium, 2009: p. 183-4.
34. Schiller, P.W., et al., *The TIPP Opioid Peptide Family: Development of detla Antagonists, delta Agonists, and Mixed mu Agonist/ delta Antagonists.* Biopolymers (Peptide Synthesis), 1999. **51**: p. 411-425.

35. Lefever, M.R., et al., *Glyscoslation of a-Amino Acids by Sugar Acetate Donors with InBR3 Minimally Competent Lewis Acids.* Carbohydrate Research, 2012. **351**: p. 121-125.
36. Przydzial, M.J., et al., *Roles of Residues 3 and 4 in Cyclic Tetrapeptide Ligand Recognition by the Kappa Opioid Receptor.* Journal of Peptide Research, 2005. **26**: p. 333-342.
37. Lee, K.O., et al., *Differential Binding Properties of Oripavines at Cloned Mu- and Delta-Opioid Receptors.* European Journal of Pharmacology, 1999(378): p. 323-330.
38. Husbands, S.M., et al., *BU74, A Complex Oripavine Derivative with Potent Kappa Opioid Receptor Agonism and Delayed Opioid Antagonism.* European Journal of Pharmacology, 2005(509): p. 117-135.
39. Traynor, J.R. and S.R. Nahorski, *Modulation by Mu-Opioid Agonists of Guanosine-5'-O(3-[35S]thio)triphosphate Binding to Membranes from Human Neuroblastoma SHY5Y Cells.* Molecular Pharmacology, 1995(47): p. 848-854.
40. Kufareva, I., et al., *Status of GPCR Modeling and Docking as Reflected by Community-wide GPCR Dock 2010 Assesment.* Structure, 2011. **19**: p. 1108-1126.
41. Congreve, M., et al., *Progress in Structure Based Drug Design for G Protein-Coupled Receptors.* Journal of Medicinal Chemistry, 2011. **54**: p. 4283-4311.
42. Michino, M., et al., *Community-wide Assesment of GPCR Structure Modeling and Ligand Docking.* Nature Reviews Drug Discovery, 2008. **8**: p. 455-463.
43. Mosberg, H.I., et al., *Cyclic Disulfide and Dithioether-Containing Opioid Tetrapeptides: Development of a Ligand with Enhanced Delta Opioid Receptor Selectivity and Potency.* Life Sciences, 1988. **43**: p. 1013-1020.
44. Manglik, A., et al., *Crystal Structure of the Mu Opioid Receptor Bound to a Morphinan Antagonist.* Nature, 2012. **doi: 10.1038/nature10954**.
45. Wu, H., et al., *Structure of the Human Kappa Opioid Receptor in Complex with JDTic.* Nature, 2012: p. doi:10.1038/nature10939.
46. Lomize, A.L., et al., *Conformational Analysis of the Delta Receptor Selective Cyclic Opioid Peptide Tyr-c[DCys-Phe-DPen]OH (JOM13). Comparison of X-ray Cystallographic Structures, Molecular Mechanics Simulations, and 1H NMR Data.* Journal of the American Chemical Society, 1994. **116**: p. 429-436.

CHAPTER 4

Opioid Receptor Trafficking Patterns

4.1 Introduction

As discussed in Chapters 1, 2, and 3, it has been demonstrated that the co-administration of a mu opioid receptor (MOR) agonist with either a delta opioid receptor (DOR) agonist or antagonist changes the *in vivo* pharmacology observed, limiting the development of tolerance to and dependence on MOR agonists, potentiating antinociception, and in some cases reducing self-administration. However, the molecular underpinnings of this phenomenon are not well understood. We know that opioid receptors, like all GPCRs, are surface expressed receptors that bind extracellular ligands and couple to intracellular downstream signaling partners. We also know that upon exposure to agonist, opioid receptors are first desensitized, then internalized into intracellular vesicles, and are then either recycled to the plasma membrane as re-sensitized receptors or degraded. This cycle of agonist binding, desensitization and internalization has been linked to development of tolerance [1-6]. As described in Chapters 1.1 and 1.3, there is a growing body of literature that suggests that many GPCRs oligomerize both *in vitro* and *in vivo* [7-9]. It has been proposed that oligomers, usually dimers, are the native functional state of opioid receptors and homo- and heterodimerization can be used to explain the wide range of functional pharmacology seen *in vivo* and under various conditions *in vitro* [10-16].

Several studies have suggested that MOR and DOR heterodimerize to form unique ligand binding and G protein activating units [9, 17-19]. This theory has been used to explain the effect that DOR and DOR ligands have on the potency and efficacy of MOR agonists, as well as the development of negative side effects and neurochemical adaptations to MOR agonists [20-25] and proposes that the native receptor state for MOR and DOR is either a homo- or heterodimer. This theory has gained support as MOR and DOR have been shown to co-localize in the dorsal

root ganglion [26-28], a region of the brain associated with pain signaling. However, previous work in the GPCR field has shown that some Class A GPCRs are able to function as monomers and that oligomerization is not necessary for normal binding and signaling in all GPCR systems [29-34]. An exploration of the viability of monomeric MOR can be found in Appendix B and is discussed in reference [35]. These data raise questions about the necessity of oligomerization for opioid function and the role that oligomerization may play *in vivo.*

At the present time researchers are deeply divided on the issue of functional opioid receptor oligomerization and whether or not it is necessary for the basic activity of the opioid receptors *in vivo*. Until recently, experiments exploring the interaction of various membrane bound receptors, such as the opioid receptors, were limited to ensemble measurements over a large population of cells (for a review of methods used see the following paper [9]). This allowed for generalizations about trends in the binding or efficacy of ligands, changes in the development of various conditions or biomarkers, or association through various intermediates, but did not speak to direct interactions between two or more receptors; measuring single molecule binding events and tracking individual receptors was below the detection limit of most techniques. However, with the correct tools, the trafficking and localization of receptors can now be monitored through fluorescence microscopy. In this chapter I will describe the design of probes and live cell platforms with which to explore the co-localization and trafficking of MOR and DOR in a single cell. With these tools I will explore how DOR and DOR ligands affect MOR trafficking and discuss what this means for the MOR/DOR effects which have been described in previous chapters.

4.2 Fluorescent Peptide Probes

4.2.1 Selective Fluorescent Opioid Ligand Design and in vitro *Pharmacological Testing*

In order to explore the function and trafficking of native opioid receptors using fluorescence microscopy we must first design selective, fluorescent ligands to use as probes. To develop these probes we started with highly selective MOR and DOR ligands and added either a Cys or Lys residue as a handle for conjugation with the fluorophores through a maleimide or NHS ester linkage, respectively. Using literature precedent [36] and our models [25, 37-44], we have determined that, generally speaking, the C-terminus of opioid peptides is the best place to

add large hydrophobic, highly conjugated substituents, such as fluorophores, without drastically altering the binding or efficacy of the ligand. As will be described later, labeling with fluorophores often results in compounds that are slightly less potent at the targeted receptor and a loss of selectivity relative to the parent compound. By examining our homology models we determined that the loss in potency is likely due to added steric bulk which hinders binding to the target receptor and that the loss of selectivity is probably caused by non-specific hydrophobic interactions between the fluorophore and the extracellular loops of the off target receptors. Consequently, the selection of the correct fluorophore is important. We initially began with the Alexafluor series of dyes, as they are fairly soluble in aqueous solutions, come in a wide variety of excitation/emission spectra, and have been used in a literature precedent with minimal loss of affinity and selectivity [36]. Unfortunately, this series of dyes was not bright enough for our purposes and was also unstable under our visualization conditions and rapidly photobleached, making time course studies unfeasible. We subsequently switched to the Cyanine dyes, Cy3 and Cy5, as they have convenient excitation/emission spectra, are cost-effective, have high quantum yields, and are photo-stable under our purification, assay, and visualization conditions.

Based on literature precedent [36], I have developed a selective, peptidic MOR ligand labeled with the fluorescent dye Cy3, [Lys^7,Cys(Cy3)^8] dermorphin (**Figure 4.1**), using as a scaffold the known MOR agonist [Lys^7] dermorphin, an opioid peptide extracted from frog skin [45]. The addition of a C-terminal Cys to [Lys^7] dermorphin left the MOR affinity and efficacy[5] relatively unchanged, but significantly reduced the selectivity of the resulting compound, [Lys^7, Cys^8] dermorphin, relative to DOR. We then

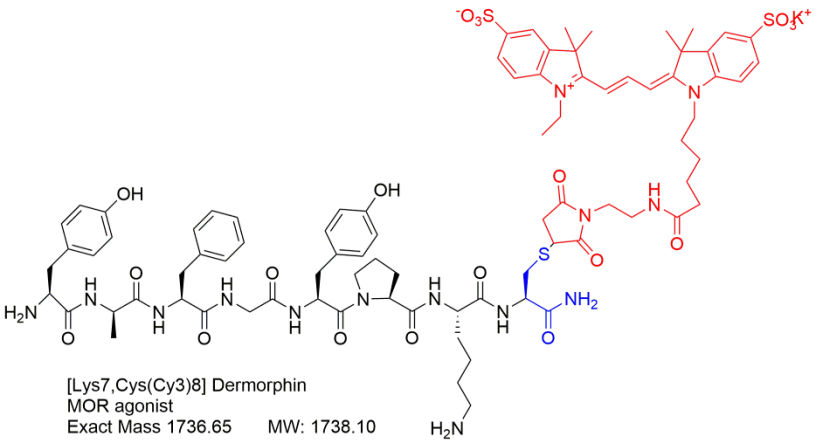

Figure 4.1: Structure of [Lys^7, Cys(Cy3)^8) Dermorphin –The core structure for dermorphin is shown in black, the C-terminal Cys extension shown in blue, and the Cy3 fluorophore shown in red.

[5] In this work "agonism" and "efficacy" refer to the ability of compounds to stimulate G protein turnover in the GTPγS assay. Details can be found in *Section 4.5.10.*

Table 4.1: *In Vitro* Binding and Efficacy Data for Selective Fluorescent MOR Agonists

	Sequence	Binding (nM)			MOR Efficacy	
		MOR	DOR	KOR	%	EC50 (nM)
[Lys7,Cys8] Dermorphin	Tyr-DAla-Phe-Gly-Tyr-Pro-Lys-Cys-NH2	0.4±0.03	240±60	240±140	104±4	18±8
[Lys7,Cys8] Dermorphin Cy3	Tyr-DAla-Phe-Gly-Tyr-Pro-Lys-Cys(Cy3)-NH2	3.8± 1.8	131±0	nd	95±3	6.2±0.1
[Lys7,Cys8] Dermorphin Cy5	Tyr-DAla-Phe-Gly-Tyr-Pro-Lys-Cys(Cy5)-NH2	11± 1	400±200	nd	nd	nd
[Lys7,Cys8] Dermorphin AF555	Tyr-DAla-Phe-Gly-Tyr-Pro-Lys-Cys(AF555)-NH2	3.5±0.5	530±140	nd	88±5	3.7±0.2
[Lys7, Cys8] Dermorphin AF488	Tyr-DAla-Phe-Gly-Tyr-Pro-Lys-Cys(AF488)-NH2	1.6±0.5	383±140	nd	nd	nd
[Lys7, Cys8] Dermorphin BodTMRX	Tyr-DAla-Phe-Gly-Tyr-Pro-Lys-Cys(BodTMRX)-NH2	0.45±0.04	37±1	nd	nd	nd

Binding affinities (K_i) were obtained by competitive displacement of radiolabeled [^{3}H] diprenorphine. Efficacy data were obtained using [^{35}S] GTPγS binding assay. Efficacy is represented as percent maximal stimulation relative to standard agonists DAMGO at 10μM . All values are expressed as mean ± SEM of three separate assays performed in duplicate. nd = not determined

conjugated various fluorophores to this modified dermorphin; the binding affinities and efficacies for the resulting analogues can be found in **Table 4.1**. We choose to use [Lys^7,Cys(Cy3)^8]dermorphin for our microscopy studies not only because it displays a desirable binding and efficacy profile, but also because the Cy dyes nicely fit our needs. As described above the Cy dyes are cost effective, have relatively high quantum yields, are photostable under our purification and assay conditions, were compatible with our microscopy facilities, and the resulting conjugated ligands are relatively straightforward to purify as compared to other fluorescently labeled derivatives.

We have also generated a selective, fluorescent, DOR antagonist, Dmt-Tic-Lys(Cy5)-OH (**Figure 4.2**), based on a previously reported selective DOR antagonist scaffold [46, 47]. (The selective fluorescent DOR antagonist Dmt-Tic-Lys(Cy5)-OH was developed and characterized by Dr. Mary F. Divin). Binding and efficacy data can be found in **Table 4.2.** Taken together, we have a MOR agonist/DOR antagonist pair that can be used with fluorescence microscopy to monitor the location of MOR and DOR in live cells.

We next sought to fill out our tool box in order to more thoroughly explore the MOR/DOR receptor/receptor interactions. While we are most interested in how a MOR agonist

and a DOR antagonist affect the trafficking, internalization, and recycling of opioid receptors, in order to fully explore the functional crosstalk between MOR and DOR a full complement of MOR and DOR ligands should be used. The state of the receptor (agonist bound vs. antagonist bound) affects the overall conformation of the receptor, may influence its ability to dimerize, and the receptors' association with downstream signaling partners and cellular scaffolding. This, in turn, may affect the trafficking of receptors or the apparent potency or efficacy of a given ligand. By monitoring the localization of MOR and DOR under various drug conditions we may be able to draw inferences as the mechanism(s) of DOR and DOR ligands' influence on MOR.

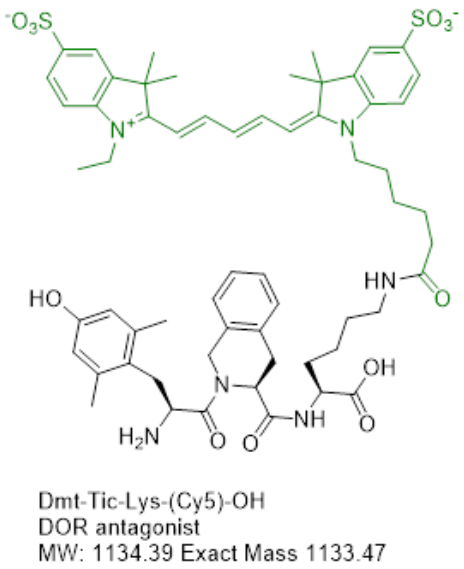

Figure 4.2: Structure of Dmt-Tic-Lys(Cy5)-OH –The core structure for Dmt-Tic-Lys is shown in black, and the Cy5 fluorophore shown in green.

Our efforts to generate a complete toolbox of MOR and DOR ligands have utilized various literature precedents to preserve or alter the selectivity and efficacy of reported ligands. Unfortunately, we have had a major problem with the selectivity of the ligands, especially after modification for and labeling with a fluorophore. Our various approaches have met with limited success; a more detailed description of our attempts to generate a selective, fluorescent MOR antagonist and DOR agonist can be found in Appendix A.

Table 4.2: *In Vitro* Binding and Efficacy Data for Selective Fluorescent DOR Antagonists

	Sequence	Binding (nM)			DOR Efficacy	
		MOR	DOR	KOR	%	Ke (nM)
Dmt-Tic-Lys-OH	Dmt-Tic-Lys-OH	>1,000	1.2±0.6	>10,000	dns	11.3±5.9
Dmt-Tic-Lys(Cy3)-OH	Dmt-Tic-Lys(Cy3)-OH	>1,000	4.6±1.2	>1,000	dns	8.5±2.3
Dmt-Tic-Lys(Cy5)-OH	Dmt-Tic-Lys(Cy5)-OH	>1,000	4.7±0.7	>1,000	dns	13.4±5.4

Binding affinities (K_i) were obtained by competitive displacement of radiolabeled [^{3}H] diprenorphine. Efficacy data were obtained using [^{35}S] GTPγS binding assay. The [^{35}S]GTPγS assay was used to determine agonist potency (EC_{50}, nM) and antagonist potency (K_e, nM) vs. known DOR agonist SNC80. All values are expressed as mean ± SEM of three separate assays performed in duplicate. dns = does not stimulate.

4.2.2 Fluorescent Ligand Viability as Probes for Confocal Microscopy in Live Cells

We have achieved some success in designing potent, selective fluorescent opioid ligands for MOR and DOR for use with confocal microscopy. We have in hand the two most interesting and clinically relevant types of opioid ligands in our toolbox: a selective fluorescent MOR agonist, [Lys^7, Cys(Cy3)^8] dermorphin, and a selective fluorescent DOR antagonist, Dmt-Tic-Lys(Cy5)-OH. [Lys^7, Cys(Cy3)^8] dermorphin potently and selectively binds to MOR and stimulates G protein turnover in membrane preparations, displaying full agonist character. When utilized in live cell fluorescence microscopy studies, [Lys^7, Cys(Cy3)^8] dermorphin is initially plasma membrane bound (**Figure 4.3C**) and the Cy3 signal internalizes over time to form intracellular puncta (**Figure 4.4C**). This signal pattern is consistent with initial binding of ligand to plasma membrane bound MOR and subsequent internalization of agonist bound MOR to intracellular vesicles. We have also demonstrated that this signal is blocked by the co-administration of 10 μM naloxone, indicating that this signal is an opioid specific one (data not shown.) Additionally, no signal is recorded when [Lys^7, Cys^8(Cy3)] dermorphin is administered to cells that express only DOR (data not shown.) This demonstrates the viability of [Lys^7,Cys (Cy3)^8] dermorphin as a MOR specific probe in live cell systems expressing both MOR and DOR.

When characterizing the DOR antagonist Dmt-Tic-Lys(Cy5)-OH in membrane preparations, we found that it potently and selectively bound to DOR, without stimulating the receptor. In live cells expressing DOR, fluorescence microscopy studies showed that Dmt-Tic-Lys(Cy5)-OH localized to the plasma membrane (**Figure 4.5**). The Cy5 signal from Dmt-Tic-Lys(Cy5)-OH was monitored over the course of 60 minutes at 37˚C and remained on the plasma membrane over this time period (data not shown). This is consistent with binding to plasma membrane bound DOR; the signal does not move over time as antagonist bound opioid receptors remain on the surface of the cell. Again, we have demonstrated that this signal is blocked by the co-administration of 10 μM naloxone, indicating that this signal is an opioid specific one (data not shown) and that no signal is recorded when Dmt-Tic-Lys(Cy5)-OH is administered to cells which express only MOR (data not shown). This demonstrates the viability of Dmt-Tic-Lys(Cy5)-OH as a DOR specific probe in live cell systems expressing both MOR and DOR.

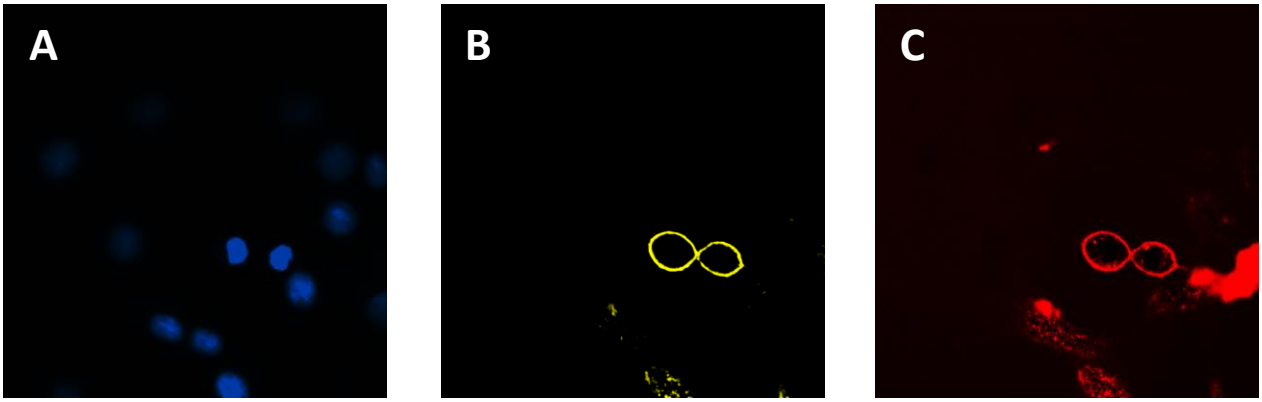

Figure 4.3: [Lys^7, Cys(Cy3)^8] Dermorphin on the Plasma Membrane - C6 cells stably expressing MOR treated with 5 ug/mL cellular stains and 100 nM [Lys^7, Cys (Cy3)^8] dermorphin for 10 mins on ice then washed an imaged at room temperature (total drug exposure approximately 15 mins). **(A)** Hoescht nuclear stain (cyan) **(B)** Wheat germ agglutinin AlexaFluor 488 plasma membrane stain (yellow) **(C)** MOR agonist [Lys^7, Cys (Cy3)^8] dermorphin (red). A clear Cy3 signal that co-localizes with the plasma membrane stain is shown, though intracellular puncta are already starting to form.

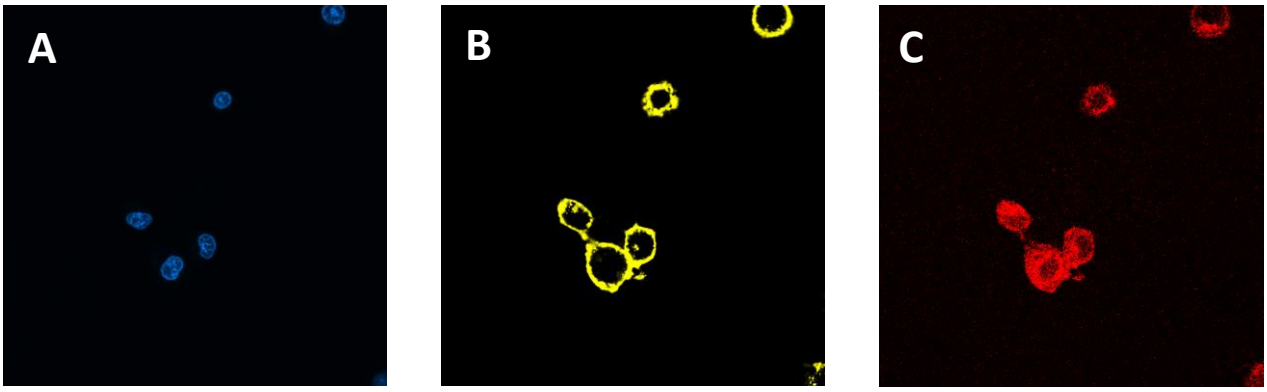

Figure 4.4: [Lys^7, Cys(Cy3)^8] Dermorphin Internalized – C6 cells stably expressing MOR treated with 5 ug/mL cellular stains and 100 nM [Lys^7, Cys^8(Cy3)] dermorphin for 20 mins at 37C then washed an imaged at 37C (total drug exposure approximately 25 mins). **(A)** Hoescht nuclear stain (cyan) **(B)** Wheat germ agglutinin AlexaFluor488 plasma membrane stain (yellow) **(C)** MOR agonist [Lys^7, Cys (Cy3) ^{8}] dermorphin (red). We can see that the Cy3 signal is internalized.

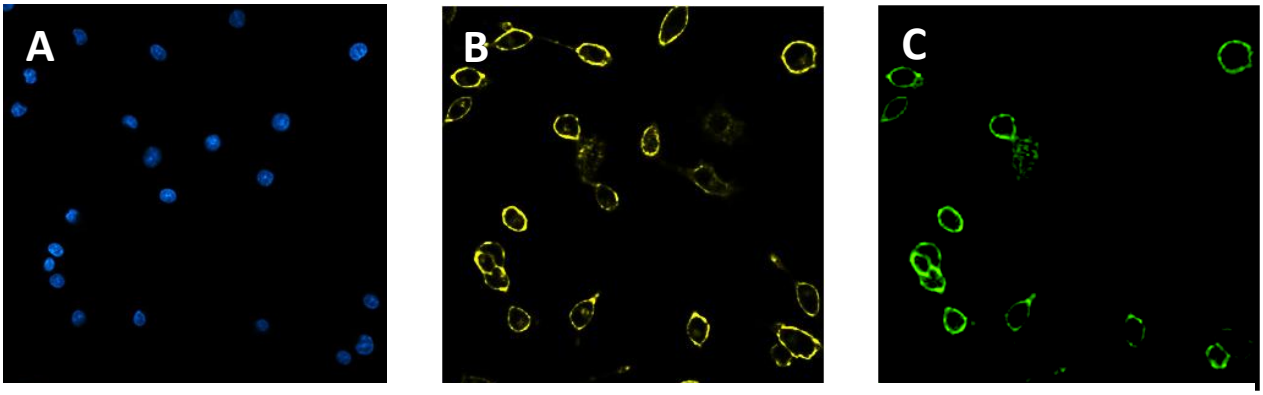

Figure 4.5: Dmt-Tic-Lys(Cy5)-OH on the Plasma Membrane – C6 cells stably expressing DOR treated with 5 ug/mL cellular stains and 100 nM Dmt-Tic-Lys(Cy5)-OH for 20 mins at 37C then washed an imaged at 37C **(A)** Hoescht nuclear stain (cyan) **(B)** Wheat germ agglutinin AlexaFluor 488 plasma membrane stain (yellow) **(C)** DOR antagonist Dmt-Tic-Lys(Cy5)-OH (green). We can see that the Cy5 signal co-localizes with the plasma membrane stain.

4.3 Live Cell Platforms to Monitor the Trafficking of MOR and DOR

The trafficking and expression patterns of opioid receptors are closely associated with their sensitivity and function. In fact, the development of tolerance to MOR agonists has been linked to a decrease in the number of active MORs available on the plasma membranes [48]. This decrease may be due to internalization of receptors after agonist treatment, which reduces the number of surface expressed receptors [1, 2]. Conversely, tolerance to MOR agonists has also been linked to a lack of internalization of MOR; it has also been proposed that MOR agonists that do not produce robust internalization, such as morphine, produce tolerance and dependence because internalization is necessary for re-sensitization of receptors and their subsequent trafficking to the cell surface [4-6, 49, 50].

In order to explore the effects of DOR and DOR antagonists on MOR trafficking we have used our selective, fluorescent, opioid ligands to monitor the trafficking and expression patterns of opioid receptors in live cell systems using fluorescence confocal microscopy. We have demonstrated that we can visualize both MOR and DOR in live cells expressing a single opioid receptor, monitor the trafficking (if any) in these cells, and that the dose of drug used is selective for the target receptor and does not interfere with imaging via fluoresence microscopy (see Chapter 4.2). However, in order to examine the trafficking of MOR and DOR, and how various drug combinations affect that trafficking, a cell line that expresses both MOR and DOR needs to be generated.

Plasmids encoding the untagged human and rat MOR and human and rat DOR (hMOR, rMOR, hDOR and rDOR respectively) with orthogonal antibiotic resistances have been generated. Both C_6 and HEK cells were stably transfected with hMOR and cell lines expressing hMOR at varying receptor expression levels were isolated and characterized. Attempts were then made to co-transfect these cell lines with hDOR. However no viable clones were isolated – cells either down-regulated receptor expression such that they were viable in selective media but did not express measurable levels of receptor or simply died in selective media. Attempts were then made to transfect our existing C_6 cells expressing rMOR with either rDOR or hDOR, however all of these attempts failed as well with cells either surviving selection but not expressing receptor or dying upon exposure to selective antibiotic. The reverse was then tried and C_6rDOR cells of

varying expression levels were transfected with hMOR or rMOR; all of these attempts also failed to produce viable clones that expressed both opioid receptors.

We next attempted to image binding of our fluorescent ligands to SH SY5Y cells; SHSY 5Y is a human derived neuroblastomal cell line which endogenously expresses both hMOR and hDOR. Unfortunately, expression levels were too low to see binding of fluorescent ligand using fluorescence confocal microscopy; experiments in SHSY 5Y cells were not pursued further.

A literature search yielded reports from the Devi lab [17] and the Whistler lab [51, 52] of cells that expressed low levels of both MOR and DOR and a report of CHO cells over-expressing both MOR and DOR from the Wang lab [53]. The Wang lab (University of Maryland) was contacted and a sample was obtained. Unfortunately, in our hands the B_{max} for total opioid receptor expression was approximately one third of that reported by the Wang lab and subsequent passages of these cells continued to lose receptor expression. By passage 5 these MOR/DOR CHO cells were expressing MOR and DOR at levels similar to SH SY5Y cells. A preliminary confocal microscopy experiment was attempted, but fluorescent ligand binding was below the detection limit and these cells were not pursued further for fluorescence microscopy use. The cells described by the Whistler lab were not thoroughly described in any publications and no further information on receptor expression levels or viability could be found.

An informal communication with the Devi lab, which works extensively with opioid receptor pharmacology, indicated that they have generated CHO cells that express low levels of both MOR and DOR [17], but that these cells lose receptor expression over time, in a manner similar to that which I found in my HEK and C_6 cell lines. Informal communications with the Akil, Wats, and Uhler labs, which were responsible for the initial cloning of the opioid receptors, yielded more information about early expression of the opioid receptors. Anecdotally, there is significant toxicity associated with the over-expression of opioid receptors; this goes a long way toward explaining why there are so few reports of cells stably over-expressing both MOR and DOR despite the interest in mixed efficacy ligands and MOR/DOR receptor-receptor interactions. This may also explain why the few viable clones which have been reported seem to down-regulate receptor expression over time and why few regions of the brain seem to co-express MOR and DOR in the same cell.

To side step the problem of stable co-expression of MOR and DOR we turned to transient transfection with fluorescently tagged receptors. We started with C_6 cells stably over-expressing rMOR and transfected in DOR. As the transfection efficiency of C_6 cells is relatively low we used cyan fluorescent protein (CFP) tagged hDOR (CDOR) to mark cells that express both the stable and transiently expressed receptors. We performed controls with CDOR to ensure that it behaved in a manner consistent with its unlabeled counterpart, DOR, when transiently expressed. C_6 wild type cells transiently expressing CDOR showed that CDOR was held primarily in internal stores, consistent with the expression pattern of unlabeled DOR [54, 55]. There was, however, enough surface expression of CDOR to bind our DOR selective antagonist Dmt-Tic-Lys(Cy5)-OH. The Cy5 signal only occurred on the plasma membrane of cells that expressed CDOR and remained there over time, consistent with the fact that opioid antagonists do not cause receptors to internalize (**Figure 4.6**).

Having confirmed that CDOR is expressed, binds antagonist, and remains surface expressed in a manner consistent with its unlabeled counterpart when transiently expressed in wild type cells, we next transiently transfected C_6rMOR with CDOR to determine if any difference in trafficking is noted when both receptors are present. We first examined the trafficking of Dmt-Tic-Lys(Cy5)-OH and [Lys^7, $Cys(Cy3)^8$] dermorphin independently to determine if the presence of both MOR and DOR in the same cells was enough to alter trafficking. Live C_6rMOR cells transiently expressing CDOR bound the delta antagonist Dmt-Tic-Lys(Cy5)-OH on the plasma membrane. Cells were imaged every 5 minutes for 30 minutes; the ligand remained plasma membrane bound over time, indicating that the presence of MOR does not alter the trafficking of antagonist bound DOR (**Figure 4.7**). Those C_6rMOR cells that did not express CDOR did not bind Dmt-Tic-Lys(Cy5)-OH. We next treated the live C_6rMOR transiently expressing CDOR with [Lys^7, $Cys(Cy3)^8$] dermorphin. Cells that expressed both MOR and CDOR bound and internalized MOR agonist in a manner similar to cells expressing only rMOR (**Figure 4.8**). Taken together, these experiments indicate that the presence of both MOR and DOR in the same cell does not alter the trafficking of MOR in the presence of a MOR agonist nor does it alter the trafficking of DOR in the presence of a DOR antagonist. This means that the effect of DOR on MOR agonist trafficking is not caused by the presence of the receptor itself, but rather by how the receptor/ligand complex interacts with MOR or other cell signaling partners.

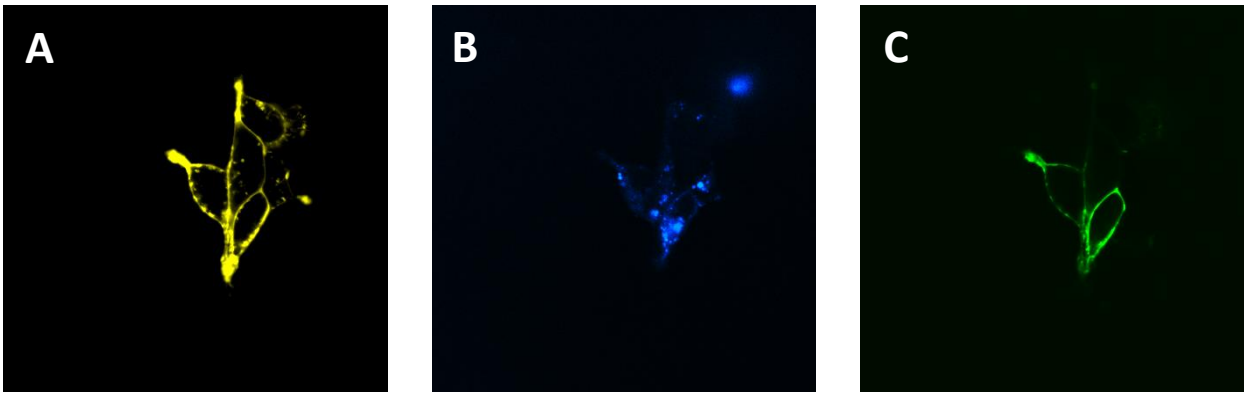

Figure 4.6: C6 Wild Type Cells Transiently Expressing CDOR Bind Dmt-Tic-Lys(Cy5)-OH – cells transiently expressing CDOR treated with 5 ug/mL cellular stains and 100 nM Dmt-Tic-Lys(Cy5)-OH for 50 mins at 37C then washed an imaged at 37C **(A)** Wheat germ agglutinin AlexaFluor488 plasma membrane stain (yellow) **(B)** CFP (cyan) **(C)** Dmt-Tic-Lys(Cy5)-OH (green) the Cy5 and plasma membrane co-localize with each other. The CFP signal is mostly held in internal stores; those cells with the strongest CFP signal bind the most DOR drug and show the strongest Cy5 signal.

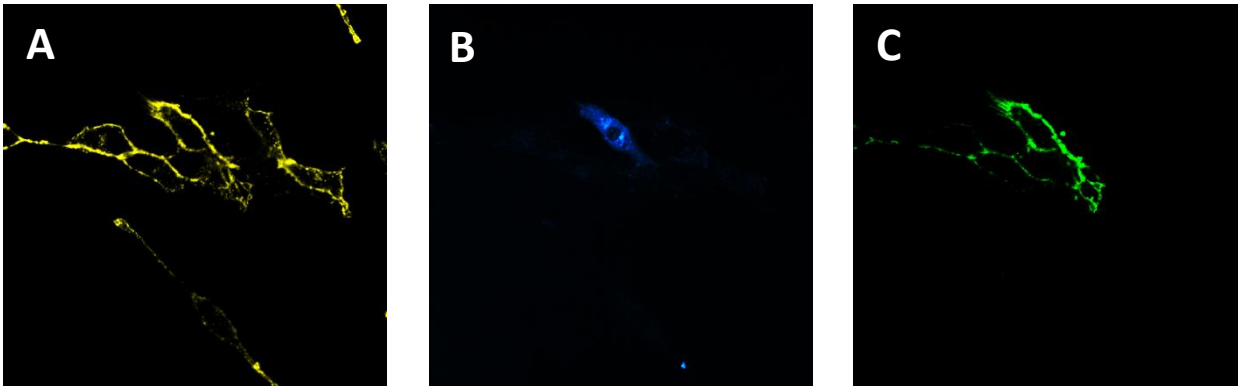

Figure 4.7: C6MOR Cells Transiently Expressing CDOR Bind Dmt-Tic-Lys(Cy5)-OH – cells stably expressing MOR and transiently expressing CDOR treated with 5 ug/mL cellular stains and 100 nM Dmt-Tic-Lys(Cy5)-OH for 5 mins at RT then washed an imaged at RT after 30 mins **(A)** Wheat germ agglutinin AlexaFluor488 plasma membrane stain (yellow) **(B)** CFP (cyan) **(C)** DOR antagonist Dmt-Tic-Lys(Cy5)-OH (green). We can see that the Cy5 and plasma membrane co-localize with each other. The CFP signal is mostly held in internal stores; those cells with the strongest CFP signal bind the most DOR drug and show the strongest Cy5 signal.

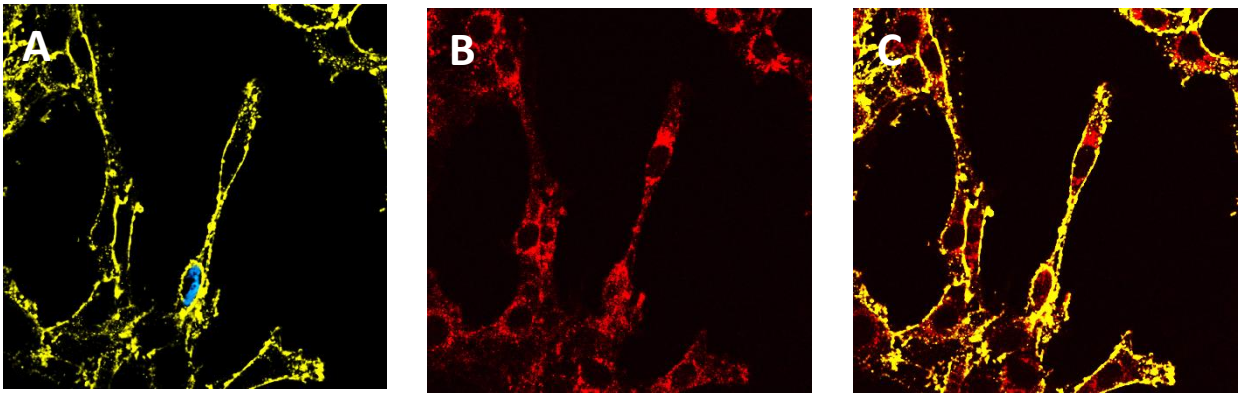

Figure 4.8: C6MOR Cells Transiently Expressing CDOR Bind and Internalize [Lys^7, Cys(Cy3)^8] Dermorphin – cells stably expressing MOR and transiently expressing CDOR treated with 5 ug/mL cellular stains and 100 nM [Lys^7, Cys(Cy3)^8] dermorphin 5 mins at RT then washed an imaged at RT after 30 mins **(A)** Wheat germ agglutinin AlexaFluor488 plasma membrane stain (yellow) and CFP (cyan) **(B)** MOR agonist [Lys^7, Cys(Cy3)^8] dermorphin (red). **(C)** Overlay of Cy3 and WGA488 signals. We can see that the Cy3 signal is internalized in all cells, regardless of the presence or absence of CDOR.

We next explored the effect of pre-treatment with DOR antagonist on MOR trafficking in cells that expressed both receptors. C_6rMOR cells transiently expressing CDOR were treated with the DOR antagonist Dmt-Tic-Lys(Cy5)-OH to ensure that all DOR binding sites were antagonist occupied. Cells were then co-treated with the MOR agonist, [Lys^7, Cys(Cy3)^8] dermorphin, and DOR antagonist Dmt-Tic-Lys(Cy5)-OH. Live cells were then imaged, the ligand only bound to cells expressing CDOR and remained on the surface of cells expressing both MOR and CDOR over time.

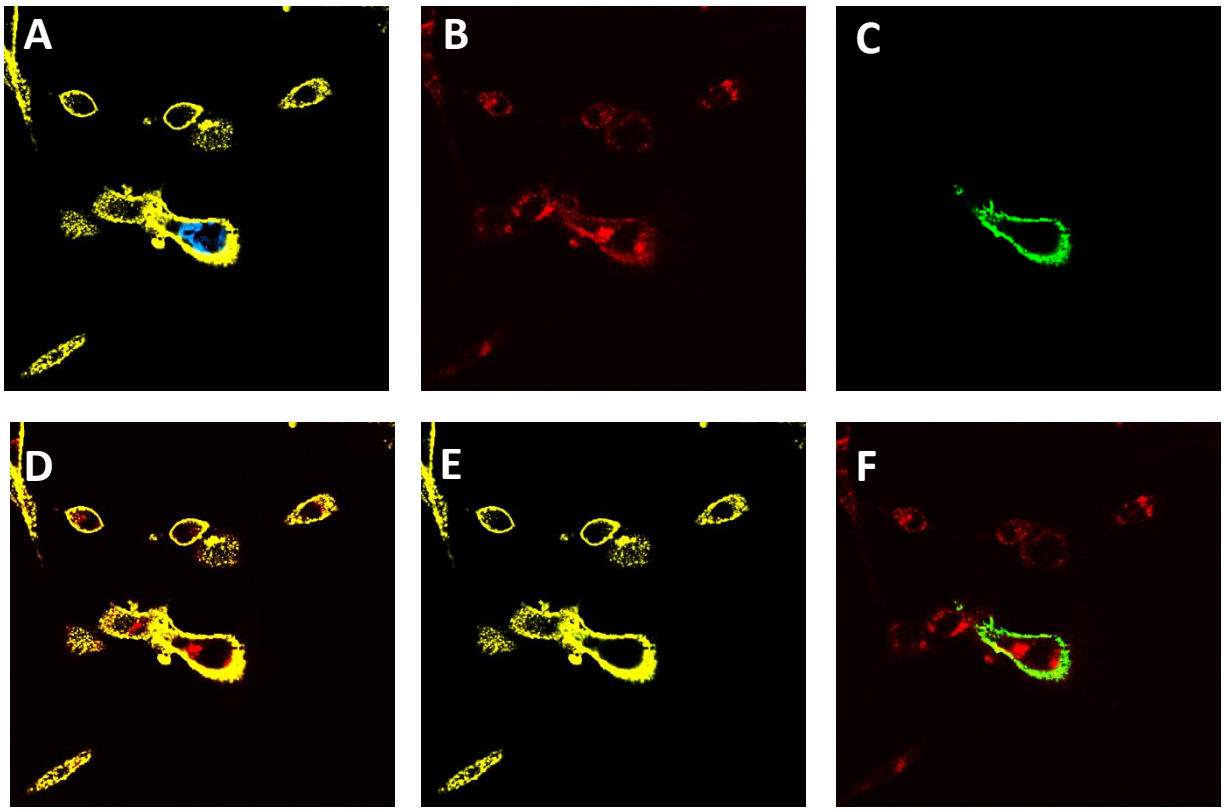

Figure 4.9: C6MOR Cells Transiently Expressing CDOR Pretreated with Dmt-Tic-Lys(Cy5)-OH, then Co-treated with Dmt-Tic-Lys(Cy5) and [Lys^7, Cys(Cy3)^8] Dermorphin – cells stably expressing MOR and transiently expressing CDOR treated with 5 ug/mL cellular stains and then pretreated with 100 nM Dmt-Tic-Lys(Cy5)-OH. Cells were then co-treated with 100 nM Dmt-Tic-Lys(Cy5)-OH and 100 nM [Lys^7, Cys(Cy3)^8] dermorphin 5 mins at RT then washed an imaged at RT after 30 mins **(A)** Wheat germ agglutinin 488 plasma membrane stain (yellow) and CFP (cyan) **(B)** MOR agonist [Lys^7, Cys(Cy3)^8] dermorphin (red). **(C)** DOR antagonist Dmt-Tic-Lys(Cy5)-OH (green) **(D)** Overlay of AF488 and Cy3 signals **(E)**Overlay of AF488 and Cy5 signals **(F)**Overlay of Cy3 and Cy5 signals. We can see that the Cy3 signal is internalized more robustly in cells that express CDOR and that the CDOR remains on the surface of the cell over time.

Interestingly, the trafficking of the MOR agonist, [Lys^7, Cys(Cy3)^8] dermorphin, was altered in cells that expressed both MOR and CDOR in the presence of DOR antagonist. Cells were pre-treated with Dmt-Tic-Lys(Cy5)-OH to occupy all DOR binding sites with a DOR

antagonist. Cells were then treated with both our MOR agonist, [Lys^7,Cys(Cy3)^8] dermorphin, and our DOR antagonist Dmt-Tic-Lys(Cy5)-OH. In cells that expressed both receptors, MOR internalized 1.66 ± 0.12 fold more robustly than in cells that expressed only MOR (n=6 images with 1-3 cells expressing both MOR and CDOR in each frame; **Figure 4.9**). It has been proposed that internalization of MOR is a key part of re-sensitization and leads to recycling of the sensitive receptor, increasing cell surface expression of functional opioid receptors [4-6, 49, 50]. I have observed that DOR antagonists increase MOR internalization. If increased internalization of MOR leads to increased recycling of MOR, this could explain how DOR antagonists reduce the development of tolerance, as reduced surface expression of active receptor is a cellular hallmark of tolerance [1-6].

The mechanism by which antagonist bound DOR increases MOR internalization and recycling upon exposure to MOR agonist is unclear. An explanation for these data involves the active and inactive receptor conformations and the G proteins they associate with. A simplified model of the association of GPCRs with G proteins and ligands states that agonists bind to the active conformation of the receptor and promote the association and turnover of G proteins while antagonists bind to the inactive conformation of the receptor and prevent the association of G proteins [56]. Given that MOR and DOR compete for the same pool of G proteins and other downstream signaling partners [57], increasing the amount of antagonist bound DOR would free G proteins to associate with MOR. This is particularly significant as DOR has a high basal signaling rate [58, 59], so that even in the absence of DOR agonist a measurable amount of G protein will be associated with DOR. By increasing the pool of available G protein, agonist bound MOR will be more able to associate with and turn over G proteins, increasing the apparent potency of MOR agonists and the rate at which receptors are marked for internalization and recycling. This may explain the ability of DOR antagonists to potentiate the potency of MOR agonists as well as the ability of DOR antagonists to slow the development of tolerance to MOR agonists.

4.4 Conclusions

The studies discussed in this chapter were designed to explore the changes in trafficking of MOR and DOR in the presence of a MOR agonist and a DOR antagonist, as this is a drug combination that has been shown to reduce the development of tolerance to and dependence on

MOR agonists [60-64]. A selective fluorescent MOR agonist, [Lys^7, Cys(Cy3)^8] dermorphin, and a selective fluorescent DOR antagonist, Dmt-Tic-Lys(Cy5)-OH, were designed and characterized. I have demonstrated these ligands behave as expected in live cells expressing only one opioid receptor and that they can be used to monitor the trafficking, or lack thereof, of both MOR and DOR. I have also developed a live cell platform stably expressing rMOR and transiently expressing hCDOR such that cells that express both receptors can be compared to cells that only express rMOR in the same frame and under exactly the same drug conditions. I have utilized these tools to explore how the trafficking of MOR is altered in the presence of CDOR and DOR antagonist.

I found that in the presence of DOR antagonist cells that expressed both MOR and CDOR, agonist bound MOR internalized more robustly than in cells that expressed only MOR. This effect was seen only in the presence of DOR antagonist; DOR itself had no effect on agonist induced MOR trafficking. Given these data, I hypothesize that DOR antagonists exert their effects on MOR agonist potency and tolerance in the following manner. Antagonist bound DOR encourages a receptor conformation which allows for the dissociation of G protein. As DOR has a high basal turnover rate [58, 59] and MOR and DOR share a pool of G proteins and other signaling partners [57] this allows for more robust stimulation, internalization, and recycling of MOR in the presence of a MOR agonist. Taken together, this increased trafficking allows for greater cell surface expression of functional opioid receptors [4-6, 49, 50], leading to improved MOR agonist potency and reduced development of tolerance to MOR agonists, features characteristic of the co-administration of MOR agonists with DOR antagonists [60-64].

Future work will explore the different effects of multifunctional ligands and drug cocktails on the trafficking of MOR and DOR. This will necessitate the development of a cell line that co-expresses two labeled receptors, as a multifunctional ligand will, by definition, bind to both MOR and DOR and therefore will not distinguish between the two receptors. Fluorescent labeling of MOR and DOR will, however, allow us to distinguish each receptor and will also expand the range of experiments that can be performed (e.g. drug cocktails of MOR agonist/DOR antagonist, MOR agonist/DOR agonist, MOR partial agonist/DOR antagonist, MOR agonist/DOR inverse agonist, various biased agonists for MOR and DOR or mixed efficacy ligands displaying any of these profiles) without the need for the difficult process of

designing fluorescent ligands that meet the desired pharmacological profile. This can be accomplished by transfecting cells with CDOR and a yellow-fluorescent protein labeled MOR (YMOR), for which I have already constructed plasmids with orthogonal antibiotic resistance. Preliminary experiments have already been performed with YMOR and I have shown that it behaves in a manner similar to unlabeled MOR in mammalian cells and that the YFP signal can be used to monitor the trafficking of MOR (*in vitro* mammalian cell data not shown and [35]). I have already generated stable cell lines that over-express YMOR. Transient transfection of these cells with CDOR will allow us to perform experiments similar to those described in Chapter 4.3, but with a wider range of drug cocktails and multifunctional ligands, further elucidating the effects of DOR ligands on MOR trafficking.

4.5 Materials and Methods

4.5.1 Materials

All reagents and solvents were purchased from commercial sources and used without further purification. All chemicals and biochemicals were purchased from Sigma Aldrich (St. Louis, MO, USA) or Fisher Scientific (Hudson, NH, USA), unless otherwise noted. All tissue culture reagents were purchased from Gibco Life Sciences (Grand Island, NY, USA). Restriction enzymes and other molecular biology tools were purchased from New England Biolabs (Ipswich MA). Radioactive compounds were purchased from Perkin-Elmer (Waltham, MA, USA). Peptide synthesis reagents, amino acids, and Rink resin were purchased from Advanced Chem Tech (Louisville, KY, USA). Wang resins were purchased from Nova Biochem, EMD (Gibbstown, NJ, USA). Cy3 and Cy5 mono-reactive dyes were purchased from GE Healthcare (Piscataway, NJ), Alexafluor dyes and Lipofectamine reagents were purchased from Invitrogen (Carlsbad, CA). Original plasmids encoding for CDOR and YMOR were a kind gift from Dr. Roger Sunahara (University of Michigan, Ann Arbor, USA). Plasmids encoding for unlabeled human MOR and DOR were purchased from cDNA.org (Rolla, MO, USA). cDNA coding for the rat mu opioid receptor (rMOR) and the rat delta opioid receptor (rDOR), both in pCMV6neo (ampicillin and neomycin resistance), were a kind gift from the Dr. Huda Akil (University of

Michigan, Ann Arbor, MI). All fluorescent microscopy images were taken at the Microscopy Image Analysis Laboratory (University of Michigan, Ann Arbor).

4.5.2 Solid-Phase Peptide Synthesis

Peptides were synthesized using standard solid phase Fmoc (fluorenylmethyloxycarbonyl) chemistry on a CS Bio CS336X Peptide Synthesizer (CS Bio Company, Menlo Park, CA, USA), using previously described protocols. [43] C-terminal amide peptides were synthesized using Rink resin. A 20% solution of piperidine in N-methyl-2-pyrrolidone (NMP) was used to remove the first Fmoc protecting group before synthesis and again to remove the Fmoc-protecting group after each coupling cycle. Coupling was performed using a four-fold excess of amino acid and a solution of 0.4 M hydroxybenzotriazole (HOBt) and O-benzotriazole-N,N,N',N'-tetramethyl-uroniumhexafluoro-phosphate (HBTU) in dimethylformamide (DMF), in the presence of diisopropylethylamine (DIEA). After the synthesis was complete, the resin was washed with NMP, then with dichloromethane, and dried under vacuum. The peptides were cleaved from the resin and side-chain-protecting groups removed by treatment at room temperature for 2 h with a cleavage cocktail consisting of 9.5 mL trifluoroacetic (TFA) acid, 0.25 mL triisopropylsilane (TIS) and 0.25 mL water for peptides with thiol containing side chains. All other peptides were cleaved with a cocktail containing 9.5 mL TFA and 0.5 mL water. The solution was concentrated *in vacuo*, and peptides were precipitated using cold, fresh diethylether. The filtered crude material was then purified using a Waters semipreparative HPLC (Waters Corporation, Milford, MA, USA) with a Vydac Protein and Peptide C18 column, using a linear gradient 10% Solvent B (0.1% TFA acid in acetonitrile) in Solvent A (0.1% TFA acid in water) to 60% Solvent B in Solvent A, at a rate of 1% per minute. The identity all peptides were determined ESI-MS performed on an Agilent Technologies LC/MS system using a 1200 Series LC and 6130 Quadrupole LC/MS (Agilent Technologies, Santa Clara, CA, USA) in positive mode with 50–100 µL injection volume and a linear gradient of 0% Solvent D (0.02% TFA and 0.1% acetic acid (AcOH) in acetonitrile) in Solvent C (0.02% TFA and 0.1% AcOH in water) to 60% Solvent D in Solvent C in 15 min. The purity of all peptides was determined using a Waters Alliance 2690 Analytical HPLC (Waters Corporation, Milford, MA, USA) and Vydac Protein and Peptide C18 reverse phase column, using a linear

gradient of 0–70% Solvent B in Solvent A at a rate of 1% per minute. Linear peptides were purified to ≥ 95% purity by UV absorbance at 230 nm.

4.5.3 Fluorescent Labeling

The purified peptide was labeled with Cy3 or Cy5 maleimide or NHS ester (GE Healthcare) according to the manufacturer's instructions using a ratio of 1.5:1 peptide to fluorophore. The labeled peptide was further purified via semi-preparative HPLC using a 5 micron Vydac C18 column as described above. The potency and efficacy labeled ligands confirmed in radiolabeled [^{3}H]DPN competition and [^{35}S]GTPγS binding assays.

4.5.4 Stable Cell Lines and Membrane Preparations

C6-rat glioma cells stably transfected with a rat μ (C6-MOR) or rat δ (C6-DOR) opioid receptor [65] and Chinese hamster ovary (CHO) cells stably expressing a human κ (CHO-KOR) opioid receptor [66] were used for all in vitro assays. Cells were grown to confluence at 37ºC in 5% CO_2 in Dulbecco's Modified Eagle's Medium containing 10% fetal bovine serum (FBS) and 5% penicillin/streptomycin. Membranes were prepared by washing confluent cells three times with ice cold phosphate-buffered saline (0.9% NaCl, 0.61 mM Na_2HPO_4, 0.38 mM KH_2PO_4, pH 7.4). Cells were detached from the plates by incubation in warm harvesting buffer (20 mM HEPES, 150 mM NaCl, 0.68 mM EDTA, pH 7.4) and pelleted by centrifugation at 200xg for 3 min. The cell pellet was suspended in ice-cold 50 mM Tris-HCl buffer, pH 7.4 and homogenized with a Tissue Tearor (Biospec Products, Inc, Bartlesville, OK, USA) for 20 s at setting 4. The homogenate was centrifuged at 20,000xg for 20 min at 4 C, and the pellet was rehomogenized in 50 mM Tris-HCl with a Tissue Tearor for 10 s at setting 2, followed by recentrifugation. The final pellet was resuspended in 50mM Tris-HCl and frozen in aliquots at -80ºC. Protein concentration was determined via Bradford assay using bovine serum albumin as the standard.

4.5.5 DNA Amplification and Purification

cDNA coding for the rat mu opioid receptor (rMOR) and the rat delta opioid receptor (rDOR), both in pCMV6neo (ampicillin and neomycin resistance), were a kind gift from the Dr. Huda Akil (University of Michigan, Ann Arbor, MI). cDNA for human MOR and DOR (hMOR and hDOR respectively) were purchased from cDNA.org (Rolla, MO, USA), both in

pcDNA3.1^{+}(ampicillin and geneticin resistance). cDNA encoding for the HA-Flag-His(10)-eYFP-hMOR and HA-Flag-His(10)-eCFP-hDOR, both in pcDNA3.1^{-}(ampicillin and geneticin resistance), were a kind gift from the Dr. Roger Sunahara (University of Michigan, Ann Arbor, MI). When stable co-transfection was desired, the gene of interest was clipped from its parent vector and using EcoRI and BamHI cut sites according to the manufacturer's protocol. An acceptor vector, pcDNAzeo^{+} ^{or} pcDNAzeo^{-} (Invitrogen, Carlsbad,CA), with ampicillin and zeocin antibiotic resistance was prepared with the same restriction enzymes and treated with calf alkaline phosphatase (New England Biolabs, Ipswich, MA) according to the manufacturer's protocol. The gene of interest and the acceptor vector were then ligated using T4 DNA ligase (New England Biolabs, Ipswich, MA) according to the manufacturer's protocol.

For amplification of DNA, XL10-Gold Ultracompetent *E. coli* (Agilent Technologies, Santa Clara, CA) were transformed according to the manufacturer's protocol and plated on LB agarose plates containing 100 µg/mL ampicillin for selection and grown at 37˚C overnight. Transformed colonies were picked and grown in 10 mL liquid LB media with 100 µg/mL ampicillin for 8 hours at 37˚C with shaking at 225 rpm. 250 mL liquid LB with 100 µg/mL ampicillin were then inoculated with 1-5 mL of the 8 hour culture and grown overnight hours at 37˚C with shaking at 225 rpm. Cells were then pelleted via centrifugation at 5,000 x g for 15 minutes and DNA was then purified using Qiagen MaxiPrep kits (Qiagen, Germantown, MD) according to the manufacturer's protocol.

Purified plasmids were digested with various restriction enzymes (HindIII, BglII, or XMaI) and run on a 1.2% (w/v) agarose gel with TAE buffer with 0.1% ethidium bromide (v/v) in 1X TAE at 80-100 V for 1.5 hours to determine the direction of insertion of the gene of interest; samples with the correct directionality were sent to the DNA sequencing Core (University of Michigan, Ann Arbor, MI) for complete sequencing to determine if the insertion of the gene of interest was correct.

4.5.6 Transient Transfection of Mammalian Cells

For transient transfection, mammalian cells, either HEK or C6, were grown to between 80 and 95 percent confluency in 6 cm dishes and transfected with 30 µL Lipofectamine 2000

(Invitrogen, Carlsbad, CA) and between 3 and 7 µg of purified DNA according to the manufacturer's protocol.

4.5.7 Stable Transfection of Mammalian Cells

Prior to transection, the minimum concentration needed to kill wild type HEK or C6 was determined for each antibiotic or combination of antibiotics, hereafter referred to as "selective media." For stable transfection, mammalian cells, either HEK or C6, were grown to between 80 and 95 percent confluency in 6 cm dishes and transfected with 30 µL Lipofectamine 2000 (Invitrogen, Carlsbad, CA) and between 7 and 10 µg of purified DNA according to the manufacturer's protocol. 24 hours post transfection cells were split with antibiotic free DMEM with 10% FBS at varying various concentrations (e.g. 1:5, 1:10, 1:20, etc) and incubated at 37˚C with 5% CO_2. 48 hours post transfection selective DMEM with 10% FBS was added to the cells and cells were incubated at 37˚C with 5% CO_2. Cells were grown at 37˚C with 5% CO_2 and media was exchanged every two days as non-transfected cells died off. When individual colonies of transfected cells emerged they were removed from the plate with 0.05% Trypsin with EDTA. Each individual colony was re-plated in 48 well plates and grown to confluency in selective media. As each clone reached confluency they were re-plated in larger and larger vessels in selective media until there were sufficient cells for a membrane preparation. Membrane preparations of each clone were prepared as described in section 4.5.4. Saturation binding assays were then performed as described in section 4.5.9 on membrane preparations to determine B_{max}.

4.5.8 Radioligand Binding Assays

Opioid ligand-binding assays were performed using competitive displacement of 0.2 nM [^{3}H]diprenorphine (250 µCi, 1.85TBq/mmol) by the test compound from membrane preparations containing opioid receptors. The assay mixture, containing membrane suspension (20 µg protein/tube) in 50 mM Tris-HCl buffer (pH 7.4), [^{3}H]diprenorphine, and various concentrations of test peptide, was incubated at room temperature for 1 h to allow binding to reach equilibrium. The samples were rapidly filtered through Whatman GF/C filters using a Brandel harvester (Brandel, Gaithersburg, MD, USA) and washed three times with 50 mM Tris-HCl buffer. The radioactivity retained on dried filters was determined by liquid scintillation counting after saturation with EcoLume liquid scintillation cocktail in a Wallac 1450 MicroBeta (Perkin-Elmer,

Waltham MA, USA). Nonspecific binding was determined using 10 μM naloxone. K_i values were calculated using nonlinear regression analysis to fit a logistic equation to the competition data using GraphPad Prism version 5.01 for Windows. The results presented are the mean ± standard error from at least three separate assays performed in duplicate.

4.5.9 Saturation Radioligand Binding Assays – Determining B_{max}

Opioid ligand-binding assays were performed using [^{3}H]diprenorphine (250 μCi, 1.85TBq/mmol). The assay mixture, containing membrane suspension (5-10 μg protein/tube) in 50 mM Tris-HCl buffer (pH 7.4), [^{3}H]diprenorphine ranging from 0 to 4 nM, and either water or 25μM naloxone, was incubated at room temperature for 1 h to allow binding to reach equilibrium. The samples were rapidly filtered through Whatman GF/C filters using a Brandel harvester (Brandel, Gaithersburg, MD, USA) and washed three times with 50 mM Tris-HCl buffer. The radioactivity retained on dried filters was determined by liquid scintillation counting after saturation with EcoLume liquid scintillation cocktail in a Wallac 1450 MicroBeta (Perkin-Elmer, Waltham MA, USA). Counts for nonspecific binding (naloxone) were substracted from total counts (water). Saturation values were calculated using saturation regression analysis using GraphPad Prism version 5.01 for Windows. The results presented are the mean ± standard error from at least three separate assays performed in duplicate.

4.5.10 Stimulation of [^{35}S]GTPγS Binding

Agonist stimulation of [^{35}S] guanosine 5'-O-[gamma-thio]triphosphate ([^{35}S]GTPγS, 1250 Ci, 46.2TBq/mmol) binding was measured as described previously [67]. Briefly, membranes (10-20 μg of protein/tube) were incubated 1 h at room temperature in GTPγS buffer (50 mM Tris-HCl, 100 mM NaCl, 5 mM $MgCl_2$, pH 7.4) containing 0.1 nM [^{35}S]GTPγS, 30 μM guanosine diphosphate **(**GDP), and varying concentrations of test peptides. Peptide stimulation of [^{35}S]GTPγS was compared with 10 μM standard compounds [D-Ala^2, N-MePhe^4, Gly-ol]-enkephalin (DAMGO) at MOR, D-Pen^{2,5}- enkephalin (DPDPE) at DOR, or U69,593 at KOR. The reaction was terminated by rapidly filtering through GF/C filters and washing ten times with GTPγS buffer, and retained radioactivity was measured as described above. The results presented are the mean ± standard error from at least three separate assays performed in

duplicate; maximal stimulation was determined using nonlinear regression analysis with GraphPad Prism.

4.5.11 Visualization of Live Cells Using Fluorescence Confocal Microscopy

Samples were imaged at ambient temperature unless otherwise specified using a 60 X water lens on an Olympus Fluo-View 500 laser scanning confocal microscope operating with FluoView FV500 *TIEMPO* software (Olympus Co, LTD, Melville, NY) at the Microscopy and Image Analysis Laboratory (University of Michigan, Biomedical Research Core Facility, Ann Arbor, MI). Samples were imaged using a four laser system includes 405 diode, multiline Argon, HeNe green and HeNe red and preprogramed filters. Invitrogen's SpectraViewer (Invitrogen, Carlsbad, CA) was used to choose appropriate laser and filter settings as well as informing our choice of cellular stains. Z stacks were 1 AU thick, set to either the 405 or 488 nm laser, whichever was in use at the time. Images were taken at 1024x1024 dpi resolution with Kalman line by line noise reduction over 4 to 8 scans.

24 hours prior to visualization, cells were split into sterile borosilicate chambered coverglasses (Lab-Tek, Fisher Scientific, Pittsburgh PA) such that they were approximately 65 to 85 percent confluent. All drug solutions for live cell sample imaging were diluted in serum and phenol red free DMEM – hereafter referred to as "media" – as fetal bovine serum (FBS) and phenol red auto-fluoresce in the Cy3 and Cy5 channels. Hoechst nuclear stain and Alexa Fluor conjugated wheat germ agglutinin plasma (WGA) membrane stains were acquired from Invitrogen (Carlsbad, CA) as lyophilized solids and 1mg/mL stock solutions were prepared in MilliQ water (EMD Millipore, Billerica, MA) and stored at -20˚C. Live cells samples were stained using 1µg/mL solutions of the cellular stains media for imaging. Stock solutions of purified fluorescent ligands were prepared at 100 µM in DMSO and stored at -20˚C. Live cell samples were exposed to 100 nM concentrations of fluorescent drug in media for imaging.

Unless otherwise specified, cells were first incubated with cellular stains in media for 10 minutes at room temperature and then washed with media and imaged to obtain control images. Cells were then incubated with drug solutions for 5 minutes at room temperature, then washed and imaged over time.

4.5.12 Quantification of Internalized [Lys^{7},Cys(Cy3)^{8}]Dermorphin

All analyses were performed on still images taken from fluorescence microscopy studies and were analyzed using Image Pro Premier version 9.0.3 (MediaCybernetics, Rockville, MD, USA). Macros for the automation of defining cell boundaries were designed by Jeff Knipe at MediaCybernetics. These boundaries were defined by smoothing the signal from the plasma membrane stain and allowed for manual separation of neighboring cells. The intensity of Cy3 signal within the cell boundaries was then measured. The Cy3 signal was divided over the area within each boundary to give an average intensity of Cy3 signal for each cell. The average intensity of signal in cells expressing both MOR and CDOR was then compared to the average intensity of signal for cells expressing only MOR in 6 separate images containing 1-3 cells that expressed both MOR and CDOR and at least 5 cells that expressed only MOR.

4.6 References

1. Bailey, C.P. and M. Connor, *Opioids: Cellular Mechanisms of Tolerance and Physical Dependence.* Current Opinion in Pharmacology, 2005. **5**: p. 60-68.
2. Ferguson, S.S., *Evolving Concepts in G Protein-Coupled Receptor Adaptation Mechanisms.* Pharmacology Reviews, 2001. **53**: p. 1-24.
3. von Zaztrow, M., et al., *Regulated Endocytosis of Opioid Receptors: Cellular Mechanisms and Proposed Roles in Physiological Adaptation to Opiate Drugs.* Current Opinion in Neurobiology, 2003. **13**: p. 348-353.
4. Martini, L. and J.L. Whistler, *The Role of Mu Opioid Receptor Densensitization and Endocytosis in Morphine Tolerance and Dependence.* Current Opinion in Neurobiology, 2007. **17**: p. 556-564.
5. He, L., et al., *Regulation of Opioid Receptor Trafficking and Morphine Tolerance by Receptor Oligomerization.* Cell, 2002. **08**: p. 271-282.
6. Whistler, J.L., et al., *Functional Dissociation of the My Opioid Receptor Signaling and Endocytosis: Implications for the Biology of Opiate Tolerance and Addiction.* Neuron, 1999. **23**: p. 737-746.
7. Bai, M., *Dimerization of G-protein-coupled receptors: roles in signal transduction.* Cell Signal, 2004. **16**(2): p. 175-86.
8. Milligan, G., et al., *The role of GPCR dimerisation/oligomerisation in receptor signalling.* Ernst Schering Found Symp Proc, 2006(2): p. 145-61.
9. Rios, C.D., et al., *G-protein-coupled Receptor Dimerization: Modulation of Receptor Function.* Pharmacology and Therapeutics, 2001. **92**: p. 71-87.
10. George, S.R., et al., *Oligomerization of mu and delta Opioid Receptors: Generation of Novel Functional Properties.* Journal of Biological Chemistry, 2000. **275**(34): p. 26128-26135.
11. Gomes, I., et al., *Heterodimerization of mu and delta Opioid Receptors: A Role in Opiate Synergy.* Journal of Neuroscience, 2000. **20**: p. 1-5.
12. Hazum, E., K.-J. Chang, and P. Cuatrecasas, *Opiate (Enkaphalin) Receptors of Neuroblastoma Cells: Occurrene in Clusters on the Cell Surface.* Science, 1979. **206**(4422): p. 1077-1079.
13. Hazum, E., K.-J. Chang, and P. Cuatrecasas, *Cluster Formation of Opiate (enkaphalin) Receptors in Neuroblastoma Cells: Differences between Agonists and Antagonists and Possible Relationships to Biological Functions.* Proceedings of the National Academy of Science USA, 1980. **77**(5): p. 3038-3041.
14. Law, P.-Y., et al., *Heterodimerization of mu - and delta-Opioid Receptors Occurs at the Cell Surface Only and Requires Receptor-G Protein Interactions.* Journal of Biological Chemistry, 2005. **280**(12): p. 11152-62.
15. Li-Wei, C., et al., *Homodimerization of the Human Mu-Opioid Receptor Overexpressed in Sf9 Insect Cells.* Protein and Peptide Letters, 2002. **9**: p. 145-152.
16. Pascal, G. and G. Millligan, *Functional Complementation and the Ananlysis of Opioid Receptor Homodimerization.* Molecular Pharmacology, 2005. **68**: p. 905-915.
17. Gomes, I., et al., *G Protein-Coupled Receptor Heteromerization: A Role in Allosteric Modulation of Ligand Binding.* Molecular Pharmacology, 2011. **79**(11): p. 1044-1052.
18. Gomes, I., et al., *Heterodimerization of the Mu and Delta Opioid Receptors: A Role in Opiate Synergy.* Journal of Neuroscience, 2000. **20**(22): p. RC110.

19. Rozenfeld, R., et al., *An Emerging Role for the Delta Opioid Receptor in the Regulation of Mu Opioid Receptor Function.* Science World Journal, 2007. **7**: p. 4-73.
20. George, S.R., et al., *Oligomerization of mu- and delta-opioid receptors. Generation of novel functional properties.* J Biol Chem, 2000. **275**(34): p. 26128-35.
21. Martin, N.A. and P.L. Prather, *Interaction of co-expressed mu- and delta-opioid receptors in transfected rat pituitary GH(3) cells.* Mol Pharmacol, 2001. **59**(4): p. 774-83.
22. Wang, D., et al., *Opioid receptor homo- and heterodimerization in living cells by quantitative bioluminescence resonance energy transfer.* Mol Pharmacol, 2005. **67**(6): p. 2173-84.
23. Gomes, I., et al., *Oligomerization of opioid receptors.* Methods, 2002. **27**(4): p. 358-65.
24. Gomes, I., et al., *Heterodimerization of mu and delta opioid receptors: A role in opiate synergy.* J Neurosci, 2000. **20**(22): p. RC110.
25. Mosberg, H.I., et al., *Cyclic Disulfide and Dithioether-Containing Opioid Tetrapeptides: Development of a Ligand with Enhanced Delta Opioid Receptor Selectivity and Potency.* Life Sciences, 1988. **43**: p. 1013-1020.
26. Wang, H.-B., et al., *Co-expression of the Delta and My Opioid Receptors in Nociceptive Sensory Neurons.* Proceedings of the National Academy of Science, 2010. **107**(29): p. 13117-13122.
27. Peng, J., S. Sarkar, and S.L. Chang, *Opioid Receptor Expression in Human Brain and Peripheral Tissues using Absolute Quantitative Real-Time RT-PCR.* Drug and Alcohol Dependence, 2012. **124**: p. 223-228.
28. Liu, N.-J., et al., *Cholecystokinin Octapeptide Reverses Mu-Opioid-Receptor Mediated Inhibition of Calcium Current in Rat Dorsal Root Ganglion Neurons.* The Joural of Pharmacology and Experimental Therapeutics, 1995. **275**(3): p. 1293-1299.
29. Leitz, A.J., et al., *Functional reconstitution of Beta2-adrenergic receptors utilizing self-assembling Nanodisc technology.* Biotechniques, 2006. **40**(5): p. 601-2, 604, 606, passim.
30. Nath, A., W.M. Atkins, and S.G. Sligar, *Applications of phospholipid bilayer nanodiscs in the study of membranes and membrane proteins.* Biochemistry, 2007. **46**(8): p. 2059-69.
31. Bayburt, T.H., et al., *Transducin activation by nanoscale lipid bilayers containing one and two rhodopsins.* J Biol Chem, 2007. **282**(20): p. 14875-81.
32. Whorton, M.R., et al., *A Monomeric G Protein-coupled Receptor Isolated in a High-density Lipoprotein Particle Efficiently Activates its G Protein.* Proc Natl Acad Sci USA, 2007. **104**(18): p. 7682-7687.
33. Whorton, M.R., et al., *Efficient Coupling of Transducin to Monomeric Rhodopsin in a Phospholipid Bilayer.* Journal of Biological Chemistry, 2008. **283**(7): p. 4387-4394.
34. Banerjee, S., T. Huber, and T.P. Sakmar, *Rapid incorporation of functional rhodopsin into nanoscale apolipoprotein bound bilayer (NABB) particles.* J Mol Biol, 2008. **377**(4): p. 1067-81.
35. Kuszak, A.J., et al., *Purification and functional reconstitution of monomeric mu-opioid receptors: allosteric modulation of agonist binding by Gi2.* The Journal of biological chemistry, 2009. **284**(39): p. 26732-41.
36. Arttamangkul, S., et al., *Binding and Internalization of Fluorescent Opioid Peptide Conjugates in Living Cells.* Molecular Pharmacology, 2000. **58**(6): p. 1570-1580.

37. Pogozheva, I.D., M.J. Przydzial, and H.I. Mosberg, *Homology Modeling of Opioid Receptor-Ligand Complexes Using Experimental Constraints.* AAPS Journal, 2005. **7**: p. 43-57.
38. Fowler, C.B., et al., *Refinement of a Homology Model of the Mu-opioid Receptor Using Distance Constraints from Intrinsic and Engineered Zinc-binding Sites.* Biochemistry, 2004. **43**: p. 8700-8710.
39. Fowler, C.B., et al., *Complex of an Active Mu-opioid Receptor with a Cyclic Peptide Agonist Modeled from Experimental Constraints.* Biochemistry, 2004. **43**: p. 15796-15810.
40. Lomize, A.L., et al., *Conformational Analysis of the Delta Receptor Selective Cyclic Opioid Peptide Tyr-c[DCys-Phe-DPen]OH (JOM13). Comparison of X-ray Cystallographic Structures, Molecular Mechanics Simulations, and 1H NMR Data.* Journal of the American Chemical Society, 1994. **116**: p. 429-436.
41. Pogozheva, I.D., A.L. Lomize, and H.I. Mosberg, *The Transmembrane 7-alpha-bundle of Rhodopsin: Distance Geometry Calculations with Hydrogen Bonding Constraints.* Biophysics, 1997. **72**: p. 1963-1985.
42. Pogozheva, I.D., A.L. Lomize, and H.I. Mosberg, *Opioid Receptor Three-Dimensional Structures from Distance Geometry Calculations with Hydrogen Bonding Constraints.* Biophysics, 1998. **75**: p. 612-634.
43. Przydzial, M.J., et al., *Roles of Residues 3 and 4 in Cyclic Tetrapeptide Ligand Recognition by the Kappa Opioid Receptor.* Journal of Peptide Research, 2005. **26**: p. 333-342.
44. Przydzial, M.J., et al., *Design of High Affinity Cyclic Pentapeptide Ligands for the Kappa Opioid Receptors.* Journal of Peptide Research, 2005. **66**: p. 255-262.
45. Erspamer, V., *The Opioid Peptides of the Amphibian Skin.* The International Journal of Developmental Neuroscience, 1992. **10**(1): p. 3-30.
46. Balboni, G., et al., *Direct Influence of C-Terminally Substituted Amino Acids in the Dmt-Tic Pharmacophore of Delta Opioid Receptor Selectivity and Antagonism.* Journal of Medicinal Chemistry, 2004. **47**(4066-4071).
47. Balboni, G., et al., *Highly Selective Fluorescent Analogue of the Potent delta-Opioid Receptor Antagonist Dmt-Tic.* Journal of Medicinal Chemistry, 2004. **47**: p. 6541-6546.
48. Bailey, C.P. and M. Connor, *Opioids: Cellular Mechanisms of Tolerance and Physical Dependence.* Current Opinion in Pharmacology, 2005. **5**(1): p. 60-8.
49. Finn, A.K. and J.L. Whistler, *Endocytosis of the Mu Opioid Receptor Reduced Tolerance and a Cellular Hallmark of Opiate Withdrawal.* Neuron, 2001. **32**: p. 829-839.
50. Whistler, J.L. and M. von Zaztrow, *Morphine-Activated Opioid Receptors Elude Desensitization by Beta-arrestin.* Proceedings of the National Academy of Science, 1998. **95**(17): p. 9914-9919.
51. Yekkirala, A.S., et al., *Clinically Employed Opioid Analgesics Produce Antinociception via Mu-Delta Receptor Heteromers in Rhesus Monkeys.* ACS Chemical Neuroscience, 2012. **3**: p. 720-727.
52. Waldhoer, M., et al., *A Heterodimer-Selective Agonist Shows In Vivo Relevance of G Protein-Coupled Receptor Dimers.* Proceedings of the National Academy of Science, 2005. **102**(25): p. 9050-9055.

53. Anathan, S., et al., *14-Alkoxy- and 14-Aculoxypyridomorphinans: Mu Agonist/Delta Antagonist Opioid Analgesics with Diminished Tolerance and Depenence Side Effects.* Journal of Medicinal Chemistry, 2012. **55**: p. 8350-8363.
54. Cheng, P.Y., et al., *Ultrasturcutual Immunolabeling Shows Prominent Presynaptic Vesicular Localization of the Delta Opioid Receptor withing both Endkphalin and Nonenkephalin Containing Axon Terminals in the Superficial Layers of the Rat Cervical Spinal Cord.* Journal of Neuroscience, 1995. **15**: p. 5976-5988.
55. Dado, R.J., et al., *Immunofluorescent Identification of a Delta Opioid Receptor on Primary Afferent Nerve Terminals.* NeuroReport, 1993. **5**(341-344).
56. Strasser, A. and H.-J. Wittmann, *Binding of Ligands to GPCRs - How Valid is a Thermodynamic Discrimination of Antagonists and Agonists.* Physical Chemistry and Biophysics, 2012: p. S1:001.
57. Levitt, E.S., L.C. Purington, and J.R. Traynor, *Gi/o Coupled Receptors Compete for Signaling to Adenylyl Cyclase in SH-SY5Y Cells and Reduce Opioid Mediated cAMP Overshoot.* Molecular Pharmacology, 2010. **79**(3): p. 461-471.
58. Wang, D., X. Sun, and W. Sadee, *Different Effects of Opioid Antagonists on Mu, Delta, and Kappa Opioid Receptors with and without Agonist Pretreatment.* Journal of Phamacology and Experimental Therapeutics, 2007. **321**: p. 544-552.
59. Costa, T. and A. Herz, *Antagonists with Negative Intrinsic Activity at Delta Opioid Receptors Coupled to GTP-binding Proteins.* Proceedings of the National Academy of Science, 1989. **86**: p. 7321-7325.
60. Abdelhamid, E.E., et al., *Selective Blockage of the Delta Opioid Receptors Prevents the Development of Morphine Tolerance and Dependence in Mice.* The Journal of Pharmacology and Experimental Therapeutics, 1991. **258**(1): p. 299-303.
61. Fundytus, M.E., et al., *Attenuation of Morphine Tolerance and Dependence with the Highly Selective Delta Opioid Receptor Antagonist TIPP(psi).* European Journal of Pharmacology, 1995. **286**: p. 105-108.
62. Hepburn, M.J., et al., *Differential Effects of Naltrindole on Morphine-Induced Tolerance and Physical Dependence in Rate.* The Journal of Pharmacology and Experimental Therapeutics, 1997. **281**(3): p. 1350-1356.
63. Purington, L.C., et al., *Pentapeptides Displaying Mu Opioid Receptor Agonist and Delta Opioid Receptor Partial Agonist/Antagonist Properties.* Journal of Medicinal Chemistry, 2009. **52**: p. 7724-7731.
64. Schiller, P.W., *Bi- or Multifunctional Opioid Peptide Drugs.* Life Sciences, 2009. **86**: p. 598-603.
65. Lee, K.O., et al., *Differential Binding Properties of Oripavines at Cloned Mu- and Delta-Opioid Receptors.* European Journal of Pharmacology, 1999(378): p. 323-330.
66. Husbands, S.M., et al., *BU74, A Complex Oripavine Derivative with Potent Kappa Opioid Receptor Agonism and Delayed Opioid Antagonism.* European Journal of Pharmacology, 2005(509): p. 117-135.
67. Traynor, J.R. and S.R. Nahorski, *Modulation by Mu-Opioid Agonists of Guanosine-5'-O(3-[35S]thio)triphosphate Binding to Membranes from Human Neuroblastoma SHY5Y Cells.* Molecular Pharmacology, 1995(47): p. 848-854.

CHAPTER 5

Conclusions

5.1 Overview of the Problem

Opioid analgesics are some of the most clinically effective compounds for treating chronic and acute pain in use today. Most clinically relevant opioid analgesics are mu opioid receptor (MOR) agonists. Unfortunately, MOR agonist analgesics have significant drawbacks, including the development of tolerance and dependence; MOR agonists also display euphorigenic qualities. Together these features limit the clinical usefulness of opioid analgesics and contribute to the social problems associated with their illicit use [1].

It has been demonstrated that the co-administration of a MOR agonist with either a delta opioid receptor (DOR) antagonist [2-5] or agonist [6-8] mitigates the development of tolerance and dependence and may even reduce the addiction liability associated with opioid use [9]. This project has explored the development of mixed efficacy MOR/DOR ligands and the functional crosstalk between the mu and delta opioid receptors.

5.2 Summary of Research

5.2.1 Development of Mixed Efficacy MOR/DOR Ligands

In order to exploit the desirable pharmacological profile displayed by the co-administration of a MOR agonist with either a DOR antagonist or agonist we sought to combine both functionalities into the same molecule. This approach is preferable to simply administering two selective ligands, as it eliminates potential problems associated with giving two separate chemical entities with possibly differing pharmacokinetic and metabolic profiles. Two families of mixed efficacy peptides were developed, cyclic and linear, which are described below.

5.2.2 Cyclic Mixed Efficacy MOR/DOR Peptides

Two series of cyclic mixed efficacy MOR agonist/DOR antagonist peptides were generated: a series of pentapeptides based on a previously developed non-selective opioid agonist, **MP-143** (MP compounds synthesized by Maggie Przydzial), and a series of tetrapeptides that improved upon a previously developed mixed efficacy ligand, **KSK-102** (KSK compounds synthesized by Kate Sobczyk-Kojiro). Information from our previously described homology models of the active and inactive states of MOR, DOR, and the kappa opioid receptor (KOR) [10-16] was used to guide the development of these ligands.

Replacement of the Phe^4 in the pentapeptide series drastically reduced KOR binding and efficacy. Docking studies showed that Phe^4 of **MP-143** is in close proximity to Tyr^{219} in the KOR active site and they likely form a favorable π-π stacking interaction. By replacing Phe^4 of the ligand with an aliphatic residue problematic KOR agonist activity is removed while preserving MOR and DOR binding and efficacy.

We next sought to reduce DOR efficacy, as we wanted to design a mixed efficacy MOR agonist/DOR antagonist. As the binding pocket for active DOR is narrower than the active MOR binding pocket we reasoned that increased steric bulk would selectively produce a steric clash in the DOR active site, thereby reducing DOR efficacy. We explored several factors: the size of the cycle between the second and fifth bridging residues, the stereochemistry of the amino acid in the fifth position, and both carboxylic acid and carboxamide C-termini. This proved to be a successful strategy. We developed two promising mixed efficacy pentapeptides – **LP-32** (LP compounds synthesized by Lauren Purington) and **JPAM3 (SS)** – demonstrating the validity of our homology models and making progress toward our goal of developing cyclic MOR agonist/DOR antagonist peptides. However, it is worth noting that in this series the reduction in DOR efficacy was not totally selective. In the instances where DOR efficacy was greatly reduced DOR binding and MOR efficacy were often negatively affected.

The next stage in the development of cyclic mixed efficacy ligands was the exploration of our tetrapeptide scaffolds. This series contained only one hydrophobic residue within the cyclized portion of the molecule. In this series the size and flexibility of the residue in the third position and the size of the cyclization between the bridging second and fourth residues were

altered to exploit the difference in the MOR and DOR active sites. We sought to balance MOR and DOR binding and remove the residual DOR efficacy found in our lead peptides from the pentapeptide series.

On the whole, the tetrapeptides displayed more balanced MOR and DOR binding with reduced selectivity relative to KOR. The two most promising ligands in this series, **JH6** (JH compounds synthesized by Jeff Ho.) and **JPAM13 (SMeS)**, both contained a homophenylalanine in the third position. These ligands were therefore modified with a C-terminal β-glucoserine, in which the side chain hydroxyl of Ser is covalently O-linked to a β-glucose, to improve blood/brain barrier penetration. Unfortunately, the effects of the modification are still somewhat unpredictable and the resulting ligands, **JPAM18 (SEtS)** and **JPAM19 (SMeS)**, did not display the desired efficacy profile.

It is worth noting that the size of the bridge between the two thiol containing side chains, methyl vs. ethyl, can have a profound impact upon the efficacy of the resulting ligands. Modeling studies suggest that the 2, 6 methyl groups on Dmt can rotate to form a steric clash with the dithioether linkage, depending on the size of the cycle and the bulk of the amino acid within the cyclized portion of the molecule. To relieve this clash the Dmt will rotate, expanding the overall profile of the molecule. This extended pose can prevent the ligand from fitting into the narrower active conformation of the opioid receptor binding pockets and reduce efficacy.

Future work will include an exploration of how the addition of a C-terminal sugar moiety affects the efficacy profile of various peptide ligands and how linker length and sugar choice change these effects. Arginine and homo-arginine extensions will also be pursued as a means of improving bioavailability. We will also explore how Tyr^1 replacements to promising sequences, such as **JPAM11** or **JPAM13**, affect binding and efficacy.

5.2.3 Linear Mixed Efficacy MOR/DOR Peptides

While we achieved success in developing cyclic mixed efficacy MOR/DOR ligands that displayed the desired binding and efficacy profile, there is still room for improvement. The yields on cyclic peptides are low and the cyclization process often produces side products, making purification difficult. As conformational restriction was initially introduced as a means to increase receptor specificity, we reasoned that linearized versions of our cyclic ligands might be

as successful as their cyclic counterparts, but with improved yields and greater ease of purification.

Two series of linear ligands were developed: direct translations of the cyclic tetrapeptides described above and modifications to the Roques scaffold of mixed efficacy MOR/DOR agonist peptides **DTLET** and **DTLES** [6, 17]. In both series we made various hydrophobic replacements; for our shorter pentapeptide translations we sought to reproduce our success with the cyclic tetrapeptides and for the longer more flexible Roques analogues we planned to add steric bulk to selectively reduce the DOR efficacy present in the parent ligands.

With only a few exceptions the direct linear translations of cyclic peptides displayed poor binding to MOR and DOR and no efficacy at any of the opioid receptors. As this series lacks the conformational restriction they adopt a more extended pose in the opioid binding site. This extended conformation is unable to fit into the relatively narrow active site of any of the opioid receptors, leading to antagonist behavior. It also forces these ligands to sit higher in the binding site of the inactive state of the receptor, preventing them from making necessary electrostatic contacts between the N-terminus and conserved residues in the binding site, lowering the affinity of this series for the opioid receptors in general.

The few exceptions to this trend were all able to adopt a more compact binding pose, lending them agonist character at MOR and/or DOR. **VRP-35** (VRP compounds synthesized by Vanessa Porter) contains an Aci^3, which is more constrained and closer to the backbone of the ligand than any other replacements in this series. **VRP-35** is the only ligand in this series that displays the desired MOR agonist/DOR antagonist profile and the selective efficacy is likely due the conformational restriction introduced by the constrained Aci^3. **JPAM7** contains a Hfe^3 residue and displays full agonist behavior at DOR and partial agonist behavior at MOR. Modeling studies suggest that the added flexibility in the Hfe side chain allows the ligand to adopt a more compact binding pose that allows it to fit deep into the narrower active site of MOR and DOR. This likely accounts for the high affinity and agonist character of **JPAM7** at DOR and MOR.

Modeling studies suggest that the bulk of $DThr^2$ in these linear pentapeptides produces a steric clash in the active site of the opioid receptors, such that these ligands bind preferentially to

the inactive conformation of the receptors, producing opioid antagonists. We therefore synthesized the $DSer^2$ analogue of **JPAM12**, **HVW-5** (HVW compounds synthesized by Helen Waldschmidt). This substitution did, in fact, rescue MOR efficacy, however the effect was not selective and **HVW-5** also displays DOR agonism. Future work will likely include exploring the SAR of these $DSer^2$ linear ligands in an effort to selectively reduce DOR efficacy.

The Roques compounds, **DTLET** and **DTLES**, display efficacy at both MOR and DOR and were used as templates for our series of hexapeptide mixed efficacy ligands. We made a series of analogues with various hydrophobic residues in the fourth position in an effort to selectively reduce DOR efficacy in a manner similar to our cyclic peptides described above. We achieved selective reduction of DOR efficacy in **JPAM16** which contains an Idg in the fourth position, though this ligand displays poor binding to MOR and DOR. **JPAM16** likely displays the desired efficacy profile because the Idg^4 is somewhat constrained and can selectively produce a steric clash in the DOR active site. We next made a Dmt^1 substitution expecting an improvement in the binding profile. The resulting ligand, **JPAM17**, displayed the desired binding profile, but no longer stimulated MOR. Modeling studies comparing **JPAM16** and **JPAM17** showed that if **JPAM17** were forced to adopt the same compact conformation as **JPAM16** the methyl groups on the Dmt^1 of **JPAM17** would clash with Idg^4. To relieve this clash **JPAM17** adopts a less compact conformation, which prevents it from binding to the narrower MOR active site, resulting in a MOR antagonist. This is a trend we have observed in our cyclic ligands as well.

Our inability to selectively reduce DOR agonism to produce a MOR agonist/DOR antagonist compound is not as problematic as it first sounds, as a MOR agonist/DOR agonist profile is also desirable. We therefore took our best MOR/DOR agonist, **VRP-39**, and added a C-terminal glucoserine, to produce **HVW-2**. This ligand binds tightly to MOR and DOR and displays selectivity relative to KOR. It is a full agonist at MOR and DOR and is a KOR antagonist. Future work will include carrying this ligand forward into *in vivo* assays to explore the development of tolerance and dependence as well as self-administration and conditioned place preference.

5.2.4 Co-Expression and Trafficking of MOR and DOR

Literature precedent states that mixed efficacy MOR/DOR ligands are slower to produce tolerance and dependence than traditional MOR agonist opioid analgesics [2-7, 9, 18-20]. Studies have also shown that some mixed efficacy MOR/DOR ligands even display reduced addiction liability as compared to MOR agonist analgesics [7, 9, 19, 20]. While the exact mechanism by which DOR ligands alter MOR agonist pharmacology is unknown, it is likely that this phenomenon is linked to the trafficking of the opioid receptors. Upon exposure to agonist MOR is first desensitized, then internalized into intracellular vesicles, and finally recycled to the plasma membrane as re-sensitized receptor; internalization without recycling leads to reduced surface expression of active receptor, a cellular hallmark of tolerance [21-26]. It has been proposed that internalization of MOR is a key part of re-sensitization and leads to recycling of the sensitive receptor, increasing cell surface expression of functional opioid receptors [24-28].

To explore the effects of DOR and DOR ligands on the trafficking of agonist stimulated MOR, a selective fluorescent MOR agonist, [Lys^{7}, Cys(Cy3)^{8}] dermorphin, and a selective fluorescent DOR antagonist, Dmt-Tic-Lys(Cy5)-OH were generated. These ligands were used in conjunction with fluorescence confocal microscopy to monitor the trafficking of MOR and DOR in live cells. We demonstrated that we can observe the initial binding of fluorescent MOR agonist to MOR on the plasma membrane and its subsequent internalization by tracking the fluorescent signal from our ligand. Similarly, we can see the binding of fluorescent DOR antagonist to DOR on the plasma membrane, where the signal remains, as antagonists do not induce internalization.

A live cell platform stably expressing unlabeled MOR and transiently expressing cyan fluorescent protein labeled DOR (CDOR) was developed to explore the effects of DOR and DOR ligands on the trafficking of MOR. The presence of CDOR in the same cells as MOR did not alter the trafficking of MOR after exposure to our selective fluorescent MOR agonist. Neither did the trafficking of CDOR change in the presence of MOR upon exposure to our selective fluorescent DOR antagonist. However, upon exposure to both ligands, cells that expressed both receptors internalized and recycled MOR more robustly than cells that expressed only MOR.

I propose that DOR antagonists exert their effects on MOR agonist potency and tolerance by encouraging a DOR receptor conformation that promotes the dissociation of G protein. DOR has a high basal turnover rate [29, 30] and MOR and DOR share a pool of G proteins and other signaling partners [31] freeing downstream effectors to stimulate, internalize and recycle MOR after exposure to MOR agonist. This increased trafficking produces greater cell surface expression of functional MOR [24-28], leading to improved MOR agonist potency and reduced development of tolerance to MOR agonists, trends observed with the co-administration of MOR agonists with DOR antagonists [15, 32-35].

Future work will include the development of live cell platforms to examine the differences in trafficking between MOR/DOR drug cocktails and MOR/DOR mixed efficacy ligands. These experiments will require the development of cells that express fluorescently tagged receptors, as multifunctional ligands will bind to both receptors and any fluorescent signal they produce will not discriminate between MOR and DOR. Additionally, the development of fluorescently tagged receptors will preclude the development of multiple fluorescently tagged ligands with specific pharmacological profiles, a task which is more difficult than it may initially seem (Chapter 4.2.1 and Appendix A). The use of fluorescently labeled receptors will allow for the exploration of biased MOR agonists with DOR antagonists, inverse agonists or biased agonists, for a fuller picture of how different ligand combinations effect receptor trafficking.

5.3 Mixed Efficacy Ligands and Receptor Trafficking: What can we do?

MOR agonist analgesics are widely used in the treatment of chronic and acute pain and are some of the most widely prescribed drugs on the market [36, 37]. Unfortunately, chronic use of opioid analgesics leads to the development of tolerance and dependence, features that complicate dosing regimens for patients and limit the clinical use of opioids; tolerance and dependence have also been linked to increased addiction liability and may contribute to the prevalence of opioid abuse [1, 38, 39]. It has been demonstrated that the co-administration of a MOR agonist with a DOR agonist or antagonist mitigates the development of these adverse neurochemical adaptations, without negatively affecting antinociceptive properties. As a result, the development of mixed efficacy ligands has been the subject of much research, as have the mechanisms by which DOR ligands affect MOR signaling and trafficking.

In this work I describe the successful rational design of mixed efficacy MOR agonist/ DOR antagonist and MOR agonist/DOR agonist peptide ligands and the development of tools to monitor the trafficking of MOR and DOR in live cells. Together these tools can be used to explore how cells expressing both receptors respond to mixed efficacy ligands and drug cocktails. This data can be correlated with parallel *in vivo* experiments to draw inferences about how changes in receptor trafficking patterns on the cellular level correspond to neurochemical adaptations or changes in animal behavior. A better understanding of the "how" and "why" of the development of tolerance to and dependence on MOR agonists will open the door for rational design of better opioid analgesics, this will allow us to better serve patients in need of pain relief and curb the addiction liability associated with opioid analgesic use.

5.4 References

1. Bailey, C.P. and M. Connor, *Opioids: Cellular Mechanisms of Tolerance and Physical Dependence.* Current Opinion in Pharmacology, 2005. **5**(1): p. 60-8.
2. Abdelhamid, E.E., et al., *Selective Blockage of the Delta Opioid Receptors Prevents the Development of Morphine Tolerance and Dependence in Mice.* The Journal of Pharmacology and Experimental Therapeutics, 1991. **258**(1): p. 299-301.
3. Fundytus, M.E., et al., *Attenuation of Morphine Tolerance and Dependence with the Highly Selective d-Opioid Receptor antagonist TIPP (psi).* European Journal of Pharmacology, 1995. **286**(1): p. 105-8.
4. Hepburn, M.J., et al., *Differential Effects of Naltrindole on Morphine-Induced Tolerance and Physical Dependence in Rats.* Journal of Pharmacology and Experimental Therapeutics, 1997. **281**(3): p. 1350-6.
5. Miyamoto, Y., P.S. Portoghese, and A.E. Takemori, *Involvement of the Delta 2 Opioid Receptors in Acute Dependence on Morphin in Mice.* Journal of Pharmacology and Experimental Therapeutics, 1993. **265**(3): p. 1325-1327.
6. Li, Y., et al., *Opioid Glycopeptide Analgesics Derived from Endogenous Enkephalins and Endorohins.* Future Medicinal Chemistry, 2012. **4**(2): p. 205-226.
7. Lowery, J.J., et al., *In Vivo Characherization of MMP-2200, a Mixed Mu/Delta Opioid Agonist, in Mice.* The Journal of Pharmacology and Experimental Therapeutics, 2011. **336**: p. 767-778.
8. Rozenfeld, R., et al., *An Emerging Role for the Delta Opioid Receptor in the Regulation of Mu Opioid Receptor Function.* Science World Journal, 2007. **7**: p. 4-73.
9. Do Carmo, G.P., et al., *Behavioral Pharmacology of the Mu/Delta Opioid Glycopeptide MMP2200 in Rhesus Monkeys.* Journal of Phamacology and Experimental Therapeutics, 2008. **326**: p. 939-948.
10. Fowler, C.B., et al., *Refinement of a Homology Model of the Mu-opioid Receptor Using Distance Constraints from Intrinsic and Engineered Zinc-binding Sites.* Biochemistry, 2004. **43**: p. 8700-8710.
11. Fowler, C.B., et al., *Complex of an Active Mu-opioid Receptor with a Cyclic Peptide Agonist Modeled from Experimental Constraints.* Biochemistry, 2004. **43**: p. 15796-15810.
12. Pogozheva, I.D., A.L. Lomize, and H.I. Mosberg, *The Transmembrane 7-alpha-bundle of Rhodopsin: Distance Geometry Calculations with Hydrogen Bonding Constraints.* Biophysics, 1997. **72**: p. 1963-1985.
13. Pogozheva, I.D., A.L. Lomize, and H.I. Mosberg, *Opioid Receptor Three-Dimensional Structures from Distance Geometry Calculations with Hydrogen Bonding Constraints.* Biophysics, 1998. **75**: p. 612-634.
14. Pogozheva, I.D., M.J. Przydzial, and H.I. Mosberg, *Homology Modeling of Opioid Receptor-Ligand Complexes Using Experimental Constraints.* AAPS Journal, 2005. **7**: p. 43-57.
15. Purington, L.C., et al., *Pentapeptides Displaying Mu Opioid Receptor Agonist and Delta Opioid Receptor Partial Agonist/Antagonist Properties.* Journal of Medicinal Chemistry, 2009. **52**: p. 7724-7731.

16. Purington, L.C., et al., *Development and in Vitro Characterization of a Novel Bifunctional Mu-Agonist/Delta-Antagonist Opioid Tetrapeptide.* ACS Chemical Biology, 2011. **6**: p. 1375-1381.
17. Zajac, J.M., et al., *Deltakephailn, Tyr-DThr-Gly-Phe-Leu-Thr: A New Highly Potent and Fully Specific Agonist for Opiate Delta Receptors.* Biochemical and Biophysical Research Communications, 1983. **111**(2): p. 390-397.
18. Elmagbari, N.O., et al., *Antinociceptive Structure-Activity Studies with Enkephalin-Based Opioid Glycopeptides.* The Journal of Pharmacology and Experimental Therapeutics, 2004. **311**: p. 290-297.
19. Keyari, C.M., et al., *Glycosylenkephalins: Synthesis and Binding at the Mu, Delta, and Kappa Opioid Receptors. Antinocicpetion in Mice.* Advances in Experimental Medicine and Biology, 2009. **611**: p. 495-496.
20. Polt, R., M. Dhanasekaran, and C.M. Keyari, *Glycosylated Neuropeptides: A New Vista for Neuropsychopharmacology?* Medicinal Research Reviews, 2005. **25**(5): p. 557-585.
21. Bailey, C.P. and M. Connor, *Opioids: Cellular Mechanisms of Tolerance and Physical Dependence.* Current Opinion in Pharmacology, 2005. **5**: p. 60-68.
22. Ferguson, S.S., *Evolving Concepts in G Protein-Coupled Receptor Adaptation Mechanisms.* Pharmacology Reviews, 2001. **53**: p. 1-24.
23. von Zaztrow, M., et al., *Regulated Endocytosis of Opioid Receptors: Cellular Mechanisms and Proposed Roles in Physiological Adaptation to Opiate Drugs.* Current Opinion in Neurobiology, 2003. **13**: p. 348-353.
24. Martini, L. and J.L. Whistler, *The Role of Mu Opioid Receptor Densensitization and Endocytosis in Morphine Tolerance and Dependence.* Current Opinion in Neurobiology, 2007. **17**: p. 556-564.
25. He, L., et al., *Regulation of Opioid Receptor Trafficking and Morphine Tolerance by Receptor Oligomerization.* Cell, 2002. **08**: p. 271-282.
26. Whistler, J.L., et al., *Functional Dissociation of the My Opioid Receptor Signaling and Endocytosis: Implications for the Biology of Opiate Tolerance and Addiction.* Neuron, 1999. **23**: p. 737-746.
27. Finn, A.K. and J.L. Whistler, *Endocytosis of the Mu Opioid Receptor Reduced Tolerance and a Cellular Hallmark of Opiate Withdrawal.* Neuron, 2001. **32**: p. 829-839.
28. Whistler, J.L. and M. von Zaztrow, *Morphine-Activated Opioid Receptors Elude Desensitization by Beta-arrestin.* Proceedings of the National Academy of Science, 1998. **95**(17): p. 9914-9919.
29. Wang, D., X. Sun, and W. Sadee, *Different Effects of Opioid Antagonists on Mu, Delta, and Kappa Opioid Receptors with and without Agonist Pretreatment.* Journal of Phamacology and Experimental Therapeutics, 2007. **321**: p. 544-552.
30. Costa, T. and A. Herz, *Antagonists with Negative Intrinsic Activity at Delta Opioid Receptors Coupled to GTP-binding Proteins.* Proceedings of the National Academy of Science, 1989. **86**: p. 7321-7325.
31. Levitt, E.S., L.C. Purington, and J.R. Traynor, *Gi/o Coupled Receptors Compete for Signaling to Adenylyl Cyclase in SH-SY5Y Cells and Reduce Opioid Mediated cAMP Overshoot.* Molecular Pharmacology, 2010. **79**(3): p. 461-471.
32. Abdelhamid, E.E., et al., *Selective Blockage of the Delta Opioid Receptors Prevents the Development of Morphine Tolerance and Dependence in Mice.* The Journal of Pharmacology and Experimental Therapeutics, 1991. **258**(1): p. 299-303.

33. Fundytus, M.E., et al., *Attenuation of Morphine Tolerance and Dependence with the Highly Selective Delta Opioid Receptor Antagonist TIPP(psi).* European Journal of Pharmacology, 1995. **286**: p. 105-108.
34. Hepburn, M.J., et al., *Differential Effects of Naltrindole on Morphine-Induced Tolerance and Physical Dependence in Rate.* The Journal of Pharmacology and Experimental Therapeutics, 1997. **281**(3): p. 1350-1356.
35. Schiller, P.W., *Bi- or Multifunctional Opioid Peptide Drugs.* Life Sciences, 2009. **86**: p. 598-603.
36. Volkow, N.D., et al., *Characteristics of Opioid Prescrpitions in 2009.* Journal of the American Medical Association, 2011. **305**(13): p. 1299-1301.
37. Volkow, N.D. and T.A. McIellan, *Curtailing Diversion and Abuse of Opioid Analgesics Without Jeopardizing Pain Treatment.* Journal of the American Medical Association, 2011. **305**(13): p. 1346-1347.
38. Ross, S. and E. Peselow, *The Neurobiology of Addicitive Disorders.* Clinical Neuropharmacology, 2009. **32**(5): p. 269-276.
39. Johnston, L.D., et al., *Monitoring the Future: National Survey Results on Drug Use.* National Institute on Drug Abuse, 2009. **1**: p. 1-721.

APPENDIX A

Failed Fluorescent Ligand Scaffolds

A.1 Introduction

As discussed in Chapter 4, we have already achieved some success in designing potent, selective fluorescent opioid ligands for MOR and DOR for use with confocal microscopy. We have in hand the two most interesting and clinically relevant types of opioid ligands in our toolbox: a selective fluorescent MOR agonist, [Lys^7, Cys^8(Cy3)] dermorphin (**A2**; **Table A.1**), and a selective fluorescent DOR antagonist, Dmt-Tic-Lys(Cy5)-OH (**A32**; **Table A.2**). We have demonstrated their viability as opioid receptor probes for fluorescence confocal microscopy in live cells. We have generated several other scaffolds in hopes of finding a selective, fluorescent MOR antagonist and a selective fluorescent DOR agonist. To date none of the ligands have proved to have sufficient affinity and selectivity profiles. (Ligands synthesized are described in **Table A.1** and **Table A.2**.) While we are most interested in how a MOR agonist and a DOR antagonist affect the trafficking, sequestering, and recycling of opioid receptors, in order to fully explore the functional crosstalk between MOR and DOR ideally a full complement of MOR and DOR ligands would be used. The state of the receptor (agonist bound vs. antagonist bound) may affect the overall conformation of the receptor and its ability to dimerize. This, in turn, may affect the co-trafficking of receptors, the development of tolerance and dependence, or alter ligand potency and efficacy. While these studies can also be completed with fluorescently labeled receptors and unlabeled ligands we first sought to produce a full toolbox of fluorescent opioid ligands.

A.2 Attempts to Complete the Fluorescent Ligand Toolbox

A.2.1 Selective Fluorescent MOR Antagonists

Our initial attempts to generate a selective, fluorescent MOR antagonist began with the selective cyclic MOR antagonist DTic-c(S-S)[Cys-Tyr-Nle-Thr-Pen]Thr-NH_2 (TCTNP; **Table**

A.1) which contains a disulfide bridge between the Cys^2 and Pen^6 side chains and is a derivative of CTAP [1]. TCTNP was then modified with a C-terminal Lys for fluorescent labeling, as a Cys modification would complicate cyclization through our thiol containing side chains, Cys^2 and Pen^6. The resulting ligand TCTNPK (**A13**) was a relatively selective, potent MOR antagonist, however, when this compound was labeled with Cy5, the resulting compound, TCTNPK(Cy3) (**A14**) was insoluble and could not be tested. We next attempted modifications of DTic-c(SS)[Cys-Tyr-Arg-Thr-Pen]Thr-NH_2 (TCTAP; **Table A.1**) [1] in hopes that the added charge would increase solubility; this compound was initially avoided as the Arg^4 residue can potentially be labeled instead of the C-terminal Lys. Both the L- and D-Lys modifications (**A15** and **A17** respectively) displayed good affinity and moderate selectivity, however once labeled the selectivity for MOR over DOR was lost and the potency at MOR was decreased (**Table A.1**). These scaffolds were then abandoned as no further logical modification were easily made.

There is literature precedent for taking existing peptide scaffolds and modifying them with unnatural amino acids to alter their selectivity or efficacy. Changes in charge and bulk at the first position of opioid peptides have been shown to alter the efficacy of the resulting ligand relative to that of the parent [2-7]. We next attempted to generate a MOR antagonist by incorporating unnatural amino acids into dermorphin, a selective potent MOR agonist. It has been reported that removing the positive charge at the first position of an opioid peptide agonist, such as [Lys^7, Cys^8] dermorphin, will generate a MOR antagonist with a similar binding profile to that of the parent compound [8]. By replacing the Tyr^1 of [Lys^7, Cys^8] dermorphin with 3-(2,6-dimethyl-4-hydroxyphenyl)propanoic acid (Dhp) we hoped to generate a selective MOR antagonist with a handle for fluorescent labeling. However, this modification decreased the affinity of the ligand, [Dhp^1, Lys^7, Cys^8] dermorphin (**A7**; **Table A.1**), to such an extent that the efficacy was moot and the scaffold was abandoned.

Table A.1: Selective MOR Agonists and Antagonists and their Fluorescent Derivatives

MOR Ligands		Sequence	Binding (nM)			MOR Efficacy
			MOR	DOR	KOR	
A1	[Lys7,Cys8] Dermorphin	Tyr-DAla-Phe-Gly-Tyr-Pro-Lys-Cys-NH2	0.4±0.03	240±60	240±140	Full
A2	[Lys7,Cys(Cy3)8] Dermorphin	Tyr-DAla-Phe-Gly-Tyr-Pro-Lys-Cys(Cy3)-NH2	3.8± 1.8	131±0	nt	Full
A3	[Lys7,Cys(Cy5)8] Dermorphin	Tyr-DAla-Phe-Gly-Tyr-Pro-Lys-Cys(Cy5)-NH2	11± 1	400±200	nt	Full
A4	[Lys7,Cys(AF555)8] Dermorphin	Tyr-DAla-Phe-Gly-Tyr-Pro-Lys-Cys(AF555)-NH2	3.5±0.5	532±138	nt	Full
A5	[Lys7, Cys(AF488)8] Dermorphin	Tyr-DAla-Phe-Gly-Tyr-Pro-Lys-Cys(AF488)-NH2	1.6±0.5	383±140	nt	Full
A6	[Lys7, Cys(BODTMRX)8] Dermorphin	Tyr-DAla-Phe-Gly-Tyr-Pro-Lys-Cys(BodTMRX)-NH2	0.45±0.04	37±1	nt	Full
A7	[Dhp1, Lys7, Cys8] Dermorphin	Dhp-DAla-Phe-Gly-Tyr-Pro-Lys-Cys-NH2	310±2	>1000	nt	nt
A8	Dmt-Sar-Phe-D2Nal-NH2	Dmt-Sar-Phe-D2Nal-NH2	0.3±0.1	10±1	nt	nt
A9	Dmt-Sar-Phe-D2Nal-Cys-NH2	Dmt-Sar-Phe-D2Nal-Cys-NH2	73±3	153±6	nt	nt
A10	Dmt-Sar-Phe-D2Nal-DCys-NH2	Dmt-Sar-Phe-D2Nal-DCys-NH2	3.6±2	82±20	nt	Neutral
A11	Dmt-Sar-Phe-D2Nal-DLys-NH2	Dmt-Sar-Phe-D2Nal-DLys-NH2	3.1±0.6	540±90	nt	Neutral
A12	Dmt-Sar-Phe-D2Nal-DLys(Cy5)-NH2	Dmt-Sar-Phe-D2Nal-Dlys(Cy5)-NH	13±1.5	30±20	nt	Partial
A13	TCTNPK (SS)	DTic-Cys-Tyr-DTrp-Nle-Thr-Pen-Thr-Lys-NH2	5±1	>1000	400±90	Neutral
A14	TCTNPK(Cy3)(SS)	DTic-Cys-Tyr-DTrp-Nle-Thr-Pen-Thr-Lys(Cy3)-NH2	nt	nt	nt	nt
A15	TCTAPK(SS)	DTic-Cys-Tyr-DTrp-Arg-Thr-Pen-Thr-Lys-NH2	2±0.7	420±90	nt	nt
A16	TCTAPK(Cy3)(SS)	DTic-Cys-Tyr-DTrp-Arg-Thr-Pen-Thr-Lys(Cy3)-NH2	38±3	160±20	nt	nt
A17	TCTAPdK(SS)	DTic-Cys-Tyr-DTrp-Nle-Thr-Pen-Thr-Lys-NH2	7±1	400±40	nt	nt
A18	TCTAPdK(Cy3)(SS)	DTic-Cys-Tyr-DTrp-Arg-Thr-Pen-Thr-DLys(Cy3)-NH2	52*	>1000	nt	nt
A19	TCTAPdK(Bod650)(SS)	DTic-Cys-Tyr-DTrp-Arg-Thr-Pen-Thr-DLys(Bod650)-NH2	1.5±0.2	234±3	nt	nt

Binding affinities (K_i) were obtained by competitive displacement of radiolabeled [^{3}H] diprenorphine. Efficacy data were obtained using [^{35}S] GTPγS binding assay. Efficacy is represented as percent maximal stimulation relative to standard agonists DAMGO (MOR), DPDPE (DOR) or U69,593 (KOR) at 10μM concentrations. All values are expressed as mean ± SEM of three separate assays performed in duplicate, except for those marked with *, where n=1. nt = not tested.

There are also reports that modifying residues of the endomorphin II scaffold, Tyr-Pro-Phe-Phe-NH_2, would generate a potent, selective MOR antagonist [9]. The resulting ligand – Dmt-Sar-Phe-D-2Nal-NH_2 (**A8**; **Table A.1**) – displayed poor selectivity. We made several C-terminal modifications for labeling purposes and the C-terminal DLys analogue displayed modest selectivity for MOR over DOR. Unfortunately, once the ligand was conjugated with the fluorescent dye, Cy5 (**A12**), the improved selectivity was lost and the scaffold was abandoned. As there is a dearth of selective, peptidic MOR antagonists, further attempts to generate a selective, fluorescent, peptidic MOR antagonist were put on hold.

A.2.2 Selective Fluorescent DOR Agonists

We attempted modifying the peptide Tyr-Tic-Phe-Phe-NH_2 (TIPP), a potent selective DOR antagonist [10], with unnatural amino acids to generate a DOR agonist, by adding hydrophobic bulk to the first position. First we demonstrated that C-terminal modification of TIPP with an L- or DCys (**A20** and **A21**) and L- or DLys (**A23** and **A25**) afforded selective DOR antagonists. Subsequent labeling of the modified TIPP analogues with Cy3 or Cy5 (**A22**, **A24**, and **A26**) yielded selective DOR antagonists (**Table A.2**), demonstrating that C-terminal modifications of the TIPP scaffold were well tolerated. The Tyr^1 of TIPP was then replaced with an 4'-[N-(2-napthalen-2-yl)ethyl)carboxamido] phenylalanine (Ncp) residue (**A27**; **Table A.2**), as added hydrophobic bulk at the first position has been reported to confer agonism to opioid peptides [2, 11]. Unfortunately, this replacement decreased the selectivity of the ligand significantly; additionally the use of Ncp did not confer full agonism. We also attempted Tyr^1 replacement with 4'[N-(hexyl) carboxamido] phenylaline] (Hcp) (**A28**) in the first position which has been reported to confer agonism to the TIPP scaffold [2]. Unfortunately the resulting ligand, Hcp-Tic-Phe-Phe-NH_2 (**A28**), was a neutral antagonist. The TIPP

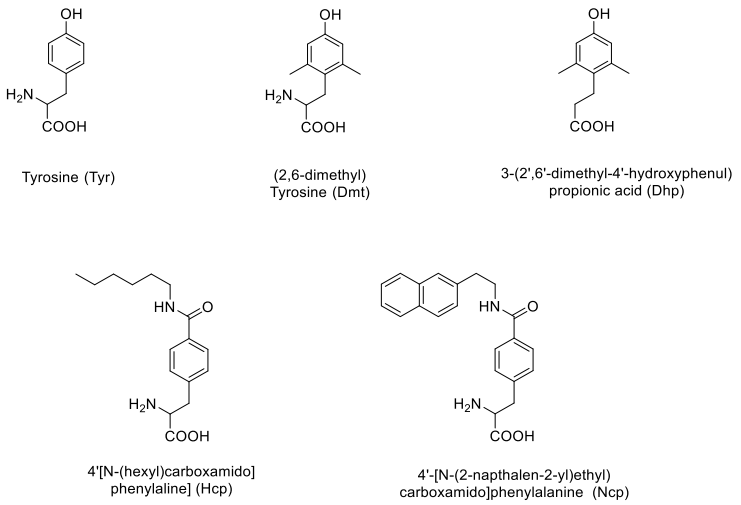

Figure A.1: Structures of Tyrosine mimics.

scaffold was subsequently abandoned.

It has been well established that diallyl substitutions on the N-terminus of opioid peptides can confer antagonism [12]. We reasoned that removal the *N*,*N*-diallyl substitution from the selective DOR antagonist ICI 174864 (*N*,*N*diallyl-Tyr-Aib-Aib-Phe-Leu-OH), might generate a selective DOR agonist. We therefore generated a new ligand, YAAFK(Ac) (Tyr-Aib-Aib-Phe-Lys(Ac)-OH; **Table A.2**), lacking the N-terminal allyl groups and replacing the Leu^5 with an acetylated Lys as a handle of later fluorescent labeling – we chose to use an acetylated Lys as acetylation masks the charge on the ε amine of the Lys and would better mimic the electronics of the labeled peptide. Unfortunately, these changes greatly reduced both the affinity for DOR and selectivity relative to MOR, so this scaffold was also abandoned. Having explored most of the reported avenues for selective, peptidic DOR agonists and antagonists, the generation of a selective fluorescent DOR agonist was also put on hold.

Table A.2: Selective DOR Agonists and Antagonists and their Fluorescent Derivatives

DOR Ligands	Sequence	Binding (nM)			DOR
		MOR	DOR	KOR	Efficacy
A20 TIPP-C	Tyr-Tic-Phe-Phe-Cys-NH2	>1000	4.6±0.8	>10,000	Neutral
A21 TIPP-dC	Tyr-Tic-Phe-Phe-DCys-NH2	>1000	4.6±0.3	>10,000	Neutral
A22 TIPP-dC(Cy5)	Tyr-Tic-Phe-Phe-Dcys(Cy5)-NH2	>1,000	4.6±0.4	>10,000	Neutral
A23 TIPP-K	Tyr-Tic-Phe-Phe-Lys-NH2	>1000	4.7±0.5	>10,000	Neutral
A24 TIPP-K(Cy3)	Tyr-Tic-Phe-Phe-Cys-NH2	130±50	40±28	nt	Neutral
A25 TIPP-dK	Tyr-Tic-Phe-Phe-DLys-NH2	>1000	2.3±0.5	>1,000	Neutral
A26 TIPP-dK(Cy3)	Tyr-Tic-Phe-Phe-DLys(Cy3)-NH2	>1,000	50±35	nt	Neutral
A27 NIPPdK	Ncp-Tic-Phe-Phe-DLys-NH2	62*	3*	nt	Partial
A28 HIPPdK	Hcp-Tic-Phe-Phe-DLys-NH2	1.0±0.03	56±5	nt	Neutral
A29 YAAFK(Ac)	Tyr-Aib-Aib-Phe-Lys(Ac)-OH	24.0±0.8	14±6	nt	nt
A30 Dmt-Tic-Lys-OH	Dmt-Tic-Lys-OH	>1,000	1.2±0.6	>10,000	Neutral
A31 Dmt-Tic-Lys(Cy3)-OH	Dmt-Tic-Lys(Cy3)-OH	>1,000	4.6±1.2	>1,000	Neutral
A32 Dmt-Tic-Lys(Cy5)-OH	Dmt-Tic-Lys(Cy5)-OH	>1,000	4.7±0.7	>1,000	Neutral

Binding affinities (K_i) were obtained by competitive displacement of radiolabeled [^{3}H] diprenorphine. Efficacy data were obtained using [^{35}S] GTPγS binding assay. Efficacy is represented as percent maximal stimulation relative to standard agonists DAMGO (MOR), DPDPE (DOR) or U69,593 (KOR) at 10μM concentrations. All values are expressed as mean ± SEM of three separate assays performed in duplicate, except for those marked with *, where n=1. nt = not tested.

A.3 Conclusions

Our efforts to generate a complete toolbox of MOR and DOR ligands have utilized literature precedents with various modifications for labeling, affinity, efficacy, and selectivity. Our major problem has been with the selectivity of the ligands, especially after labeling with a fluorophore. We have had some success using our homology models to predict the best site and stereochemistry of modifications for fluorophore labeling. We initially chose to use the Cy dyes as labels for our opioid ligands based on their excitation/emission spectra, extinction coefficient, and photostability; other fluorophores may be explored to determine if the affinity and selectivity of the labeled ligands can be improved while maintaining the desired label properties. With the correct label we may be able to rescue some of the ligands previously abandoned due to selectivity or affinity issues.

A.4 Materials and Methods

A.4.1 Materials

All reagents and solvents were purchased from commercial sources and used without further purification. All chemicals and biochemicals were purchased from Sigma Aldrich (St. Louis, MO, USA) or Fisher Scientific (Hudson, NH, USA), unless otherwise noted. All tissue culture reagents were purchased from Gibco Life Sciences (Grand Island, NY, USA). Radioactive compounds were purchased from Perkin-Elmer (Waltham, MA, USA). Peptide synthesis reagents, amino acids, and Rink resin were purchased from Advanced Chem Tech (Louisville, KY, USA). All other chemicals and ligands were from either Sigma-Aldrich (St. Louis, MO) or Fisher Scientific (Pittsburgh, PA).

A.4.2 Solid Phase Peptide Synthesis

Peptides were synthesized using standard solid phase Fmoc (fluorenylmethyloxycarbonyl) chemistry on a CS Bio CS336X Peptide Synthesizer (CS Bio Company, Menlo Park, CA, USA), using previously described protocols. [13] C-terminal amide peptides were synthesized using Rink resin, C-terminal acid peptides were synthesized using Fmoc-Wang resin preloaded with the C-terminal amino acid. A 20% solution of piperidine in N-

methyl-2-pyrrolidone (NMP) was used to remove the first Fmoc protecting group before synthesis and again to remove the Fmoc-protecting group after each coupling cycle. Coupling was performed using a four-fold excess of amino acid and a solution of 0.4 M hydroxybenzotriazole (HOBt) and O-benzotriazole- N, N, N ', N '-tetramethyl-uroniumhexafluoro- phosphate (HBTU) in dimethylformamide (DMF), in the presence of diisopropylethylamine (DIEA). After the synthesis was complete, the resin was washed with NMP, then with dichloromethane, and dried under vacuum. Difficult couplings of the artificial amino acids Dmt, Dhp, Ncp, and Hcp were performed with coupling times lasting 4-16 hours. The peptides were cleaved from the resin and side-chain-protecting groups removed by treatment at room temperature for 2 h with a cleavage cocktail consisting of 9.5 mL trifluoroacetic (TFA) acid, 0.25 mL triisopropylsilane (TIS) and 0.25 mL H_2O. The solution was concentrated *in vacuo*, and peptides were precipitated using cold, fresh diethylether. The filtered crude material was then purified using a Waters semipreparative HPLC (Waters Corporation, Milford, MA, USA) with a Vydac Protein and Peptide C18 column, using a linear gradient 10% Solvent B (0.1% TFA acid in acetonitrile) in Solvent A (0.1% TFA acid in water) to 60% Solvent B in Solvent A, at a rate of 1% per minute. The identity all peptides were determined ESI-MS performed on an Agilent Technologies LC/MS system using a 1200 Series LC and 6130 Quadrupole LC/MS (Agilent Technologies, Santa Clara, CA, USA) in positive mode with 50–100 µL injection volume and a linear gradient of 0% Solvent D (0.02% TFA and 0.1% acetic acid (AcOH) in acetonitrile) in Solvent C (0.02% TFA and 0.1% AcOH in water) to 60% Solvent D in Solvent C in 15 min. The purity of all peptides was determined using a Waters Alliance 2690 Analytical HPLC (Waters Corporation, Milford, MA, USA) and Vydac Protein and Peptide C18 reverse phase column, using a linear gradient of 0–70% Solvent B in Solvent A at a rate of 1% per minute. Linear peptides were purified to ≥ 95% purity by UV absorbance at 230 nm.

A.4.3 Fluorescent Labeling

The purified peptide was labeled with Cy3 or Cy5 maleimide or NHS ester (GE Healthcare) according to the manufacturer's instructions using a ratio of 1.5:1 peptide to fluorophore. The labeled peptide was further purified via semi-preparative HPLC using a 5 micron Vydac C18 column as described above. The potency and efficacy labeled ligands confirmed in radiolabeled [^{3}H]DPN competition and [^{35}S]GTPγS binding assays.

A.4.4 Cell Lines and Mammalian Membrane Preparations

C6-rat glioma cells stably transfected with a rat μ (C6-MOR) or rat δ (C6-DOR) opioid receptor [14] and Chinese hamster ovary (CHO) cells stably expressing a human κ (CHO-KOR) opioid receptor [15] were used for all in vitro assays. Cells were grown to confluence at 37ºC in 5% CO_2 in Dulbecco's Modified Eagle's Medium containing 10% fetal bovine serum and 5% penicillin/streptomycin. Membranes were prepared by washing confluent cells three times with ice cold phosphate-buffered saline (0.9% NaCl, 0.61 mM Na_2HPO_4, 0.38 mM KH_2PO_4, pH 7.4). Cells were detached from the plates by incubation in warm harvesting buffer (20 mM HEPES, 150 mM NaCl, 0.68 mM EDTA, pH 7.4) and pelleted by centrifugation at 200xg for 3 min. The cell pellet was suspended in ice-cold 50 mM Tris-HCl buffer, pH 7.4 and homogenized with a Tissue Tearor (Biospec Products, Inc, Bartlesville, OK, USA) for 20 s at setting 4. The homogenate was centrifuged at 20,000xg for 20 min at 4 C, and the pellet was rehomogenized in 50 mM Tris-HCl with a Tissue Tearor for 10 s at setting 2, followed by recentrifugation. The final pellet was resuspended in 50mM Tris-HCl and frozen in aliquots at -80ºC. Protein concentration was determined via Bradford assay using bovine serum albumin as the standard.

A.4.5 Radioligand Binding Assays in Mammalian Membrane Preparations

Opioid ligand-binding assays were performed using competitive displacement of 0.2 nM [^{3}H]diprenorphine (250 μCi, 1.85TBq/mmol) by the test compound from membrane preparations containing opioid receptors. The assay mixture, containing membrane suspension (20 μg protein/tube) in 50 mM Tris-HCl buffer (pH 7.4), [^{3}H]diprenorphine, and various concentrations of test peptide, was incubated at room temperature for 1 h to allow binding to reach equilibrium. The samples were rapidly filtered through Whatman GF/C filters using a Brandel harvester (Brandel, Gaithersburg, MD, USA) and washed three times with 50 mM Tris-HCl buffer. The radioactivity retained on dried filters was determined by liquid scintillation counting after saturation with EcoLume liquid scintillation cocktail in a Wallac 1450 MicroBeta (Perkin-Elmer, Waltham MA, USA). Nonspecific binding was determined using 10 μM naloxone. K_i values were calculated using nonlinear regression analysis to fit a logistic equation to the competition

data using GraphPad Prism version 5.01 for Windows. The results presented are the mean ± standard error from at least three separate assays performed in duplicate.

A.4.6 Stimulation of [^{35}S]GTPγS Binding in Mammalian Membrane Preparations

Agonist stimulation of [^{35}S] guanosine 5'-O-[gamma-thio]triphosphate ([^{35}S]GTPγS, 1250 Ci, 46.2TBq/mmol) binding was measured as described previously [16]. Briefly, membranes (10-20 μg of protein/tube) were incubated 1 h at room temperature in GTPγS buffer (50 mM Tris-HCl, 100 mM NaCl, 5 mM $MgCl_2$, pH 7.4) containing 0.1 nM [^{35}S]GTPγS, 30 μM guanosine diphosphate **(**GDP), and varying concentrations of test peptides. Peptide stimulation of [^{35}S]GTPγS was compared with 10 μM standard compounds [DAla^2, N-MePhe^4, Gly-ol]-enkephalin (DAMGO) at MOR, DPen^{2,5}- enkephalin (DPDPE) at DOR, or U69,593 at KOR. The reaction was terminated by rapidly filtering through GF/C filters and washing ten times with GTPγS buffer, and retained radioactivity was measured as described above. The results presented are the mean ± standard error from at least three separate assays performed in duplicate; maximal stimulation was determined using nonlinear regression analysis with GraphPad Prism.

A.5 References

1. Pelton, J.T., et al., *Design and Synthesis of Conformationally Constrained Somatostatin Analogues with HIgh Potency and Specificity for Mu Opioid Receptors.* Journal of Medicinal Chemistry, 1986. **29**: p. 2370-2375.
2. Berezowska, I., et al., *Replacement of the Tyr1 Hydroxyl Group of TIPP Peptides with N-(Alkyl)carboxamido Groups Results in Potent and Selective d Opioid Agonists or Antagonists.* Proceedings of the 21st American Peptide Symposium, 2009: p. 183-4.
3. Lu, Y., et al., *Replacement of the N-terminal Tyrosine Redisue in Opioid Peptides with 3-(2,6-Dimethyl-4-carbamoyl)propanoic Acid (Dcp) Results in Novel Opioid Antagonists.* Journal of Medicinal Chemistry, 2006. **49**: p. 5382-5385.
4. Lu, Y., et al., *Stereospecific Synthesis of (2S)-2-Methyl-3-(2',6'-dimethyl-4'-hydroxyphenul)-propionic Acid (Mdp) and its Incorporatiuon into an Opioid Peptide.* Bioorganic and Medicinal Chemistry Letters, 2001. **11**: p. 323-325.
5. Salvadori, S., et al., *Evolution of the Dmt-Tic Pharmacophore: N-Terminal Methylated Derivatives with Extraordinary delta Opioid Antagonist Activity.* Journal of Medicinal Chemistry, 1997. **40**: p. 3100-3108.
6. Schiller, P.W., et al., *Novel Ligands Lacking a Positive Charge for the delta and mu Opioid Receptors.* Journal of Medicinal Chemistry, 2000. **43**: p. 551-559.
7. Schiller, P.W., et al., *Differential Stereochemical Requirements of mu and delta Opioid Receptors for Ligand Binding and Signal transduction: Development of a Class of Potent and Highly delta-Selective Peptide Antagonists.* Pharmacology, 1992. **89**: p. 11871-11875.
8. Weltrowska, G., et al., *A Chimeric opioid peptide with mixed u agonist/ d antagonist properties.* Journal of Peptide Research, 2004. **63**: p. 63-8.
9. Finchna, J., et al., *Novel Highly Potent mu-opioid Receptor Antagonist Based on Endomorphin-2 Structure.* Bioorganic and Medicinal Chemistry Letters, 2008. **18**: p. 1350-1353.
10. Fundytus, M.E., et al., *Attenuation of Morphine Tolerance and Dependence with the Highly Selective Delta Opioid Receptor Antagonist TIPP(psi).* European Journal of Pharmacology, 1995. **286**: p. 105-108.
11. Schiller, P.W., et al., *The TIPP Opioid Peptide Family: Development of detla Antagonists, delta Agonists, and Mixed mu Agonist/ delta Antagonists.* Biopolymers (Peptide Synthesis), 1999. **51**: p. 411-425.
12. Shaw, J.S., et al., *Selective Antagonists at the Opiate Delta Receptor.* Life Sciences, 1984. **31**: p. 1259-1262.
13. Przydzial, M.J., et al., *Roles of Residues 3 and 4 in Cyclic Tetrapeptide Ligand Recognition by the Kappa Opioid Receptor.* Journal of Peptide Research, 2005. **26**: p. 333-342.
14. Lee, K.O., et al., *Differential Binding Properties of Oripavines at Cloned Mu- and Delta-Opioid Receptors.* European Journal of Pharmacology, 1999(378): p. 323-330.
15. Husbands, S.M., et al., *BU74, A Complex Oripavine Derivative with Potent Kappa Opioid Receptor Agonism and Delayed Opioid Antagonism.* European Journal of Pharmacology, 2005(509): p. 117-135.

16. Traynor, J.R. and S.R. Nahorski, *Modulation by Mu-Opioid Agonists of Guanosine-5'-O(3-[35S]thio)triphosphate Binding to Membranes from Human Neuroblastoma SHY5Y Cells.* Molecular Pharmacology, 1995(47): p. 848-854.

APPENDIX B

The Minimal Functional Unit of the Mu Opioid Receptor is Monomeric

B.1 Introduction

As discussed in chapters 1 and 4 receptor homo- and heterodimerization has been used to explain the wide array of pharmacological responses displayed by opioid receptors [1-6]. It has been suggested that these oligomers regulate opioid ligand binding, the association of downstream signaling partners, amplification of signal, and even trafficking and expression of receptors [6-14]. It has even been proposed that oligomerization is necessary for normal opioid function and that opioid homo- and heterodimers are the native receptor state [15-21]. There exists a plethora of indirect evidence suggesting that opioid dimers or higher order oligomers occur [1, 4-6] and that these dimers explain the effects DOR and DOR ligands have on MOR agonist behavior [2, 22-24]. However these experiments rely on ensemble measurements and do not look directly at the association of individual receptors on the molecular level. Previous work in the GPCR field has shown that some Class A GPCRs are able to function as monomers and that oligomerization is not necessary for normal binding and signaling in all GPCR systems [26-31]. These data raise questions about the necessity of oligomerization for opioid function and the role it plays *in vivo.*

At the present time researchers are deeply divided on the issue of functional opioid receptor oligomerization. However, novel techniques now allow us to explore the minimal functional unit needed for signaling, the examination of which was previously below the detection limit. Using single molecule total internal reflection fluorescence microscopy (SM-TIRF-M) and the fluorescent MOR ligands developed in chapter 4, single molecule binding events can be studied directly in isolated receptor systems using characterized selective fluorescent ligands, a feat which is impossible to accomplish in ensemble measurements. These data can then be compared to data collected from more natural systems and inferences drawn about opioid receptor function *in vivo.* In this chapter I will explore the functionality of

MORisolated systems to determine if a monomeric MOR is capable of normal signaling, as measured *in vitro.* (Please note: This work has already been published [32].)

B.2 Characterization of Monomeric MOR

B.2.1 Isolation of Purified MOR

In order to study the binding of a single ligand to a single receptor we must first purify monomeric receptor and isolate it in a pseudo-membrane. A construct expressing yellow fluorescent protein (YFP) conjugated human MOR with His, FLAG, and HA tags for purification (YMOR; note the YFP was used in other experiments to monitor the location of MOR, additionally, the yellow color of YFP aided in locating the fractions containing receptor during purification; **Figure B.1**), was expressed in Sf9 and HighFive^{TM} insect cells. The potency and efficacy of DAMGO in membrane preparations of insect cells expressing YMOR was tested and was well in line with its observed pharmacological characteristics in mammalian cells expressing unlabeled human MOR [33]. We chose a high density lipoprotein (HDL) reconstitution system to isolate monomeric YMOR (**Figure B.2**), however reconstitution requires the purification of active receptor in large enough quantities for subsequent biochemical manipulation and analysis. Previous reports of MOR purification from endogenous or recombinant sources have yielded either low quantities [34-38] or poor agonist binding affinities [39-41]. We were able to successfully purify large quantities of active YMOR monomer [33]; several aspects were key to the expression and purification of YMOR: a cleavable hemagglutinin signal sequence at the receptor's N-terminus [42], the presence of naltrexone during expression, and the inclusion of cholesteryl hemisuccinate and naltrexone during the entire purification process. These modifications contributed to the stabilization of YMOR, leading to an increase in yields during the chromatography process as well as increasing the specific activity of the detergent solubilized receptor [33]. (Plasmid design, expression systems, and purification techniques for YMOR developed by Adam Kuszak [32].)

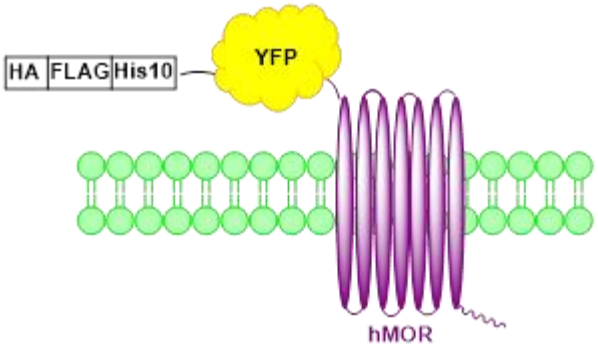

Figure B.1: Cartoon of the fluorescently tagged hMOR receptor.

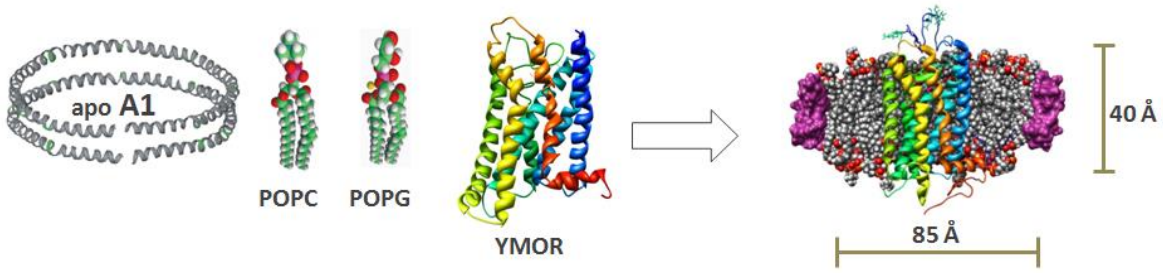

Figure B.2: Schematic for the Incorporation of GPCRs into HDL Particles – Purified apo A1 protein is incubated with the lipids POPC and POPG and purified receptor in a solution containing detergent. Detergent is then removed using Biobeads ®. Upon detergent removal the apo A1 protein corrals lipids and receptor, spontaneously forming monodispersed receptor isolated in HDL discs. Modified from Whorton *et al.* 2007.[25]

The purified YMOR was then reconstituted into the phospholipid bilayer of a HDL particle. The HDL particles are monodispersed, uniform in size, and preferentially incorporate a GPCR monomer; G proteins were also incorporated into these discs to assess the functionality of the isolated receptor [29, 33, 43]. The ability of the YMOR isolated in HDL discs to bind ligand and turn over G proteins was also characterized and shown to be within the normal range of unlabeled MOR expressed in mammalian systems (**Table B.1**) [33, 44-46]. Having generated a platform for testing purified, non-membrane bound MOR, we next needed to develop selective, fluorescent ligands as tools to confirm that the receptor was indeed in a monomeric state and to further characterize of the HDL disc bound receptor.

Table B.1: Comparison of *in vitro* Binding and Efficacy for Dermorphin Derivatives in Membrane Preparations and HDL Particles

Compound	Binding (nM)		Efficacy			
	Membranes	Particles	Membranes		Particles	
			Agonist	EC50 (nM)	Agonist	EC50 (nM)
[Lys7,Cys8] Dermorphin	0.4±0.3	2.1±0.3	Full	17.7±0.8	Full	23±3
[Lys7,Cys(AF555)8] Dermorphin	3.5±0.5	16±0.9	Full	30±4	Full	24±2
[Lys7, Cys(Cy3)8] Dermorphin	3.8±1.8	3±0.5	Full	6.2±0.1	Full	32±7

Binding affinities (K_i) were obtained by competitive displacement of radiolabeled [^{3}H] diprenorphine. Efficacy data were obtained using [^{35}S] GTPγS binding assay. Efficacy is represented as percent maximal stimulation relative to standard agonists DAMGO (MOR), DPDPE (DOR) or U69,593 (KOR) at 10μM concentrations. All values are expressed as mean ± SEM of three separate assays performed in duplicate.

B.2.2 Selective Fluorescent MOR Ligands

In order to explore the individual ligand binding events via fluorescence microscopy, we must first develop selective, potent, fluorescent ligands for the receptor in question. Since we plan to explore the functionality of isolated MOR we need to develop a fluorescent MOR agonist, as discussed in Chapter 4.2 and Appendix A we have successfully generated such a ligand, [Lys^7, Cys(Cy3)^8] dermorphin, which we can now use in our fluorescent microscopy experiments to study isolated MOR

B.2.3 Single Molecule Photobleaching in HDL Particles

Having developed a selective fluorescent MOR ligand and a system in which to isolate MOR, we next sought to confirm that the YMOR isolated in HDL particles was in fact monomeric. Binding of a saturating concentration of our fluorescent probe, [Lys^7, Cys(Cy3)^8] dermorphin, to YMOR reconstituted in HDL discs was imaged with single molecule total internal reflection fluorescence microscopy (SM-TIRF-M). Samples containing 50 pmolar receptor were continuously excited at 532 nm, the excitation wavelength of Cy3, and fluorescence intensity traces were analyzed for step-wise photo-bleaching. Approximately 95% of the fluorescent traces exhibited single-step photo-bleaching, indicating that a single fluorophore, in other words only one [Lys^7, Cys(Cy3)^8]dermorphin, was localized within each fluorescence focus. This would indicate that there is a single binding site located in each fluorescence foci, the corollary being that each foci contains a single receptor. This would mean that the HDL discs do indeed contain monomeric YMOR and that this receptor is fully functional in the monomeric state.

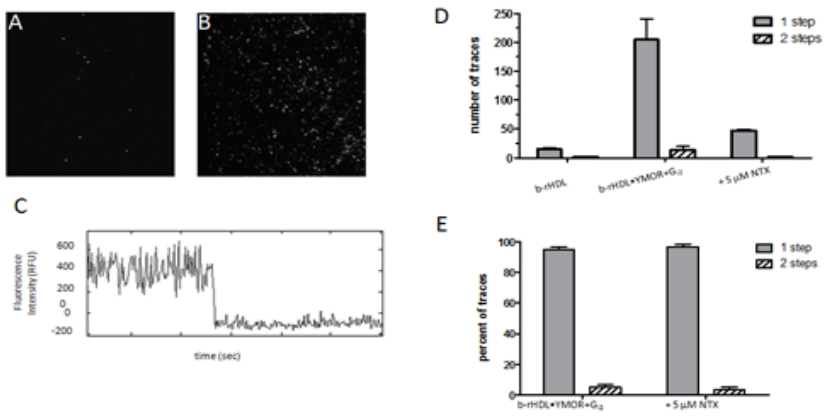

Figure B.3: Photobleaching of Monomeric MOR – (**A**) Reconstituted HDL without receptor was incubated with fluorescent agonist. No significant binding was observed, indicating that the fluorescently labeled peptide has minimal non-specific binding. (**B**) HDL particles containing YMOR+Gi2 were incubated with fluorescently labeled agonist. Significant binding was observed. (**C**) Representative single step photobleaching data. (**D**) Quantification of the number of traces with single and double step photobleaching. (**E**) Single and double step photobleaching data graphed as

B.3 Conclusions

We have successfully isolated pure monomeric YMOR in HDL discs and designed selective, fluorescent opioid probes to explore the characteristics of these isolated receptors. We have demonstrated that these monomeric YMORs bind ligand and turn over G protein in a manner comparable to assays performed in membrane preparations or *in vivo.* [33] Although we have illustrated the functionality of monomeric MOR, these data do not preclude the existence of opioid receptor oligomerization *in vitro* or *in vivo*. It is possible that homo- and heterodimerization creates unique receptor conformations that may be subject to differential regulation, desensitization, and trafficking. HDL reconstitution of YMOR provided a platform for analysis of ligand binding using single molecule microscopy. In this study we examined the reversible binding of a MOR specific agonist [Lys^7, $Cys(Cy3)^8$]dermorphin with SM-TIRF-M. To the best of our knowledge these data [33] represent the first reported observation of a peptide agonist binding to an isolated GPCR in a lipid bilayer using single molecule imaging.

B.4 Materials and Methods

B.4.1 Materials

All reagents and solvents were purchased from commercial sources and used without further purification. All chemicals and biochemicals were purchased from Sigma Aldrich (St. Louis, MO, USA) or Fisher Scientific (Hudson, NH, USA), unless otherwise noted. All tissue culture reagents were purchased from Gibco Life Sciences (Grand Island, NY, USA). Radioactive compounds were purchased from Perkin-Elmer (Waltham, MA, USA). Peptide synthesis reagents, amino acids, and Rink resin were purchased from Advanced Chem Tech (Louisville, KY, USA). Wang resins were purchased from Nova Biochem, EMD (Gibbstown, NJ, USA). G protein baculoviruses encoding rat $G\alpha_{i2}$, His_6-$G\alpha_1$ and $G\alpha_2$ were provided by Dr. Alfred G. Gilman (University of Texas Southwestern, Dallas, TX). DNA encoding human μ opioid receptor was generously provided by Dr. John R. Traynor (University of Michigan, Ann Arbor, MI). *Spodoptera frugiperda* (Sf9) and *Trichoplusia ni* (HighFive™) cells, pFastBac™ Baculovirus expression vectors and Sf900™ Serum Free Medium were from Invitrogen (Carlsbad, CA). InsectExpress™ medium was purchased from Lonza (Allendale, NJ). N-decyl-

β-D-maltoside was from Dojindo (Rockville, MD). All lipids were from Avanti Polar Lipids (Alabaster, AL). [^{3}H]diprenorphine (DPN) and [^{35}S]GTP□S were obtained from PerkinElmer (Waltham, MA). EZ-Link™ NHS-Biotin reagent was from Pierce (Rockford, IL). Ovomucoid Trypsin Inhibitor was purchased from United States Biological (Swampscott, MA). All other chemicals and ligands were from either Sigma-Aldrich (St. Louis, MO) or Fisher Scientific (Pittsburgh, PA). GF/B and BA85 filters, Cy3 and Cy5 NHS-ester mono-reactive dyes, and Source15Q and Superdex200 chromatography resins were from GE Healthcare (Piscataway, NJ). Talon™ resin was from Clontech (Mountain View, CA). BioBeads absorbant resin was from Bio-Rad (Hercules, CA). Chromatography columns were run using a BioLogic Duo-Flow Protein Purification System from Bio-Rad. Amicon Ultra centrifugation filters were from Millipore (Billerica, MA). Amino acids for ligand synthesis were obtained from Advanced ChemTech (Louisville, KY) or Sigma-Aldrich (St. Louis, MO).

B.4.2 [^{3}H]DPN Saturation and Agonist Competition Binding Assays in HDL Particles

Binding reactions were prepared in 100 µL volumes. Membrane fractions prepared from Sf9 or HighFive™ cells expressing YMOR (0.5 to 5 µg total protein, prepared as above) were incubated with [^{3}H]DPN (0.25 to 4 nM) for 1 hr at room temperature in 25 mM Tris pH 7.7, 136 mM NaCl, 2.7 mM KCl (TBS) buffer. Nonspecific binding was determined in the presence of 20 µM (NTX). Bound [^{3}H]DPN was separated from free by rapid filtration through GF/B filters and three 200 µL washes of ice cold TBS. [^{3}H]DPN saturation binding reactions on YMOR incorporated into rHDL particles were prepared in TBS pH 7.7, 0.1% BSA and Sephadex G-50 Fine (GE Healthcare) gravity-flow columns were used to separate bound from free [^{3}H]DPN. Agonist competition assays in HDL particles were performed in 25 mM Tris pH 7.7, 5 mM NaCl, 0.1% BSA. [^{3}H]DPN binding assays on detergent-solubilized YMOR were performed in 50 mM Tris pH 8, 136 mM NaCl, 0.1% DDM, 0.01% CHS and separated on Sephadex G-50 gravity flow columns. For agonist competition assays receptor samples were incubated with 0.5 to 1 nM [^{3}H]DPN and increasing concentrations of agonist (1 pM to 1 mM) in the absence or presence of 10 µM GTPγS. Samples were measured for radioactivity on a liquid scintillation counter and data was fit to one-site saturation, one-site competition or two-site competition binding models using Prism 5.0 (GraphPad, San Diego, CA).

B.4.3 [^{35}S]GTPγS Binding Assay in HDL Particles

One hundred µL volume reactions were prepared containing 1-10 µg total membrane protein from YMOR expressing HighFive™ cells or ~80 fmoles of YMOR incorporated into rHDL particles in 30mM Tris pH 7.4, 100 mM NaCl, 5 mM $MgCl_2$, 0.1 mM DTT, 1 or 10 □M GDP (membranes or HDL particles), and 10 nM isotopically diluted [^{35}S]GTP□S. YMOR samples were incubated with increasing concentrations of agonists (1 pM to 1 mM) for 1 hr at room temperature, then rapidly filtered through GF/B (membrane samples) or BA85 filters (HDL samples) and washed three times with 2 mL ice cold 30 mM Tris pH 7.4, 100 mM NaCl, 5 mM $MgCl_2$. Samples were measured for radioactivity on a liquid scintillation counter and data was fit to a log dose-response model using Prism 5.0.

B.4.4 Solid Phase Peptide Synthesis

Peptides were synthesized using standard solid phase Fmoc (fluorenylmethyloxycarbonyl) chemistry on a CS Bio CS336X Peptide Synthesizer (CS Bio Company, Menlo Park, CA, USA), using previously described protocols. [47] C-terminal amide peptides were synthesized using Rink resin, C-terminal acid peptides were synthesized using Fmoc-Wang resin preloaded with the C-terminal amino acid. A 20% solution of piperidine in N-methyl-2-pyrrolidone (NMP) was used to remove the first Fmoc protecting group before synthesis and again to remove the Fmoc-protecting group after each coupling cycle. Coupling was performed using a four-fold excess of amino acid and a solution of 0.4 M hydroxybenzotriazole (HOBt) and O-benzotriazole- N, N, N ', N '-tetramethyl-uroniumhexafluoro- phosphate (HBTU) in dimethylformamide (DMF), in the presence of diisopropylethylamine (DIEA). After the synthesis was complete, the resin was washed with NMP, then with dichloromethane, and dried under vacuum. Difficult couplings of the artificial amino acids Dmt, Dhp, Ncp, and Hcp were performed with coupling times lasting 4-16 hours. The peptides were cleaved from the resin and side-chain-protecting groups removed by treatment at room temperature for 2 h with a cleavage cocktail consisting of 9.5 mL trifluoroacetic (TFA) acid, 0.25 mL triisopropylsilane (TIS) and 0.25 mL H_2O. The solution was concentrated *in vacuo*, and peptides were precipitated using cold, fresh diethylether. The filtered crude material was then purified using a Waters semipreparative HPLC (Waters Corporation, Milford, MA, USA) with a Vydac Protein and Peptide C18 column, using a linear gradient 10% Solvent B

(0.1% TFA acid in acetonitrile) in Solvent A (0.1% TFA acid in water) to 60% Solvent B in Solvent A, at a rate of 1% per minute. The identity all peptides were determined ESI-MS performed on an Agilent Technologies LC/MS system using a 1200 Series LC and 6130 Quadrupole LC/MS (Agilent Technologies, Santa Clara, CA, USA) in positive mode with 50–100 µL injection volume and a linear gradient of 0% Solvent D (0.02% TFA and 0.1% acetic acid (AcOH) in acetonitrile) in Solvent C (0.02% TFA and 0.1% AcOH in water) to 60% Solvent D in Solvent C in 15 min. The purity of all peptides was determined using a Waters Alliance 2690 Analytical HPLC (Waters Corporation, Milford, MA, USA) and Vydac Protein and Peptide C18 reverse phase column, using a linear gradient of 0–70% Solvent B in Solvent A at a rate of 1% per minute. Linear peptides were purified to ≥ 95% purity by UV absorbance at 230 nm.

B.4.5 Fluorescent Labeling

The purified peptide was labeled with Cy3 or Cy5 maleimide or NHS ester (GE Healthcare) according to the manufacturer's instructions using a ratio of 1.5:1 peptide to fluorophore. The labeled peptide was further purified via semi-preparative HPLC using a 5 micron Vydac C18 column as described above. The potency and efficacy labeled ligands confirmed in radiolabeled [^{3}H]DPN competition and [^{35}S]GTPγS binding assays.

B.4.6 Cell Lines and Mammalian Membrane Preparations

C6-rat glioma cells stably transfected with a rat µ (C6-MOR) or rat δ (C6-DOR) opioid receptor [48] and Chinese hamster ovary (CHO) cells stably expressing a human κ (CHO-KOR) opioid receptor [49] were used for all in vitro assays. Cells were grown to confluence at 37ºC in 5% CO_2 in Dulbecco's Modified Eagle's Medium containing 10% fetal bovine serum and 5% penicillin/streptomycin. Membranes were prepared by washing confluent cells three times with ice cold phosphate-buffered saline (0.9% NaCl, 0.61 mM Na_2HPO_4, 0.38 mM KH_2PO_4, pH 7.4). Cells were detached from the plates by incubation in warm harvesting buffer (20 mM HEPES, 150 mM NaCl, 0.68 mM EDTA, pH 7.4) and pelleted by centrifugation at 200xg for 3 min. The cell pellet was suspended in ice-cold 50 mM Tris-HCl buffer, pH 7.4 and homogenized with a Tissue Tearor (Biospec Products, Inc, Bartlesville, OK, USA) for 20 s at setting 4. The homogenate was centrifuged at 20,000xg for 20 min at 4 C, and the pellet was rehomogenized in 50 mM Tris-HCl with a Tissue Tearor for 10 s at setting 2, followed by recentrifugation. The

final pellet was resuspended in 50mM Tris-HCl and frozen in aliquots at -80ºC. Protein concentration was determined via Bradford assay using bovine serum albumin as the standard.

B.4.7 Radioligand Binding Assays in Mammalian Membrane Preparations

Opioid ligand-binding assays were performed using competitive displacement of 0.2 nM [^{3}H]diprenorphine (250 µCi, 1.85TBq/mmol) by the test compound from membrane preparations containing opioid receptors. The assay mixture, containing membrane suspension (20 µg protein/tube) in 50 mM Tris-HCl buffer (pH 7.4), [^{3}H]diprenorphine, and various concentrations of test peptide, was incubated at room temperature for 1 h to allow binding to reach equilibrium. The samples were rapidly filtered through Whatman GF/C filters using a Brandel harvester (Brandel, Gaithersburg, MD, USA) and washed three times with 50 mM Tris-HCl buffer. The radioactivity retained on dried filters was determined by liquid scintillation counting after saturation with EcoLume liquid scintillation cocktail in a Wallac 1450 MicroBeta (Perkin-Elmer, Waltham MA, USA). Nonspecific binding was determined using 10 µM naloxone. K_i values were calculated using nonlinear regression analysis to fit a logistic equation to the competition data using GraphPad Prism version 5.01 for Windows. The results presented are the mean ± standard error from at least three separate assays performed in duplicate.

B.4.8 Stimulation of [^{35}S]GTPγS Binding in Mammalian Membrane Preparations

Agonist stimulation of [^{35}S] guanosine 5'-O-[gamma-thio]triphosphate ([^{35}S]GTPγS, 1250 Ci, 46.2TBq/mmol) binding was measured as described previously [50]. Briefly, membranes (10-20 µg of protein/tube) were incubated 1 h at room temperature in GTPγS buffer (50 mM Tris-HCl, 100 mM NaCl, 5 mM $MgCl_2$, pH 7.4) containing 0.1 nM [^{35}S]GTPγS, 30 µM guanosine diphosphate **(**GDP), and varying concentrations of test peptides. Peptide stimulation of [^{35}S]GTPγS was compared with 10 µM standard compounds [DAla^2, N-MePhe^4, Gly-ol]-enkephalin (DAMGO) at MOR, DPen^{2,5}- enkephalin (DPDPE) at DOR, or U69,593 at KOR. The reaction was terminated by rapidly filtering through GF/C filters and washing ten times with GTPγS buffer, and retained radioactivity was measured as described above. The results presented are the mean ± standard error from at least three separate assays performed in duplicate; maximal stimulation was determined using nonlinear regression analysis with GraphPad Prism.

B.4.9 Prism-based Single Molecule TIRF and Step-Photobleaching analysis of [Lys^7, Cys(Cy3)^8]dermorphin binding to rHDL-YMOR+G_{i2}.

Purified recombinant apoA-1 was biotinylated at a 4:1 molar ratio of biotin:apoA-1 using EZ-Link^{TM} NHS-Biotin (Pierce), according to the manufacturer's protocol. Biotin-apoA-1 was separated from unconjugated biotin on a Superdex200 gel filtration column. Purified YMOR was then reconstituted with biotin-apoA-1, POPC, POPG, and brain lipid extract as above. Purified Gi_2 heterotrimer was added to reconstituted receptor as above, and coupling was confirmed by observing high affinity competition of [^{3}H]DPN binding by DAMGO. Five nanomolar biotin-rHDL-YMOR+G_{i2} was then incubated with 5 □M [Lys^7, Cys^8]dermorphin-Cy3 for 45 minutes at 25^{o}C in a 25 mM Tris pH 7.7. Samples were diluted 100-fold in 25 mM Tris and imaged as described above. Fluorophore intensity time-traces were collected for 30 to 100 seconds at 10 frames per second and analyzed for photo-bleaching with in-house software (MatLab 7.0).

B.5 References

1. Conn, P.M. and A. Ulloa-Aguirre, *Trafficking of G-protein-coupled Receptors to the Plasma Membrane: Insights for Pharmacoperone Drugs.* Cell, 2009. **21**(3): p. 190-198.
2. George, S.R., et al., *Oligomerization of Mu and Delta Opioid Receptors.* The Journal of biological chemistry, 2000. **275**(34): p. 26128-26135.
3. Law, P.-Y., et al., *Heterodimerization of Mu and Delta Opioid Receptors Occurs at the Cell Surface Only and Requires Receptor-G Protein Interactions.* The Journal of biological chemistry, 2006. **280**(12): p. 11152-11164.
4. Milligan, G., *G Protein-coupled Receptor Hetero-dimerization: Contribution to Pharmacology and Function.* British Journal of Pharmacology, 2009. **158**: p. 5-14.
5. Milligan, G., *The Role of Dimerization in Cellular Trafficking of G-protein-coupled Receptors.* Current Opinion in Pharmacology, 2010. **10**: p. 23-29.
6. Rios, C.D., et al., *G-protein-coupled Receptor Dimerization: Modulation of Receptor Function.* Pharmacology and Therapeutics, 2001. **92**: p. 71-87.
7. Breitwieser, G.E., *G Protein coupled Receptor Oligomerization: Implications for G Protein Activation and Cell Signaling.* Circulation Research, 2004. **94**: p. 17-27.
8. Fotiadis, D., et al., *Rhodopsin dimers in native disc membranes.* Nature, 2003. **421**: p. 127-8.
9. Gether, U. and B.K. Kobilka, *G Protein-coupled Receptors.* Journal of Biological Chemistry, 1998. **273**(29): p. 17979-17982.
10. Lee, C., et al., *Two Defective Heterozygous Lutenizing Hormone Receptors can Rescue Hormone Action.* Journal of Biological Chemistry, 2002. **277**: p. 15795-15800.
11. Maggio, R., Z. Vogel, and J. Wess, *Co-expression studies with mutant muscarinic/adrenergic receptors provide evidence for intermolecular ''cross-talk'' between G-protein linked receptors.* Proc Natl Acad Sci USA, 1993. **90**: p. 3103–3107.
12. McVey, M., et al., *Monitoring Receptor Oligomerization Using Time-resolved Fluorescence Resonance Energy Transfer and Bioluminescence Resonance Enerty Transfer.* Journal of Biological Chemistry, 2001. **276**(17): p. 14092-14099.
13. Milligan, G., *G Protein Coupled Receptor Dimerization: Function and Ligand Pharmacology.* Molecular Pharmacology, 2004. **66**: p. 1-7.
14. Ramsay, D., et al., *Homo- and Heterooligomeric Interactions Between G Protein-Coupled Receptors in Living Cells Monitored by Two Variants of Bioluminesence Resonance Energy Transfer. Heterooligomers Between Receptor Subtypes form More Effiency than between less Closely Related Sequences.* Biochemistry, 2002. **365**: p. 429-440.
15. George, S.R., et al., *Oligomerization of mu and delta Opioid Receptors: Generation of Novel Functional Properties.* Journal of Biological Chemistry, 2000. **275**(34): p. 26128-26135.
16. Gomes, I., et al., *Heterodimerization of mu and delta Opioid Receptors: A Role in Opiate Synergy.* Journal of Neuroscience, 2000. **20**: p. 1-5.
17. Hazum, E., K.-J. Chang, and P. Cuatrecasas, *Opiate (Enkaphalin) Receptors of Neuroblastoma Cells: Occurrene in Clusters on the Cell Surface.* Science, 1979. **206**(4422): p. 1077-1079.
18. Hazum, E., K.-J. Chang, and P. Cuatrecasas, *Cluster Formation of Opiate (enkaphalin) Receptors in Neuroblastoma Cells: Differences between Agonists and Antagonists and*

Possible Relationships to Biological Functions. Proceedings of the National Academy of Science USA, 1980. **77**(5): p. 3038-3041.
19. Law, P.-Y., et al., *Heterodimerization of mu - and delta-Opioid Receptors Occurs at the Cell Surface Only and Requires Receptor-G Protein Interactions.* Journal of Biological Chemistry, 2005. **280**(12): p. 11152-62.
20. Li-Wei, C., et al., *Homodimerization of the Human Mu-Opioid Receptor Overexpressed in Sf9 Insect Cells.* Protein and Peptide Letters, 2002. **9**: p. 145-152.
21. Pascal, G. and G. Millligan, *Functional Complementation and the Ananlysis of Opioid Receptor Homodimerization.* Molecular Pharmacology, 2005. **68**: p. 905-915.
22. Gomes, I., et al., *Heterodimerization of the Mu and Delta Opioid Receptors: A Role in Opiate Synergy.* Journal of Neuroscience, 2000. **20**(22): p. RC110.
23. Law, P.-Y., et al., *Heterodimerization of the Mu and Delta Opioid Receptros Occurs at the Cell Surface Only and Requires Receptor-G Protein Interactions.* The Journal of biological chemistry, 2005. **280**(12): p. 11152-11164.
24. He, S.-Q., et al., *Facilitation of My Opioid Receptor Activity by Preventing Delta Opioid Receptor Mediated Codegradation.* Neuron, 2011. **69**: p. 120-131.
25. Whorton, M.R., et al., *A Monomeric G Protein-Coupled Receptor Isolated in a High Density Lipoprotein Particle Efficently Activates its G Protein.* Proceedings of the National Academy of Science, 2007. **104**(18): p. 7682-7687.
26. Leitz, A.J., et al., *Functional reconstitution of Beta2-adrenergic receptors utilizing self-assembling Nanodisc technology.* Biotechniques, 2006. **40**(5): p. 601-2, 604, 606, passim.
27. Nath, A., W.M. Atkins, and S.G. Sligar, *Applications of phospholipid bilayer nanodiscs in the study of membranes and membrane proteins.* Biochemistry, 2007. **46**(8): p. 2059-69.
28. Bayburt, T.H., et al., *Transducin activation by nanoscale lipid bilayers containing one and two rhodopsins.* J Biol Chem, 2007. **282**(20): p. 14875-81.
29. Whorton, M.R., et al., *A Monomeric G Protein-coupled Receptor Isolated in a High-density Lipoprotein Particle Efficiently Activates its G Protein.* Proc Natl Acad Sci USA, 2007. **104**(18): p. 7682-7687.
30. Whorton, M.R., et al., *Efficient Coupling of Transducin to Monomeric Rhodopsin in a Phospholipid Bilayer.* Journal of Biological Chemistry, 2008. **283**(7): p. 4387-4394.
31. Banerjee, S., T. Huber, and T.P. Sakmar, *Rapid incorporation of functional rhodopsin into nanoscale apolipoprotein bound bilayer (NABB) particles.* J Mol Biol, 2008. **377**(4): p. 1067-81.
32. Kuszak, A.J., et al., *Purification and functional reconstitution of monomeric mu-opioid receptors: allosteric modulation of agonist binding by Gi2.* The Journal of biological chemistry, 2009. **284**(39): p. 26732-41.
33. Kuszak, A.J., et al., *Purification and reconstitution of a mu-opioid receptor monomer: functional G protein activation and allosteric regulation.* Journal of Biological Chemistry, 2009. **284**(39): p. 26732-41.
34. Gioannini, T.L., et al., *Purification of an active opioid-binding protein from bovine striatum.* J Biol Chem, 1985. **260**(28): p. 15117-21.
35. Li, L.Y., et al., *Purification of opioid receptor in the presence of sodium ions*. Life Sci, 1992. **51**(15): p. 1177-85.

36. Talmont, F., et al., *Expression and pharmacological characterization of the human mu-opioid receptor in the methylotrophic yeast Pichia pastoris.* FEBS Lett, 1996. **394**(3): p. 268-72.
37. Obermeier, H., A. Wehmeyer, and R. Schulz, *Expression of mu-, delta- and kappa-opioid receptors in baculovirus-infected insect cells.* Eur J Pharmacol, 1996. **318**(1): p. 161-6.
38. Massotte, D., et al., *Characterization of delta, kappa, and mu human opioid receptors overexpressed in baculovirus-infected insect cells.* J Biol Chem, 1997. **272**(32): p. 19987-92.
39. Sarramegna, V., et al., *Optimizing functional versus total expression of the human mu-opioid receptor in Pichia pastoris.* Protein Expr Purif, 2002. **24**(2): p. 212-20.
40. Sarramegna, V., et al., *Green fluorescent protein as a reporter of human mu-opioid receptor overexpression and localization in the methylotrophic yeast Pichia pastoris.* J Biotechnol, 2002. **99**(1): p. 23-39.
41. Sarramegna, V., et al., *Solubilization, purification, and mass spectrometry analysis of the human mu-opioid receptor expressed in Pichia pastoris.* Protein Expr Purif, 2005. **43**(2): p. 85-93.
42. Guan, X.M., T.S. Kobilka, and B.K. Kobilka, *Enhancement of membrane insertion and function in a type IIIb membrane protein following introduction of a cleavable signal peptide.* J Biol Chem, 1992. **267**(31): p. 21995-8.
43. Whorton, M.R., et al., *Efficient coupling of transducin to monomeric rhodopsin in a phospholipid bilayer.* J Biol Chem, 2008. **283**(7): p. 4387-94.
44. Emmerson, P.J., et al., *Characterization of opioid agonist efficacy in a C6 glioma cell line expressing the mu opioid receptor.* J Pharmacol Exp Ther, 1996. **278**(3): p. 1121-7.
45. Alt, A., et al., *Stimulation of guanosine-5'-O-(3-[35S]thio)triphosphate binding by endogenous opioids acting at a cloned mu receptor.* J Pharmacol Exp Ther, 1998. **286**(1): p. 282-8.
46. Clark, M.J., et al., *Comparison of the relative efficacy and potency of mu-opioid agonists to activate Galpha(i/o) proteins containing a pertussis toxin-insensitive mutation.* J Pharmacol Exp Ther, 2006. **317**(2): p. 858-64.
47. Przydzial, M.J., et al., *Roles of Residues 3 and 4 in Cyclic Tetrapeptide Ligand Recognition by the Kappa Opioid Receptor.* Journal of Peptide Research, 2005. **26**: p. 333-342.
48. Lee, K.O., et al., *Differential Binding Properties of Oripavines at Cloned Mu- and Delta-Opioid Receptors.* European Journal of Pharmacology, 1999(378): p. 323-330.
49. Husbands, S.M., et al., *BU74, A Complex Oripavine Derivative with Potent Kappa Opioid Receptor Agonism and Delayed Opioid Antagonism.* European Journal of Pharmacology, 2005(509): p. 117-135.
50. Traynor, J.R. and S.R. Nahorski, *Modulation by Mu-Opioid Agonists of Guanosine-5'-O(3-[35S]thio)triphosphate Binding to Membranes from Human Neuroblastoma SHY5Y Cells.* Molecular Pharmacology, 1995(47): p. 848-854.